Aus der Klinik für Kardiovaskuläre Chirurgie

der Heinrich-Heine-Universität Düsseldorf

Direktor: Univ.-Prof. Dr. med. Artur Lichtenberg

Optimization of the biocompatibility of cardiovascular implants

in a standardized rat model

Habilitationsschrift

zur Erlangung der *Venia Legendi*

an der Hohen Medizinischen Fakultät

der Heinrich-Heine-Universität Düsseldorf

vorgelegt von

Dr. med. Alexander Assmann

2014

Publications

The present habilitation thesis summarizes the results of the five thematically connected original articles which are listed below. Details with regard to methodology and results or the elaborate discussion thereof are part of the included writings.

- **Assmann A**, Delfs C, Munakata H, Schiffer F, Horstkötter K, Huynh K, Barth M, Stoldt VR, Kamiya H, Boeken U, Lichtenberg A, Akhyari P. Acceleration of autologous *in vivo* recellularization of decellularized aortic conduits by fibronectin surface coating. **Biomaterials**. 2013; 34:6015-6026. **IF 8,3**
- **Assmann A**, Zwirnmann K, Heidelberg F, Schiffer F, Horstkötter K, Munakata H, Gremse F, Barth M, Lichtenberg A, Akhyari P. The degeneration of biological cardiovascular prostheses under pro-calcific metabolic conditions in a small animal model. **Biomaterials**. 2014; 35:7416-7428. **IF 8,3**
- **Assmann A**, Horstkötter K, Munakata H, Schiffer F, Delfs C, Zwirnmann K, Barth M, Akhyari P, Lichtenberg A. Simvastatin does not diminish the *in vivo* degeneration of decellularized aortic conduits. **J Cardiovasc Pharmacol**. 2014; 64:332-342. **IF 2,1**
- **Assmann A**, Akhyari P, Delfs C, Flögel U, Jacoby C, Kamiya H, Lichtenberg A. Development of a growing rat model for the *in vivo* assessment of engineered aortic conduits. **J Surg Res**. 2012; 176:367-375. **IF 2,1**
- Munakata H, **Assmann A**, Poudel-Bochmann B, Horstkötter K, Kamiya H, Okita Y, Lichtenberg A, Akhyari P. Aortic conduit valve-model with controlled moderate aortic regurgitation in rats: A technical modification to improve short- and long-term outcome and to increase the functional results. **Circ J**. 2013; 77:2295-2302. **IF 3,7**

The scientific findings summarized in the present habilitation thesis were awarded the Ulrich Karsten Scientific Award of the German Society for Thoracic and Cardiovascular Surgery in February 2014.

Table of contents

1 Objectives

1.1 Epidemiological background

Valvular heart disease has become an emerging challenge in modern cardiovascular medicine [1]. In 2000, 2.5% of the US citizens suffered from valvular diseases, whereas in the subgroup >75 years, the percentage amounted for 13.2% [2]. From 1979 to 2009, the annual number of deaths related to valvular heart disease in the US has risen from 15,054 to 26,663, reflecting the significance of these pathologies [3]. In the developing world, rheumatic valve disease is a major factor of morbidity and mortality especially in younger patients with more than 282,000 deaths per year worldwide [4]. Predominantly in the Western world, degenerative entities increase in quantity due to the rapidly ageing population. In most of these cases, the status of the leaflet tissue does not allow for reconstructive approaches anymore, so that valve replacement procedures have to be taken into account. Therefore, heart valve prosthesis implantations are standard procedures in cardiovascular surgery and cardiology with more than 32,000 reported cases per year in Germany in 2012 [5] and more than 300,000 annual operations worldwide, whereas the number is expected to exceed 1,000,000 cases by 2050 [6]. Among patients who undergo heart valve procedures, calcifying aortic valve disease (CAVD) leading to functional stenosis is the most frequent underlying pathology, which compromised 47% of all treated patients in a European survey in 25 countries [7].

The aforementioned statistics highlight the importance of developing optimized therapeutic strategies against CAVD from a patient-centered as well as from a socio-economic point of view.

1.2 Pathophysiology of calcifying aortic valve disease

CAVD is a pathological process that seems to have multiple parallels to atherosclerosis. Most of the major risk factors of atherosclerosis, as e.g. arterial hypertension, diabetes mellitus, hypercholesterinemia and smoking, have been reported to be also predictors of CAVD, and CAVD is associated in turn with adverse cardiovascular events [8,9]. However, recent publications have pointed out that it is a separate disease with at

least partially different pathophysiological mechanisms and resulting characteristics of the degenerative lesions.

Over a long time, mechanical stress has been considered to be the major determinant of CAVD development resulting in damage of the leaflet tissue with subsequent passive calcium deposition [10]. On the contrary, current theories claim active cellular and inflammatory processes to initiate and sustain the disease.

Supported by genetic and acquired cardiovascular risk factors, local inflammation predominantly driven by tissue-invading macrophages and T-lymphocytes disrupts the endothelium of aortic valve leaflets [11]. At the first stage of this process, valvular endothelial cells upregulate pro-inflammatory receptors, as e.g. intercellular adhesion molecule-1, vascular cell adhesion molecule-1 or E-selectin, resulting in enhanced adhesion of monocytes and T-lymphocytes. Due to disturbed flow on the aortic side of the leaflets, valvular endothelial cells on this side are more responsive to inflammatory cytokines and exhibit in turn higher production rates [12,13]. Upregulation of cytokines as e.g. tumor necrosis factor-alpha, transforming growth factor-beta or bone morphogenetic proteins adversely activates valvular interstitial cells (VICs) [14]. These myofibroblasts and the invaded inflammatory cells produce matrix metalloproteinases (MMPs) and cathepsins which destroy the fibrous architecture of the extracellular matrix [15].

Similarly to atherosclerotic plaques, lesions in CAVD contain low-density lipoproteins [16]. Extracellular deposition of oxidized low-density lipoproteins further aggravates binding and effect of inflammatory cytokines, thus catalyzing the degenerative processes [17].

At an advanced stage of CAVD, osteoblastic transformation of VICs, neoangiogenesis and hydroxyapatite deposition occur [11]. Osteogenic differentiation of VICs is characterized by upregulation of pro-osteogenic (e.g. alkaline phosphatase, osteocalcin and runt-related transcription factor-2) as well as anti-osteogenic markers (e.g. osteopontin and osteoprotegerin) [18-20], and seems to be additionally influenced by further substances regulating the bone metabolism, as e.g. vitamin D (VD) or phosphate (PH) [21,22]. Interestingly, skeletal calcification was reported to inversely

correlate with CAVD and arterial degeneration [23]. Besides active transformation of VICs, dystrophic calcification is regarded to play a role in CAVD as well. In calcified areas, apoptotic and necrotic cells additionally stimulate calcium deposition [24], whereas the amount of these dying cells is low as compared to that of activated VICs, supporting the hypothesis that CAVD predominantly is an active process of valvular degeneration.

In contrast to atherosclerosis, that is a typical disease of the elderly, CAVD also occurs in younger patients, especially in case of bicuspid aortic valves which are present in 1% of all neonates [25]. The compositions of atherosclerotic and CAVD lesions are different from each other. While atherosclerotic plaques exhibit extensive lipid content and fibrous tissue, CAVD lesions predominantly consist of calcified extracellular matrix. This conditions different events to result in symptomatic transformation of the diseases. In atherosclerosis, clinical symptoms frequently arise after plaque rupture and subsequent thrombus formation leading to vascular occlusion. On the contrary, CAVD results in progressive leaflet stiffening creating aortic valve stenosis. On the cellular level, atherosclerosis is characterized by de-differentiation of smooth muscle cells towards myofibroblasts [26], while in CAVD, quiescent VICs are activated and finally undergo osteoblastic transformation [27].

1.3 **Therapeutic approaches against calcifying aortic valve disease**

In spite of all the knowledge about pathophysiological mechanisms in CAVD and the obvious parallels to atherosclerosis, no medication, including drugs with therapeutic efficiency against atherosclerosis, has proven yet to be effective against progression of CAVD [28]. In case of 3-hydroxy-3-methyl-glutaryl coenzyme A (HMG-CoA) reductase inhibitors, the primary lipid-lowering mechanism as well as the known pleiotropic effects, as e.g. plaque stabilization, improvement of endothelial function and reduction of platelet aggregation, should beneficially influence the course of CAVD. However, recent large clinical trials resulted in conflicting data, currently not supporting any recommendation for statin therapy in CAVD patients [29-31].

Advanced stages of CAVD are associated with high morbidity and mortality. Once symptoms as e.g. dyspnea, fatigue or syncopes have occurred, the average survival amounts to only two to three years [28]. Since the necessity of treatment is urgent in these patients, and conservative therapy is ineffective to slow down or reverse the progression of CAVD, aortic valve replacement is the measure of choice.

Independently on the choice of interventional or operative approaches, all currently available heart valve implants are characterized by inherent limitations and drawbacks. The durability of all clinically established biological grafts is restricted predominantly due to their immunogenicity resulting in calcifying degeneration and subsequent necessity of redo replacement. On the other hand, mechanical implants are highly thrombogenic and therefore require strictly monitored life-long anticoagulation to avoid major thrombotic or bleeding complications. Both classes of prostheses do not grow with the recipient, which limits their use in pediatric patients.

1.4 **The ideal heart valve prosthesis**

In order to set targets for future research on implant development, the following specifications of an ideal heart valve prosthesis have been defined [32]:

- Physiological hemodynamics
- No degeneration
- No thrombogenicity
- No hemolysis
- No impairment of the patient‘s daily life
- Resistance against infection
- Growth potential
- Simple implantation

In biological implants, thrombogenicity and hemolysis are aspects of minor importance. While some modern bioprostheses allow for fast and even minimally invasive implantation techniques, as e.g. sutureless grafts or implants for transcatheter approaches, and their hemodynamic performance is similar to that of native valves, the major problems of graft degeneration and lack of growth are unsolved yet.

In this context, methods of tissue engineering, an interdisciplinary field of science aiming at the development of functional replacement tissues, could serve as tools to generate and modify tissue scaffolds in order to create improved heart valve implants.

1.5 **Decellularization of cardiovascular grafts**

Decellularization describes the process of destruction and elution of all cellular components of native tissues in order to obtain a cell-free extracellular matrix scaffold. Common protocols for decellularization of cardiovascular tissues employ ionic and non-ionic detergents, osmotic shock, proteolytic digestion, DNase/RNase treatment and biological cell toxins [33]. One of the major challenges of developing efficient decellularization techniques is to induce destruction of the cytoskeleton while preserving the extracellular matrix proteins and their architecture. Therefore, multiple combinations of the above mentioned components have been examined, though an ideally balanced protocol has not been found yet. However, the joint application of the detergents sodium dodecyl sulfate and deoxycholic acid has been reported to efficiently decellularize native heart valves tissues [34].

Decellularized cardiovascular implants are promising alternatives to overcome the inherent limitations of clinically available grafts, since they do not require anticoagulation, are nearly non-immunogenic and potentially allow for graft growth *in vivo* after recellularization. The reason for low immunogenicity is the lack of major cell-bound antigens triggering the adaptive immune response of the recipient, e.g. human leukocyte antigens or alpha-Gal epitopes, which induce degeneration and implant failure in both, animals and humans [35,36]. Furthermore, decellularization has been reported to reduce retrovalvular thrombus formation after heterotopic aortic conduit implantation in rats [37]. Previously, decellularized pulmonary as well as aortic heart valves have been successfully implanted in preclinical models with encouraging short- to mid-term functional outcome [34,38]. These results have been confirmed in clinical series of decellularized allogenic valve implantation in the pulmonary as well as in the aortic position [39,40].

In the aortic valve position, cryopreserved allografts still are the clinical gold standard providing good long-term results in adults [41]. Nevertheless, their availability is limited, and especially in younger patients, accelerated calcific degeneration causes early implant failure and a redo operation with increased risk of morbidity and mortality [42]. As pediatric pulmonary valve substitutes, decellularized allografts showed superior performance in terms of freedom from explantation up to 5 years, transvalvular pressure gradients, and adaptive growth, as compared to cryopreserved allografts [39].

While the reduction of early graft inflammation by decellularization has been analyzed in small as well as large animal models [37,43,44], the impact of decellularization on the progression of deteriorating graft calcification in the middle- and long-term has not been investigated extensively yet.

1.6 **Recellularization of decellularized grafts**

In opposite to multiple studies claiming advantages of decellularized prostheses, a few failure reports have raised caution: After implantation of decellularized porcine heart valves in pediatric patients, severe calcifying degeneration and early graft failure were observed, which may be attributed to thrombogenesis, inflammation and immune response against remnants of donor cells in the transplant [45-47]. Possible reasons for these processes are incomplete removal of cell fragments during decellularization and the exposure of extracellular matrix proteins on the luminal prosthesis surface to the blood stream [48,49]. Therefore, it is crucial that decellularized cardiovascular grafts undergo autologous endothelialization on the luminal side either before or within a short time period after implantation. Furthermore, a closed endothelial layer may prevent pannus formation on the inner graft surface, which regularly occurs in the absence of intact endothelium.

Endothelialization of decellularized scaffolds can be conducted prior to implantation, or *in vivo* recellularization after implantation can be awaited or induced, respectively.

The main advantage of cellular seeding *in vitro* is the option to achieve a closed endothelial layer at the time of implantation. However, this approach necessitates choosing and harvesting of an appropriate autologous cell source, which is a drawback particularly in patients with dysfunctional or quantitatively reduced endothelial progenitor cells, and requires an additional intervention, as e.g. bone marrow puncture, in order to harvest the cells. Once the cells are collected, they have to be expanded to generate a sufficient amount of cells for the seeding process. In order to allow for stable attachment of the cells to the graft surface and to avoid sudden loss of the seeded cells after implantation into the circulatory system, the hemodynamic and metabolic conditions in the recipient organism have to be mimicked already during the *in vitro* cellularization procedure. Thus, utilization of a pulsatile bioreactor applying sophisticated hemodynamic protocols and physiological metabolic conditions seems to be inevitable [50]. Such bioreactors increase the production costs of tissue-engineered cardiovascular implants as well as the risk of graft contamination. The aforementioned scenario of seeding autologously harvested cells in a bioreactor is a time-consuming approach and rules out affordable off-the-shelf production of implants. As a further consequence, these individually engineered prostheses could not be used for patients in need of urgent or emergency solutions.

Implantation of acellular scaffolds implies the potential risk of thrombus or pannus formation on the exposed extracellular matrix surface. Otherwise, previous reports have shown that decellularized valvular and arterial grafts do not exhibit relevant thrombogenicity [34,38,43]. Furthermore, decellularized scaffolds can be produced time- and cost-effectively as off-the-shelf grafts with low risk of microbial contamination.

In spite of low thrombogenicity of decellularized implants, extensive efforts to accelerate autologous *in vivo* recellularization are justified, in particular since endothelium-free surfaces are known to induce hyperplastic intima formation [51,52]. In this context, graft surface coating with agents supporting attachment or proliferation of endothelial cells is a promising approach. Previously, surface treatment of artificial and biological vascular grafts with biofunctional proteins, such as fibronectin (FN), fibrin or vascular endothelial growth factor, has been shown to

accelerate the *in vivo* adhesion of recipient cells, thereby improving the *in vivo* performance of the implants [53,54].

FN surface coating has been reported to improve the initial attachment of endothelial cells to polytetrafluorethylene prostheses *in vitro* as well as the stability of endothelial cell adhesion to polyethylene terephthalate grafts under physiological shear stress in a pulsatile bioreactor [55,56]. Beyond the beneficial effects on cell attachment, FN-coated surfaces have been observed to inhibit the formation of calcium noduli in VIC cultures, which hints at multimodal anti-degenerative potential of FN [57].

While there is some evidence that FN might be useful as coating substance for vascular polymer grafts, neither the stability nor the effect of FN surface coating of decellularized implants has been examined. In particular, there have been no reports on FN treatment of aortic valve grafts.

1.7 **Degeneration of decellularized grafts**

Besides optimization of the initial biocompatibility of the implants, their durability in the long term is decisive to avoid graft failure requiring redo replacement procedures. Therefore, protective *in vitro* treatment of the implant or systemic anti-degenerative therapy in the recipient should be considered. Statins, inhibitors of the HMG-CoA reductase, are known to beneficially influence the course of atherosclerosis due to their lipid-lowering and pleiotropic effects. As a consequence, they have been implemented in the first line therapy of coronary artery disease.

On the contrary, their influence on the calcification of the native aortic valve is controversially discussed [58,59], and there is even less evidence on the role of statins in preserving biological heart valve grafts *in vivo* [60].

Neither experimental nor clinical data on the effect of statins on the deterioration of decellularized cardiovascular implants have been published before.

1.8 **Animal models to study the *in vivo* fate of cardiovascular grafts**

In order to study the above introduced aspects of biocompatibility and *in vivo* degeneration of cardiovascular implants as well as to comparatively examine different intervention techniques to optimize the graft durability, the development of a suitable small animal implantation model is necessary. While large animal models are advantageous when evaluating the hemodynamic performance of cardiovascular implants, rodent models allow for examination and comparison of basic principles of engineering grafts. In rodents, larger numbers of different groups and animals per group can be tested, in terms of ethical as well as technical and economic considerations. Additionally, the repertoire of available disease models as well as established readout methods, as e.g. antibody-based immunohistology or protein analysis, is relevantly more expanded in rodents than in large animals. Thus, rodent models seem to be most desirable for comparative *in vivo* testing of different tissue-engineered implants.

Aiming to allow for the examination of graft degeneration *in vivo* within short observation periods, a reliable well characterized model of accelerated cardiovascular calcification has to be also implemented. Knockout models mimicking degenerative cardiovascular diseases are frequently associated with high project costs, low animal robustness, and the limitation that a combination with other disease models might require time- and resource-consuming breeding of double knockout animals. Diet-based accelerated cardiovascular calcification would provide a flexible model that could be applied to different strains or existing disease models. Since mice aortic valves are very small, which would impair aortic valve graft implantation and later readout, and rabbit experiments would result in e.g. higher costs, larger housing space and reduced availability of established readout methods, the species rat seems to be a well-balanced choice.

Increased levels of VD, cholesterol (CH) and PH are associated with cardiovascular calcification and have been shown to enhance tissue sclerosis in rat arteries as well as in rabbit aortic valves [61-63]. All these components can be added as rodent diet supplements at high dosage without producing extensive costs. The effect of VD, CH

and PH on the degeneration of rat aortic valves, or even rat aortic valve grafts, has not been described before.

Combining an animal model of systemic implantation of cardiovascular implants with a model of accelerated cardiovascular calcification would provide a worthwhile platform to comparatively examine biocompatibility and *in vivo* degeneration of biological and tissue-engineered aortic valve and vessel grafts within short time periods.

2 Specific aims of the present study

I-a) To develop a standardized functional *in vivo* model of aortic conduit implantation into the systemic circulation of rats

I-b) To develop and characterize a diet-based model of accelerated cardiovascular calcification in rats

In these models, the following questions should be investigated:

II) Does decellularization diminish the *in vivo* degeneration of aortic conduit grafts?

III) Does FN surface coating improve the biocompatibility of aortic conduit implants?

IV) Does systemic statin treatment influence the prosthesis deterioration *in vivo*?

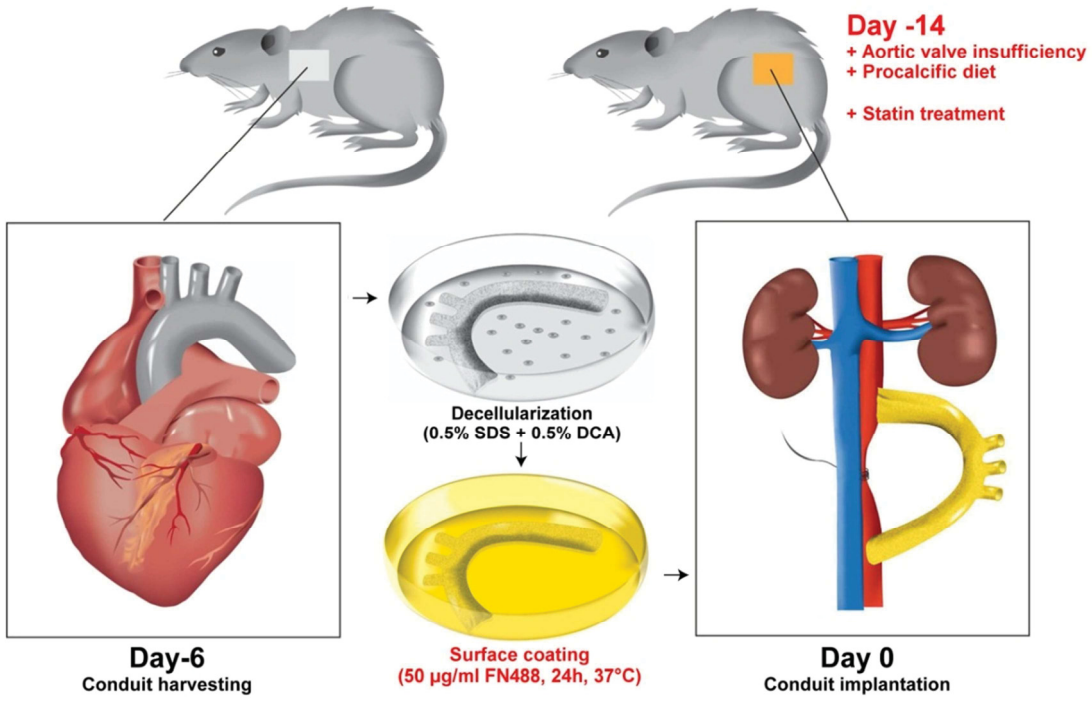

Figure 1: Overview of the rat aortic conduit implantation model. Grafts were harvested at day-6, detergent-decellularized and infrarenally implanted into the systemic circulation of recipient rats at day0. Depending on the project (red text), conduits were surface-coated with FN before implantation, or the recipients underwent aortic valve insufficiency generation at day-14 with simultaneous onset of pro-calcific diet and systemic statin treatment as indicated. SDS, sodium dodecyl sulfate; DCA, deoxycholic acid [adapted from Assmann et al. *Biomaterials* 2013].

3 Own projects

The following sections present and briefly comment on the main results of each project only, while detailed description and discussion of the findings are subject to the underlying original articles which are attached at the end of each corresponding section.

3.1 Development and optimization of the animal model

3.1.1 Aortic conduit implantation

***Assmann A**, Akhyari P, Delfs C, Flögel U, Jacoby C, Kamiya H, Lichtenberg A. Development of a growing rat model for the in vivo assessment of engineered aortic conduits. **J Surg Res**. 2012; 176:367-375.*

The first aim was to develop a standardized functional *in vivo* model of aortic conduit implantation into the systemic circulation of rats.

Based on previous reports on end-to-side anastomoses or interposition models of heterotopic graft implantation in rats [37,44,64], we chose to implant U-shaped decellularized aortic conduits with end-to-side anastomoses to the infrarenal aorta. This approach allows for coping with size mismatching which regularly occurs when grafts from the thoracic aorta with large diameters are sutured to the smaller abdominal aorta. Moreover, a larger implant size can be selected as compared to interposition models which require short straight graft segments. Thereby, more prosthesis material is available to be examined for the readout.

Unimpaired perfusion of the implants as well as of the downstream vasculature without signs of thromboembolism was shown by Doppler sonography at days 0 and 56, magnetic resonance imaging at day 5 and vascular plastination *post mortem* at day 56. In contrast to previous reports on implantation models, our study on developing the surgical model proved this approach to be safe and feasible even in young rats weighing 70-80 g, which allows for examining the implant fate also in growing organisms. This aspect is of particular interest since decellularized valve prostheses have been reported to carry the potential to grow with the recipient [38].

Journal of Surgical Research **176,** 367–375 (2012)
doi:10.1016/j.jss.2011.10.009

Development of a Growing Rat Model for the *In Vivo* Assessment of Engineered Aortic Conduits

Alexander Assmann, M.D.,* Payam Akhyari, M.D.,*,[1] Christofer Delfs,* Ulrich Flögel, Ph.D.,† Christoph Jacoby, Ph.D.,† Hiroyuki Kamiya, M.D., Ph.D.,* and Artur Lichtenberg, M.D., Ph.D.*

**Clinic for Cardiovascular Surgery, Heinrich Heine University Medical School, Duesseldorf, Germany; and †Department of Cardiovascular Physiology, Heinrich Heine University Medical School, Duesseldorf, Germany*

Originally submitted July 26, 2011; accepted for publication October 12, 2011

Background. **Numerous limitations of aortic valve grafts currently used in pediatric patients cause the need for alternative prostheses. For the purpose of *in vivo* evaluation of novel engineered aortic conduit grafts, we aimed at downsizing a previously described model to create a growing rodent model.**

Materials and Methods. **U-shaped aortic conduits were sutured to the infrarenal aorta of young Wistar rats (70–80 g, $n = 10$) in an end-to-side manner. Functional assessment was performed by Doppler sonography and high resolution rodent MRI. Histology and immunohistochemistry followed after 8 wk.**

Results. **Postoperative recovery rate was 80%. Conforming to clinical observations, postoperative MRI (d 5) and Doppler sonography (wk 8) revealed unimpaired conduit perfusion. Explanted implants were luminally completely covered by an endothelial cell layer with local hyperplasia and accumulation of α-smooth muscle actin (+) cells. Moreover microcalcification of the decellularized scaffolds was observed.**

Conclusions. **Our downsized model of aortic conduit transplantation enables overall characterization with detailed analysis of maturation of engineered aortic grafts in a growing organism.**

Key Words: **tissue engineering; aortic conduit transplantation; growing rat model; magnetic resonance imaging; cardiovascular degeneration.**

INTRODUCTION

Implantation of aortic valve allografts is a standard procedure in modern cardiac surgery with good long-term results in adults [1, 2]. However, depending on the expected lifespan of each individual patient, a final implant failure is inevitable, which is all the more noteworthy in children. Moreover, development of allograft failure in pediatric patients occurs much more rapidly than in adults [3, 4]. Adaptive immunity is accused of causing accelerated implant failure in both animals [5, 6] and humans [7], especially after pediatric cardiac surgery [8–10]. Since this type of immune response is primarily dependent on the recognition of major cell bound antigens, e.g., human leukocyte antigens in case of allografts [11] or α-Gal-epitopes in case of xenografts, preoperative decellularization of the prosthesis is a promising option to reduce the rate of degenerative events [12]. Tissue-engineered pulmonary valves have been successfully used in preclinical [13] and clinical [14] settings and aortic valve grafts were implanted in juvenile sheep revealing encouraging short-term function and integrity [15]. Following the implantation of decellularized porcine heart valves ("SYNERGRAFT") in pediatric patients, serious calcification and early failure have been reported [16], which have been related to an inflammatory response and thrombogenesis [17]. Different results in view of implant immunogenicity may be partially attributed to different decellularization protocols [18]. In a very recent report, the clinical feasibility and safety of decellularization as a method of improvement of aortic heart valve prostheses has been demonstrated [19]. However, crucial questions concerning the maturation of decellularized heart valve prostheses remain unresolved. The molecular mechanisms underlying the diverse *in vivo* development of tissue-engineered heart valve grafts, including the triggers for degeneration, are not fully understood. Furthermore, technical details of implantation and potential

[1] To whom correspondence and reprint requests should be addressed at Clinic for Cardiovascular Surgery, Heinrich Heine University Medical School, Moorenstr. 5, D – 40225 Duesseldorf, Germany. E-mail: payam.akhyari@med.uni-duesseldorf.de.

0022-4804/$36.00

pharmacologic means capable of limiting these adverse effects and thus improving graft patency need to be elucidated. For that reason, *in vivo* models in well characterized small animals are worthwhile tools.

Preoperative decellularization of aortic conduits has been reported as a measure not only to diminish the recipient immune response, but also to decrease the rate of retrovalvular thrombus formation in adult rats [20, 21]. To study the fate of aortic valve grafts *in vivo*, different rat models of heterotopic aortic valve interposition [20, 22] as well as an end-to-side transplantation model [21, 23] have been described previously. In all existing reports, a functional *in vivo* assessment of graft patency was at best performed by echocardiography.

In order to observe the *in vivo* maturation processes of implanted decellularized aortic conduits, in particular those related to the immune response and thrombogenesis of the grafts, we aimed for developing a growing rodent model (Fig. 1), that mimics the setting in pediatric cardiac surgery. Functional evaluation should be enabled by the use of small rodent magnetic resonance imaging (MRI).

MATERIALS AND METHODS

Animals

Wistar rats (donors: 200–250 g; recipients: 70–80 g) (Fig. 2A) were purchased from the in-house breed of the local animal care facility and fed ad libitum. All experiments were approved by the state animal care committee and conducted according to the national animal welfare act.

Donor Graft Harvesting

Donor animals were euthanized by CO_2 insufflation. After thoracotomy, the heart and the thoracic aorta were dissected from surrounding tissue and explanted en bloc, followed by thorough antegrade as well as retrograde rinsing with phosphate buffered saline (PBS) + 12.5 IU/mL Heparin. Using a stereomicroscope (Nikon, Duesseldorf, Germany) at 7-fold to 10-fold magnification, a U-shaped aortic conduit with a small myocardial cuff was prepared (Fig. 2B). The coronary arteries and the left subclavian and common carotid artery were ligated by 8-0 monofilament, nonabsorbable polypropylene sutures (Ethicon, Norderstedt, Germany).

Graft Engineering

Aortic conduits were decellularized following a detergent-based protocol consisting of 4 cycles of 12 h with 0.5% sodium dodecyl sulfate + 0.5% deoxycholate, 24 h rinsing with distilled water and 3 cycles of 24 h with PBS + 1% penicillin/streptomycin, in the presence of sodium azide (0.05%; Sigma-Aldrich, Taufkirchen, Germany) (Fig. 2C).

Graft Implantation Procedure

Infrarenal aortic conduit implantation was performed as a modified variant of the size-matching procedure previously described [23]. Young recipient rats ($n = 10$) were intubated, anesthetized with 2.0%–2.5% isoflurane, and a central venous jugular vein catheter was inserted. All animals underwent median laparotomy, lateralization of intestines, and dissection of the infrarenal aorta from the inferior vena cava. After systemic administration of 300 IU/kg heparin and aortic clamping, a U-shaped, decellularized aortic conduit was sutured to the infrarenal aorta in an end-to-side manner (Fig. 2D), using a 10-0 monofilament, nonabsorbable polypropylene suture (Ethicon, Norderstedt, Germany). Intermittent reperfusion was used to keep limb ischemia times below 30 min. Following release of blood flow through the conduit, the native aorta between the two anastomoses was ligated to improve perfusion of the implant (Fig. 3). After clinical observation over a reperfusion period of at least 10 min, particularly paying attention to the perfusion of the lower extremities, the abdomen was closed, and recipients were allowed to recover from anesthesia.

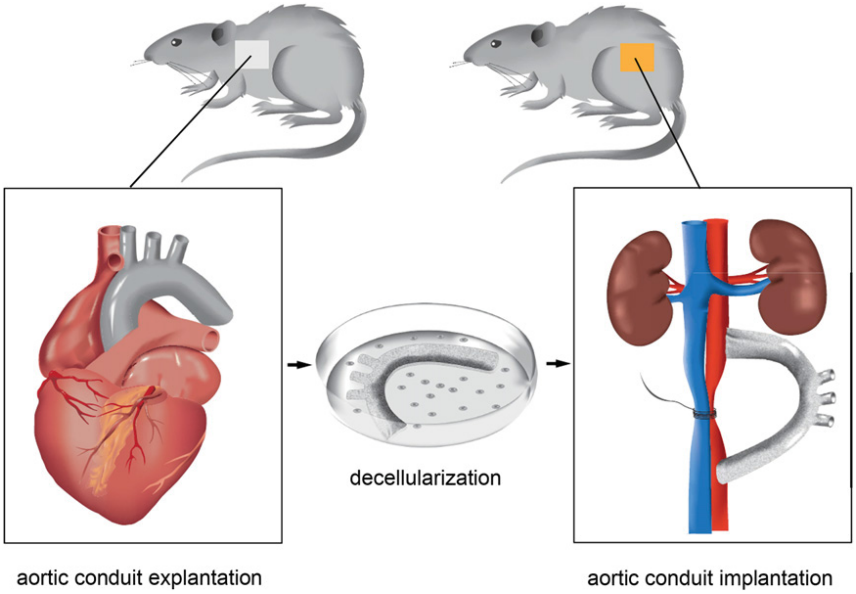

FIG. 1. Experimental design of decellularized aortic conduit transplantations. (Color version of figure is available online.)

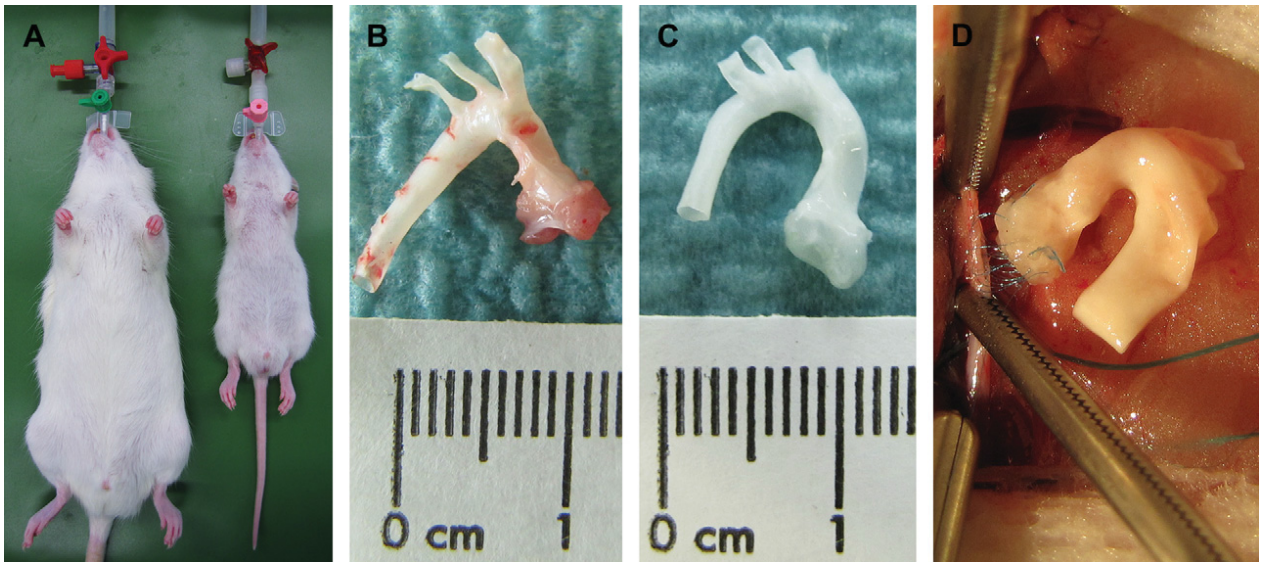

FIG. 2. Donor (A, left) and recipient rat (A, right), native explanted aortic conduit (B), decellularized aortic conduit (C), and proximal anastomosis during the implant procedure (D). (Color version of figure is available online.)

Functional Implant Evaluation

On d 5 after implantation, a functional assessment of the conduit perfusion was conducted by small rodent MRI. Experiments were carried out on a vertical Bruker DRX 9.4 Tesla WB NMR spectrometer operating at 400.13 MHz using a microimaging unit (Mini 0.5, Bruker, Ettlingen, Germany) equipped with an actively shielded 57-mm gradient set (capable of 200 mT/m maximum gradient strength and 110 μs rise time at 100% gradient switching) and a 38-mm birdcage resonator. Rats were anesthetized with isoflurane (1.5%) and kept at 37°C. Images were acquired using a fast gradient echo sequence with a flip angle $> 75°$, echo time 2.2 ms, and a repetition rate of about 40 ms. The resulting in-plane resolution was 160×160 μm^2 (field of view 40×40 mm^2, 256×256 matrix, 1 mm slice thickness).

Immediately after the implantation and at 8 wk, a Doppler sonography evaluation of the implant was conducted with a Philips HDX11 ultrasonography system equipped with a 15 MHz probe.

Perfusion of the aortic conduit and the distal arterial vasculature were displayed by intra-arterial administration of red plastic adhesive ($n = 2$).

Explantation and Tissue Analysis

Eight weeks after implantation, rats underwent laparotomy in general anesthesia and the proximal abdominal aorta was canulated to rinse the conduit with heparinized PBS solution (12.5 IU/mL Heparin in PBS).

In two rats, the visualization of the vascular system was achieved by injection of a red colored polymerizing solution (plastic adhesive Acrifix 190 + Acrifix CO 3075 red; ThyssenKrupp Plastics, Cologne, Germany). After 30 min, the lower body of the rat was cut off, skinned and transferred into 25% KOH solution (24 h at 50°C). Finally the preparation was air-dried.

In all other rats the aortic conduits were excised with adjacent recipient tissue and further processed for histology ($n = 3$) and immunohistochemistry ($n = 3$).

Histology

Explanted tissue blocks were fixated in buffered formalin solution for 24 h, dehydrated in a series of solutions with increasing alcohol concentrations, and paraffin embedded according to standard protocols. Sections of 4 μm thickness were stained with hematoxylin/eosin, von Kossa and Movat's pentachrome as previously described [13].

Immunohistochemistry

For cryo-embedding, tissue blocks were rinsed in PBS, embedded in TissueTek mounting medium (Sakura Finetek, Alphen aan den Rijn, The Netherlands) at −20°C and cut into 4 μm cryosections, using a cryostat CM 1950 (Applied Biosystems, Darmstadt, Germany). Further processing was immediately carried out by 10 min of fixation with 4% paraformaldehyde, followed by 1 h incubation with 5% bovine serum albumin at room temperature (RT). Incubation with primary antibodies (anti-von Willebrand factor (vWF); DAKO, Hamburg, Germany; anti-α-smooth muscle actin (SMA); Sigma-Aldrich, Taufkirchen, Germany; anti-CD3; Sigma-Aldrich, Taufkirchen, Germany; anti-CD68; Abcam, Cambridge, UK) lasted 1 h at 37°C. Secondary antibodies linked to fluorophores (Alexa 488, Alexa 546; both from

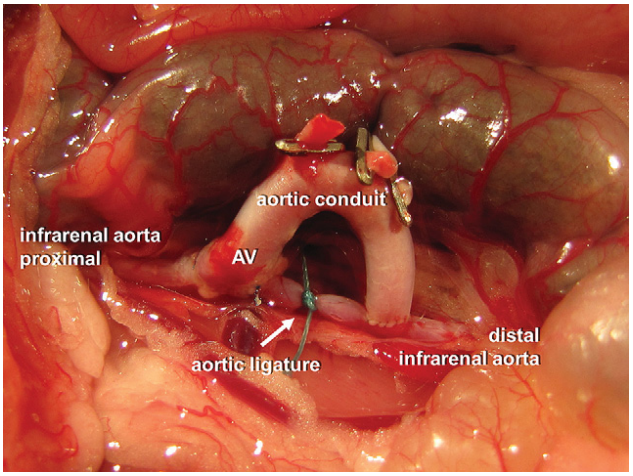

FIG. 3. Representative photograph of a transplanted aortic conduit after release of blood flow. (AV = aortic valve of the conduit). (Color version of figure is available online.)

Invitrogen, Carlsbad, CA; Cy3, Sigma-Aldrich, Taufkirchen, Germany) were utilized for 45 min in a dark and humid chamber at 37°C. Sections were covered with Vectashield mounting medium containing DAPI (Vector Labs, Peterborough, UK), and image acquisition was performed using a microscope system DM2000, equipped with a digital camera DFC 425C (Leica, Wetzlar, Germany), with Leica Application Suite ver. 3.7 software.

RESULTS

Operative Outcome

The mean graft harvesting time was 14.3 ± 2.6 min, while graft implantation cut-suture time was 93.7 ± 16.6 min and single infrarenal aortic clamping times ranging from 9 to 28 min (19.2 ± 5.7 min). As a consequence of the technical demands of the implantation of decellularized grafts, a learning curve of 10 initial animals was experienced, in which seven animals did not survive the procedure due to bleeding ($n = 2$), paraplegia ($n = 2$), or ischemic lower limbs ($n = 3$). Improving the procedure decreased the operative mortality rate from 70% to 20% in our hereby presented study group ($n = 10$). Here, one rat died of excessive intraoperative bleeding and the other one due to lower limb ischemia. At the end of the surgical procedure, clinical observation revealed sufficient perfusion of the lower limbs in all surviving animals ($n = 8$). Eight weeks after surgery, no adverse events had occurred and the body weight had increased adequately from 75 ± 4 g to 221 ± 22 g. Untreated, age- and gender-matched peers of the same in-house strain weighed 77 ± 3 g and 230 ± 27 g, respectively (five randomly chosen rats were weighed).

Functional Transplant Evaluation

On d 5, MRI analyses confirmed unrestricted aortic blood flow via the implanted conduit (Fig. 4). Doppler sonography on d 0 and d 56 revealed unimpaired conduit perfusion (Fig. 5). Red plastic adhesive preparations after 8 wks confirmed patency of the implants and showed no signs of peripheral arterial thrombosis or embolism (Fig. 6).

Histology and Immunohistochemistry

Histologic assessment after 8 wk showed a predominantly cell-free tunica media of the decellularized aortic conduits (Fig. 7). Eight weeks after transplantation, a continuous *de novo* repopulation on the luminal side of the conduits was observed. While in most parts of the conduit there were cells with an endothelial phenotype (Fig. 7A and C), in some regions a pronounced hyperplasia (Fig. 7B and D) occurred. However, the structural integrity of the collagen and elastic fibers was maintained on the histologic level (Fig. 7C and D). After 8 wk *in vivo*, von Kossa staining showed microcalcification in the tunica media and in the tunica adventitia of the decellularized implants, but not in the neointimal layer (Fig. 8).

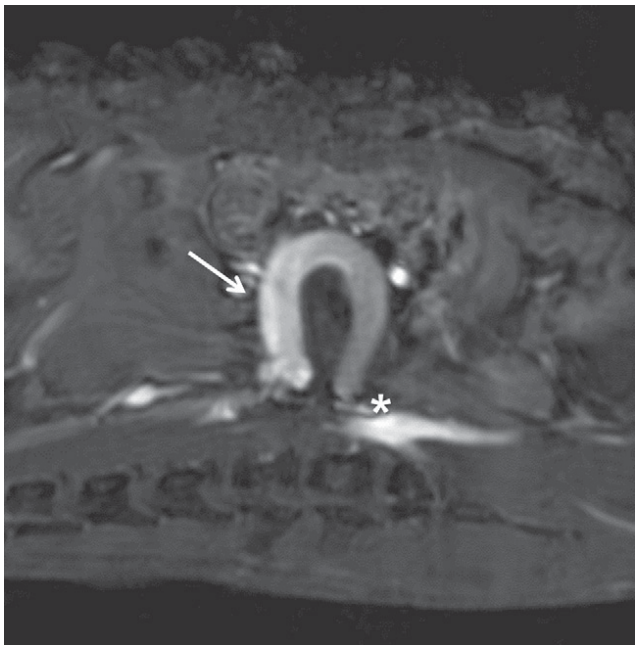

FIG. 4. Sagittal gradient echo MR image (field of view 40 × 40 mm^2; slice thickness 1 mm) showing unrestricted flow through the aortic conduit implant (arrow = proximal aortic conduit; asterisk = distal native aorta) 5 d after surgery.

Staining against vWF revealed a continuous band on the luminal surface of the aortic conduits (Fig. 9A) indicating an endothelial lining. In areas of hyperplastic recellularization, most invaded cells were positive for SMA (Fig. 9B). Moreover, CD3 staining of explants resulted in ubiquitarily negative and CD68 staining in predominantly negative results (Fig. 9C).

Due to thrombus formation in the aortic sinuses, all aortic valves of the transplants were retracted to the aortic wall and a specific examination of the valvular cusp tissue became mostly impossible. In some areas, distinguishing the cusp tissue from the thrombus material and the implant sinus tissue was attempted, however, at the current time, the resulting data do not allow for a robust and detailed analysis. Thus, an extensive histologic analysis with focus on the cusp tissue was not performed.

DISCUSSION

Biological aortic valve grafts (chemically fixed xenografts) are routinely used in cardiac surgery with an increasing trend because of the omission of lifelong anticoagulation and the favourably lower rate of thromboembolic events compared with mechanical prostheses. Yet the major limitation of these implants is

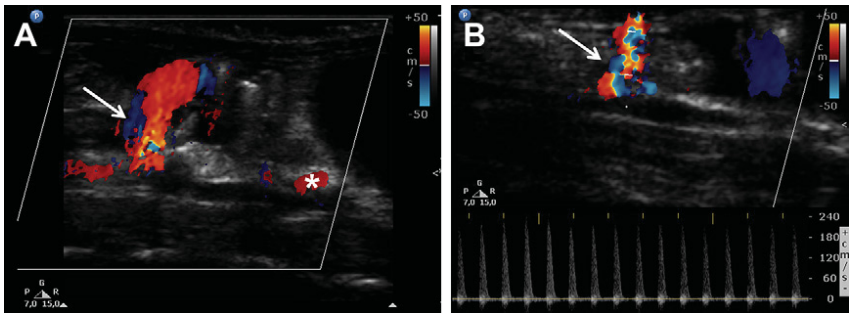

FIG. 5. Color (A) and pulse wave (B) Doppler sonography of aortic conduits 8 wk after infrarenal implantation (arrows = proximal aortic conduit; asterisk = distal native aorta). (Color version of figure is available online.)

a progressive degeneration, which is reported for both, cryopreserved allografts (so called 'homografts') as well as for xenografts during the long-term follow-up [2, 24–26]. While freedom from reoperation for structural deterioration of aortic allografts seems to be rather acceptable for follow-up times of up to 15 y in adults (85% for 21–40 y-old patients, 81% for patients with 41–60 y, and 94% for patients > 60 years at the time of operation), results in children and adolescents (0–20 y) are disappointing (47% freedom from reoperation after 15 y) [27], particularly for an implantation during the first 3 y of life [3, 4]. As a consequence, improving the long-term performance of aortic valve grafts should be particularly addressed in the context of pediatric cardiac surgery, as the presently available solutions in children may not fulfil the requirements of a lifelong lasting functional heart valve to the same degree as it can be observed in the case of biological grafts implanted in the majority of adults. Therefore, we developed a small animal model, which allows for studying the mechanisms underlying graft deterioration in a growing organism.

Surgical Aspects of the Model

Simulating the clinical setting for children with aortic allografts originating from adult donors, we transplanted aortic conduits obtained from rats weighing 200–250 g into rats weighing 70–80 g. As this technique is accompanied by a relevant size mismatch, our surgical approach was based on a model involving end-to-side anastomoses of U-shaped aortic conduits, a method first described by Oei *et al*. [23], which allowed for coping with the present mismatch. Thus this technique was preferred over to the alternative approach of an end-to-end interposition [20, 22].

Lethality of 70% in the first 10 animals reflected the complexity of the microsurgical model presented here. Yet having passed this learning curve, a reduction of mortality to 20% confirmed the feasibility of the method after an appropriate pilot phase. Eight weeks after transplantation, the plastination of the lower body arterial system proved not only unimpaired perfusion of the implanted conduit, but also the absence of relevant local thrombosis or distal embolism. We regard this particular finding as an evidence for the effectiveness of the intraoperative anticoagulation.

Functional Transplant Evaluation

To the best of the authors' knowledge, the study presented here is the first one in which a functional evaluation of infrarenally grafted aortic conduits was performed using MRI-based imaging modalities. Although the resolution of the examined structures was excellent, the projection of the perfusion along the entire conduit and the adjacent aortic up- as well as downstream segments in one single image was considerably demanding. This is related to the shift of the blood flow direction and the occurrence of turbulent flow patterns, particularly due to the end-to-side anastomoses, which impeded an unproblematic capture of the blood flow.

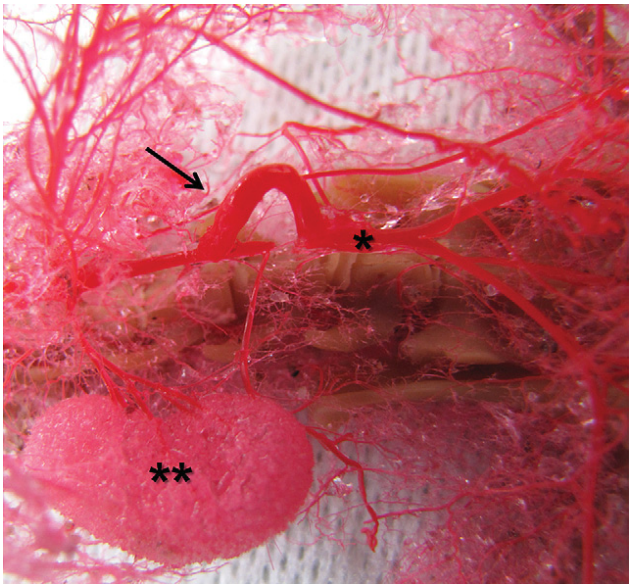

FIG. 6. Photograph of a plastination of a lower rat body arterial system (arrow = proximal aortic conduit; single asterisk = distal native aorta; double asterisk = kidney vasculature). (Color version of figure is available online.)

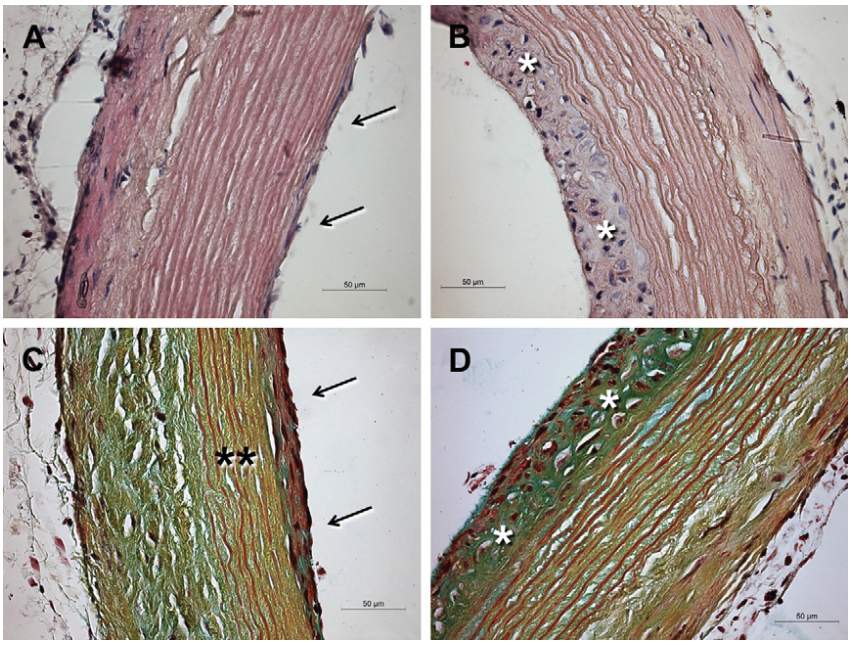

FIG. 7. Hematoxylin/eosin (A) and (B) and Movat's pentachrome (C) and (D) staining of decellularized aortic conduits 8 wk after implantation revealed a confluent luminal cell layer (arrows in A and C), partially accompanied by a local intimal hyperplasia (single asterisks in B and D), as well as no cell remnants in the tunica media and preserved structure of collagen and elastic fibers (double asterisk in C). (Color version of figure is available online.)

Nevertheless, an unimpaired perfusion via the conduits could be demonstrated. In this context, the excellent early results were additionally confirmed by Doppler sonography measurements conducted with a 15 MHz ultrasound probe. However, establishing the MRI application in our small animal model may enable us to perform repeated *in vivo* observation studies of the morphologic graft maturation. Moreover, using novel contrast dye enhanced MRI imaging techniques, for the first time a noninvasive detection of early graft rejection in small animals may become feasible, as very recently demonstrated by MRI-based measurement of (19) F uptake in rodent cardiac transplant recipients [28]. In an upcoming study, we plan to perform a similar combination of methods during the follow-up, where in the early post-implantation phase a MRI-based detection of inflammatory response in the region of the implant may become feasible, whereas functional data, e.g., graft patency, flow direction reversal during diastole and velocity measurements are planned to be determined by US in later stages of the study.

Naturally derived extracellular matrix scaffolds have been demonstrated to carry the properties to grow along with the somatic growth of the recipient organism [15]. Although our growing model discloses transplant growth, we did not observe an increase of graft diameters during the study follow up period of 8 wk. This may be related to the size-mismatch at implant time, which avoided the occurrence of graft growth. However, at the same time, the absence of a dilatative degeneration speaks in favor of the employed implants.

Structural Maturation and Repopulation of the Implants

Histological staining of re-explanted aortic conduits revealed conserved structure and integrity of collagen and elastic fibres in the tunica media. Therefore, it can be supposed that the chosen graft engineering protocol guarantees sufficient preservation of the extracellular matrix.

Cellular repopulation of decellularized tissues has been performed under defined *in vitro* conditions [29–31]. Yet it remains unclear whether preoperative *in vitro* cell reseeding or postoperative *in vivo*

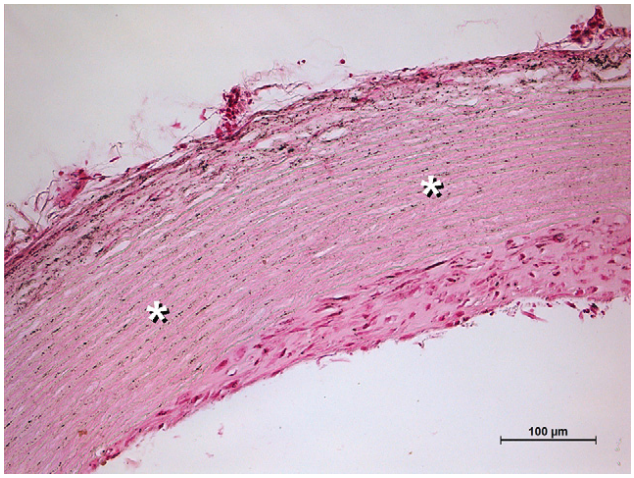

FIG. 8. Microcalcification in the tunica media (asterisks) and the tunica adventitia of decellularized aortic conduits, 8 wk after implantation (von Kossa staining). (Color version of figure is available online.)

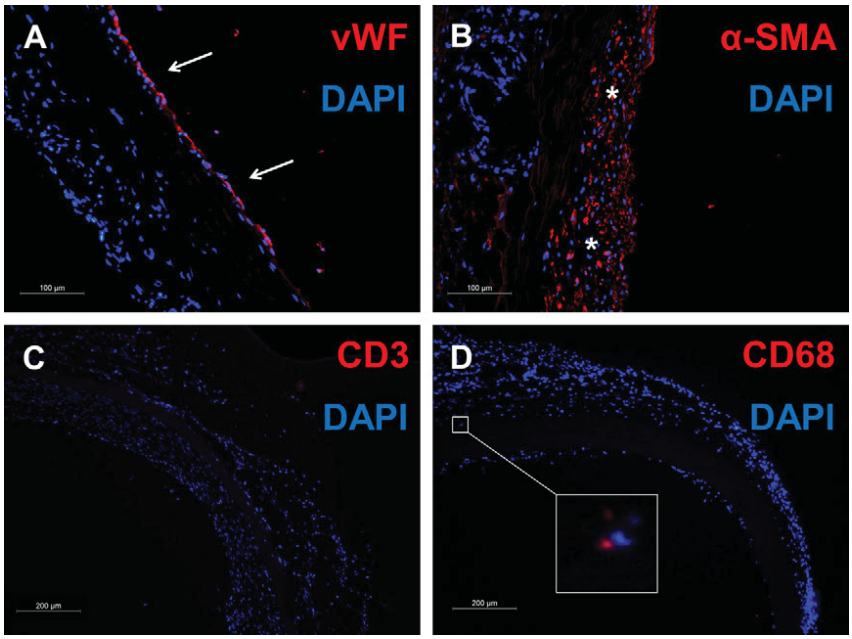

FIG. 9. Immunohistochemical staining against von Willebrand factor (VWF) (arrows in A) and α-smooth muscle actin (αSMA) (asterisks in B) on the luminal surface of decellularized aortic conduits, as well as against CD3 (C), and CD68 (D) after 8 wk *in vivo*. (Color version of figure is available online.)

migration of autologous cells into the graft tissue results in better tissue formation. The present model is suitable to examine graft integration and the process of *in vivo* recellularization. In our experiments, after 8 wk of *in vivo* perfusion, the luminal surface of decellularized rat aortic conduits was completely covered with cell layers. Besides neoendothelialized parts, we observed areas of intimal hyperplasia with SMA-positive cells. Differentiated myofibroblasts, which typically express SMA, are known to occur at sites of connective tissue proliferation and wound healing. These cells support the *de novo* generation of extracellular matrix and are capable of contracting granulation tissue [32]. The occurrence of neointimal hyperplasia with SMA-positive cells is in line with the results from many other groups, including a study involving decellularized canine vein allografts, which were implanted for 8 wk *in vivo* [33], as well as findings related to tissue-engineered pulmonary valves in a sheep model previously reported by our group [13]. The origin of these cells is not clearly elucidated. However, myofibroblasts have been shown to derive from CD34-positive mesenchymal progenitor cells, circulating in the peripheral blood, as well as from resident fibroblasts, fibrocytes, endothelial, or also smooth muscle cells [34, 35]. Eight weeks after transplantation of decellularized aortic conduits in our rat model, the whole intimal surface was covered with SMA-positive cells. Therefore, it is difficult to decide whether the neoepithelial cells had grown from the anastomotic regions towards the aortic arch of the conduit, or whether they originated from the peripheral blood and ubiquitarily attached to the surface. To this point, the almost cell-free region of the implant-media suggests that the mechanism of trans-implant migration appears as rather unlikely to explain for the neo-intimal formation. Further experiments with shorter observation periods are necessary to clarify this question.

Endothelial vWF is reported to augment platelet adhesion after endothelial injury favoring the development of atherosclerosis [36]. Whether this also holds true for the continuous luminal vWF observed in aortic conduit re-explants remains to be elucidated.

It is remarkable that after 8 wk, the luminal surface of the implanted conduits was completely neoendothelialized, while the aortic media showed only detached nuclei. This observation conforms to previous implantation studies of decellularized rat aortic prostheses, where the amount of cells repopulating the medial aortic layer was reported to be sparse [37] or even not existing [21]. We speculate that the preserved layered architecture of the aortic grafts with the pronounced proportion of intact collagen layers substantially inhibits a migration of recipient interstitial cells into the media region.

Eight weeks after implantation, there was no sign of relevant inflammatory activity in the conduit implant, which may point to a diminished inflammatory response against decellularized grafts as compared to cellular allografts. These findings are in agreement with published data of significantly decreased inflammatory infiltration of decellularized aortic conduit implants as compared to non-decellularized controls, 4 wk after

implantation [20]. Further detailed studies are necessary to confirm that hypothesis and elucidate the time course of implant inflammation.

A limitation of our study is the loss of aortic valve functionality that was caused by retro-semilunar thrombus formation. The finding, that the loss of an intact endothelial barrier in decellularized aortic conduits may represent a thrombogenic factor, is consistent with observations in previous rat transplantation studies [20, 21]. In large animal models, sinus thrombus formation does not seem to play such a crucial role [13, 38], which may be a consequence of the orthotopic implantation with predominantly physiologic hemodynamics in these models. In contrast, all rodent studies that have been published so far were conducted by heterotopic implantation, so that the blood flow profile was significantly affected, and may have supported the formation of thrombotic structures.

Another aspect of graft degeneration is the microcalcification, which was observed in all parts of the decellularized scaffolds after 8 wk *in vivo*. Several studies reported signs of moderate calcification in the wall of decellularized sheep pulmonary artery alloimplants [39] and pulmonary homografts [40], as well as in decellularized porcine heart valve xenografts [16]. Intramural deposition of calcium may be related to extracellular matrix components, cell remnants, or the decellularization protocol. Therefore, more detailed and comparative *in vivo* analyses of these potential causes should be conducted.

CONCLUSIONS

In the present study we developed a rat model, with which the *in vivo* fate of decellularized aortic conduits can be examined in a growing organism. This model allows us to study the mechanisms of autologous *in vivo* recellularization, the growth potential of the graft, and the immune as well as the inflammatory response of the recipient to the implants. Due to downsizing of the model, rodent MRI analyses become feasible and extend the spectrum of methods available for a functional evaluation by an observer-independent technique.

After 8 wk of *in vivo* perfusion, aortic conduit transplants were continuously neo-endothelialized, but local intimal hyperplasia and microcalcification were also observed. Further studies are necessary to test graft treatment options, which may reduce hyperplastic tissue formation and implant microcalcification for a sustained graft function *in vivo*.

REFERENCES

1. Ross DN. Evolution of the homograft valve. Ann Thorac Surg 1995;59:565.
2. O'Brien MF, Stafford EG, Gardner MA, et al. Allograft aortic valve replacement (long-term follow-up). Ann Thorac Surg 1995;60(Suppl):S65.
3. Clarke DR, Campbell DN, Hayward AR, et al. Degeneration of aortic valve allografts in young recipients. J Thorac Cardiovasc Surg 1993;105:934.
4. Yankah AC, Alexi-Meskhishvili V, Weng Y, et al. Accelerated degeneration of allografts in the first two years of life. Ann Thorac Surg 1995;60(Suppl):S71.
5. Green MK, Walsh MD, Dare A, et al. Histologic and immunohistochemical responses after aortic valve allografts in the rat. Ann Thorac Surg 1998;66(Suppl):S2160.
6. Légaré JF, Lee TD, Creaser K, et al. T lymphocytes mediate leaflet destruction and allograft aortic valve failure in rats. Ann Thorac Surg 2000;70:1238.
7. Hogan P, Duplock L, Green M, et al. Human aortic valve allografts elicit a donor-specific immune response. J Thorac Cardiovasc Surg 1996;112:1260.
8. Shaddy RE, Hunter DD, Osborn KA, et al. Prospective analysis of HLA immunogenicity of cryopreserved valved allografts used in pediatric heart surgery. Circulation 1996;94:1063.
9. Hawkins JA, Breinholt JP, Lambert LM, et al. Class I and class II anti-HLA antibodies after implantation of cryopreserved allograft material in pediatric patients. J Thorac Cardiovasc Surg 2000;119:324.
10. Vogt PR, Stallmach T, Niederhäuser U, et al. Explanted cryopreserved allografts: A morphological and immunohistochemical comparison between arterial allografts and allograft heart valves from infants and adults. Eur J Cardiothorac Surg 1999; 15:639. discussion 644.
11. Welters MJ, Oei FB, Witvliet MD, et al. A broad and strong humoral immune response to donor HLA after implantation of cryopreserved human heart valve allografts. Hum Immunol 2002; 63:1019.
12. Vesely I. Heart valve tissue engineering. Circ Res 2005;97:743.
13. Lichtenberg A, Tudorache I, Cebotari S, et al. Preclinical testing of tissue-engineered heart valves re-endothelialized under simulated physiological conditions. Circulation 2006; 114(1 Suppl):I559.
14. Cebotari S, Lichtenberg A, Tudorache I, et al. Clinical application of tissue engineered human heart valves using autologous progenitor cells. Circulation 2006;114(1 Suppl):I132.
15. Akhyari P, Kamiya H, Gwanmesia P, et al. *In vivo* functional performance and structural maturation of decellularized allogenic aortic valves in the subcoronary position. Eur J Cardiothorac Surg 2010;38:539.
16. Simon P, Kasimir MT, Seebacher G, et al. Early failure of the tissue engineered porcine heart valve SYNERGRAFT in pediatric patients. Eur J Cardiothorac Surg 2003;23:1002. discussion 1006.
17. Kasimir MT, Rieder E, Seebacher G, et al. Decellularization does not eliminate thrombogenicity and inflammatory stimulation in tissue-engineered porcine heart valves. J Heart Valve Dis 2006; 15:278. discussion 286.
18. Meyer SR, Chiu B, Churchill TA, et al. Comparison of aortic valve allograft decellularization techniques in the rat. J Biomed Mater Res A 2006;79:254.
19. da Costa FD, Costa AC, Prestes R, et al. The early and midterm function of decellularized aortic valve allografts. Ann Thorac Surg 2010;90:1854.
20. Meyer SR, Nagendran J, Desai LS, et al. Decellularization reduces the immune response to aortic valve allografts in the rat. J Thorac Cardiovasc Surg 2005;130:469.
21. Grauss RW, Hazekamp MG, van Vliet S, et al. Decellularization of rat aortic valve allografts reduces leaflet destruction and extracellular matrix remodeling. J Thorac Cardiovasc Surg 2003; 126:2003.
22. Légaré JF, Nanton MA, Bryan P, et al. Aortic valve graft implantation in rats: A new functional model. J Thorac Cardiovasc Surg 2000;120:679.

23. Oei FB, Welters MJ, Bonthuis F, et al. A size-matching heterotopic aortic valve implantation model in the rat. J Surg Res 1999;87:239.
24. Ali A, Patel A, Ali Z, et al. Medium to long-term clinical outcome following stentless aortic valve replacement: Comparison between allograft and xenograft valves. Interact Cardiovasc Thorac Surg 2010;11:166. Epub 2010 Mar 31.
25. Luciani GB, Casali G, Auriemma S, et al. Survival after stentless and stented xenograft aortic valve replacement: A concurrent, controlled trial. Ann Thorac Surg 2002;74: 1443.
26. Kirklin JK, Smith D, Novick W, et al. Long-term function of cryopreserved aortic homografts. A 10-year study. J Thorac Cardiovasc Surg 1993;106:154. discussion 165.
27. O'Brien MF, Harrocks S, Stafford EG, et al. The homograft aortic valve: A 29-year, 99.3% follow up of 1022 valve replacements. J Heart Valve Dis 2001;10:334. discussion 335.
28. Flögel U, Su S, Kreideweiss I, et al. Noninvasive detection of graft rejection by *in vivo* (19) F MRI in the early stage. J Transplant 2011;11:235. Epub 2011 Jan 7.
29. Lichtenberg A, Tudorache I, Cebotari S, et al. *In vitro* reendothelialization of detergent decellularized heart valves under simulated physiological dynamic conditions. Biomaterials 2006;27:4221. Epub 2006 Apr 18.
30. Lee DJ, Steen J, Jordan JE, et al. Endothelialization of heart valve matrix using a computer-assisted pulsatile bioreactor. Tissue Eng Part A 2009;15:807.
31. Schenke-Layland K, Opitz F, Gross M, et al. Complete dynamic repopulation of decellularized heart valves by application of defined physical signals-an *in vitro* study. Cardiovasc Res 2003; 60:497.
32. Tomasek JJ, Gabbiani G, Hinz B, et al. Myofibroblasts and mechano-regulation of connective tissue remodeling. Nat Rev Mol Cell Biol 2002;3:349.
33. Martin ND, Schaner PJ, Tulenko TN, et al. *In vivo* behavior of decellularized vein allograft. J Surg Res 2005;129:17. Epub 2005 Aug 31.
34. Li J, Sensebe L, Hervé P, et al. Nontransformed colony-derived stromal cell lines from normal human marrows. III. The maintenance of hematopoiesis from CD34+ cell populations. Exp Hematol 1997;25:582.
35. Forte A, Della Corte A, De Feo M, et al. Role of myofibroblasts in vascular remodeling: Focus on restenosis and aneurysm. Cardiovasc Res 2010;88:395. Epub 2010 Jul 8.
36. Theilmeier G, Michiels C, Spaepen E, et al. Endothelial von Willebrand factor recruits platelets to atherosclerosis-prone sites in response to hypercholesterolemia. Blood 2002;99:4486.
37. Hwang SJ, Kim SW, Choo SJ, et al. The decellularized vascular allograft as an experimental platform for developing a biocompatible small-diameter graft conduit in a rat surgical model. Yonsei Med J 2011;52:227.
38. Goldstein S, Clarke DR, Walsh SP, et al. Transpecies heart valve transplant: Advanced studies of a bioengineered xenoautograft. Ann Thorac Surg 2000;70:1962.
39. Lehr EJ, Rayat GR, Chiu B, et al. Decellularization reduces immunogenicity of sheep pulmonary artery vascular patches. J Thorac Cardiovasc Surg 2011;141:1056. Epub 2010 Jul 15.
40. Hopkins RA, Jones AL, Wolfinbarger L, et al. Decellularization reduces calcification while improving both durability and 1-year functional results of pulmonary homograft valves in juvenile sheep. J Thorac Cardiovasc Surg 2009;137:907. 913e1. Epub 2009 Feb 23.

3.1.2 **Aortic valve insufficiency in the recipient**

*Munakata H, **Assmann A**, Poudel-Bochmann B, Horstkötter K, Kamiya H, Okita Y, Lichtenberg A, Akhyari P. Aortic conduit valve-model with controlled moderate aortic regurgitation in rats: A technical modification to improve short- and long-term outcome and to increase the functional results. **Circ J**. 2013; 77:2295-2302.*

Implantation of aortic valve grafts in the infrarenal position of hemodynamically unimpaired rats resulted in restricted movement of the implant valve, since there was no diastolic pressure drop directly upstream of the implant valve. Searching for a solution to mimic the hemodynamic situation of a native aortic valve, we hypothesized that severe insufficiency of the recipient's native aortic valve would create a diastolic backflow in the whole aorta supporting adequate diastolic closing of the implant valve. Thus, aortic valve insufficiency was generated in the recipients 14 days before aortic conduit implantation. After cannulation of the right common carotid artery, the recipient's aortic valve was perforated with a guide-wire under echocardiographic control of the procedure as well as the hemodynamic result. Only insufficiencies with grade II-III were accepted for further experiments.

Postoperative Doppler analyses revealed relevant diastolic backflow in all parts of the aorta. Aortic conduits implanted 14 days later were observed to exhibit adequate functionality of the implant valve as shown by Doppler sonography. Previous studies had focused on trying to directly visualize leaflet movement in aortic valve grafts by M-mode sequences, which is quite challenging and marginally reliable in rodents. In contrast, the present pulse-wave Doppler-based approach of proving leaflet functionality by showing the disappearance of diastolic aortic backflow downstream of the implant valve is a technically easier and reliable method. Furthermore, it allows for quantifying regurgitation through the implant valve that might occur during the follow-up. Additionally, we revealed that echocardiography-controlled generation of moderate recipient aortic valve insufficiency grade II-III improved the survival of the recipients when compared to severe insufficiencies. In this context, high-quality live echocardiography is crucial to obtain optimal results.

The functionally optimized implantation model allows for comparative *in vivo* observation of valvular as well as vascular structures of biological grafts.

Circulation Journal
Official Journal of the Japanese Circulation Society
http://www.j-circ.or.jp

ORIGINAL ARTICLE
Cardiovascular Surgery

Aortic Conduit Valve Model With Controlled Moderate Aortic Regurgitation in Rats

– A Technical Modification to Improve Short- and Long-Term Outcome and to Increase the Functional Results –

Hiroshi Munakata; Alexander Assmann; Bhawana Poudel-Bochmann; Kim Horstkötter; Hiroyuki Kamiya; Yutaka Okita; Artur Lichtenberg; Payam Akhyari

Background: The objective of this study was to describe a small animal aortic conduit model that could analyze long-term conduit valve (CV) function by echocardiography.

Methods and Results: Recipient Wistar rats (200–250 g, n=20) underwent aortic leaflet injury of their native aortic valve under echocardiographic control. After 2 weeks, U-shaped decellularized CVs obtained from other rats were implanted onto the abdominal aorta. Implanted CVs were analyzed via pulsed-wave echocardiography at day 0, 4 and 12 weeks. CV stenosis was assessed as systolic flow velocity (post-pre CV)/flow velocity in the ascending aorta. CV regurgitation was assessed as the ratio of the amount of reversed diastolic flow to forward systolic flow in post-pre CV. The endpoint was set at 12 weeks. Three rats died immediately after aortic valve injury and all surviving rats received CV implantation (n=17, 85%). The survival rate after conduit implantation was 100% at 4 weeks and 88% (15/17) at 12 weeks. Regarding the CV function at 0, 4 and 12 weeks, the average observed value of CV stenosis was 3.8±7.9%, 3.1±4.1% and 14±10% (P<0.01), respectively. The average value of CV regurgitation was 0%, 12±27% and 52±43%, respectively (P<0.001).

Conclusions: By using this model, the degeneration of implanted CV could be assessed not only qualitatively, but also quantitatively. (*Circ J* 2013; **77:** 2295–2302)

Key Words: Echocardiography; Small animal model; Valves

Cardiovascular calcification remains a global health burden with unmet challenges to health-care systems globally.[1] Currently available aortic valvular prostheses and aortic valve conduits have several limitations. Mechanical valves require lifelong anticoagulation, which might cause bleeding or thromboembolic complications and bear a risk for prosthetic infection, and tissue valves are prone to progressive degeneration.[2–4] Tissue engineering might bear promising solutions for overcoming the limitations of biological and mechanical heart valve substitutes. One popular concept of heart valve tissue engineering bases itself on decellularized biological matrices. The removal of cellular components is practised to reduce immunological reactions, which are thought to be responsible for accelerated valvular graft deterioration, and for subsequent repopulation of the transplanted valves with autologous cells.

We and others have performed heart valve implantation studies in vivo using large animal models, involving decellularized valves in the pulmonary and in the aortic position.[5,6] Similarly, several groups have published results about small animal models of heterotopic aortic valve interposition,[7,8] as well as end-to-side transplantation.[9,10] However, in small animal aortic position models, the physiological function of the implanted valves remains questionable.

In order to preserve the functional hemodynamic load on a heterotopic aortic valve implant, there must be some turbulence and reversal of blood flow in the aorta that permits leaflet closure. Légaré et al[8,11] have previously reported on the experimental creation of native aortic regurgitation (AR) for allowing flow reversal in the abdominal aorta in rats. However, a major problem observed in this model is the rather high mortality rate due to cardiac failure associated with the acute AR. In addition,

Received November 21, 2012; revised manuscript received April 1, 2013; accepted April 25, 2013; released online May 29, 2013 Time for primary review: 69 days

Department of Cardiovascular Surgery and Research Group for Experimental Surgery, Heinrich Heine University, Medical Faculty, Duesseldorf (H.M., A.A., B.P.-B., K.H., H.K., A.L., P.A.), Germany; Department of Surgery, Division of Cardiovascular Surgery, Kobe University Graduate School of Medicine, Kobe (H.M., Y.O.), Japan

Mailing address: Hiroyuki Kamiya, MD, PhD, Department of Cardiovascular Surgery, Heinrich Heine University, Moorenstrasse 5, 40225 Duesseldorf, Germany. E-mail: hkamiya88@yahoo.co.jp

ISSN-1346-9843 doi:10.1253/circj.CJ-12-1439

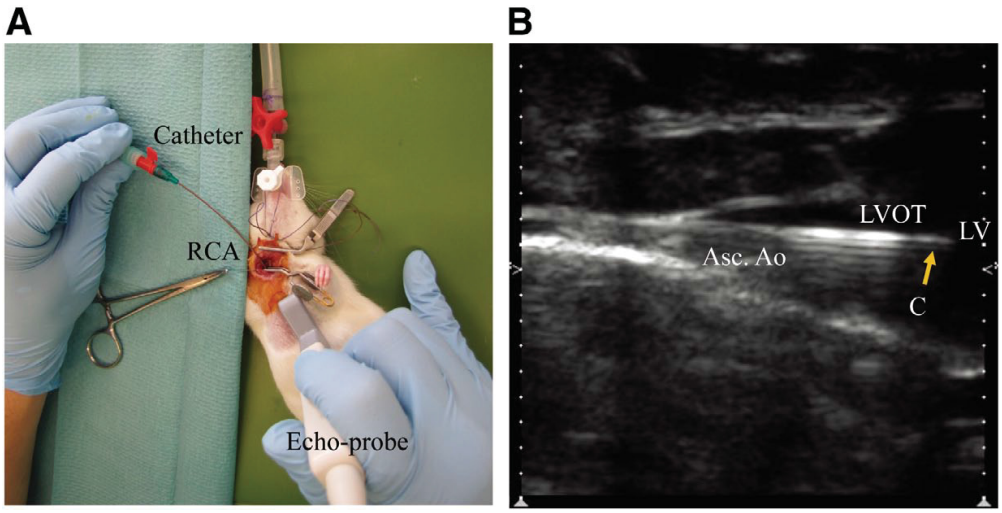

Figure 1. Creation of aortic regurgitation (AR) in recipient animals. (**A**) Picture of the creation of AR. Right hand holds the echocardiography probe and left hand controls the catheter. (**B**) Under continuous echocardiographic guidance, a catheter is advanced towards the aortic valve. The image is taken in the parasternal long-axis view. The catheter (C, arrow) has entered the left ventricle via the perforated aortic valve. RCA, right carotid artery; Echo-probe, echocardiographic probe; LV, left ventricle; LVOT, left ventricular outflow tract; Asc. Ao, ascending aorta.

according to the authors, this model did not prove a complete closure of the conduit valve (CV). Moreover, because the implanted CV is too small in these small animal models, one of the major limitations is the difficulty to perform measurements by directly targeting the CV for a quantitative analysis of the valve function, that is, as it is regularly done in the clinical field.

Considering these studies, we hypothesized that a further improvement of the described aortic conduit model with controlled AR, generated by using improved echocardiographic techniques during the operation and the follow-up time, might more soundly: (1) reduce short- and long-term mortality; (2) demonstrate a complete closure of the valve; and (3) allow for a quantitative analysis of the CV function. We tested this hypothesis using our standardized small animal aortic conduit implantation model.

Methods

Animals

Male rats (donors: Lewis, recipients: Wistar, n=20) weighing 200–250 g were purchased from the in-house breed of animals from the local animal care facility and used for the investigation. All experiments were approved by the State animal care committee and conducted according to the National Animal Welfare Act. During the whole study, all animals were fed with a procalcific diet supplemented with 300,000 U/kg vitamin D, 1.5% calcium phosphate and 2% cholesterol.

Echocardiography

The recipient rats were intubated and anesthetized with 2.0–2.5% isoflurane. Standard 2-dimensional, M-mode, color- and pulsed-wave Doppler transthoracic and transabdominal measurements were conducted with a Philips HDX11 ultrasonography system equipped with a 15 MHz transducer. Pulsed-wave Doppler recordings were taken. Left ventricular (LV) dimensions, ejection fraction (EF), ratio of AR jet width to LV outflow tract diameter (AR jet/LVOT), ratio of time-velocity integral of reversed diastolic flow to forward systolic flow (RVTI), and maximum forward systolic flow velocity (MSV) in the ascending thoracic (Asc. Ao) and the abdominal aorta (Abd. Ao) were evaluated as previously reported.[12] All images were recorded digitally for later analysis.

Creation of AR

Creation of AR was performed with a modification to a previously reported method.[13] In anesthetized animals, a right lateral neck incision was used to expose the right carotid artery. The distal common carotid artery was ligated with 4-0 nylon suture. An arteriotomy was then performed to allow the insertion of a 0.9-mm guide wire. The echocardiographic probe was positioned on the thorax to obtain a good view of the left ventricle, the aortic valve and the ascending aorta equivalent to a parasternal long-axis view in standard echocardiography in humans. Under continuous echocardiographic guidance, an arterial leader catheter (20 gauge) was advanced towards the aortic valve in a retrograde manner (**Figure 1A**). The sonographer guided the position and advancement of the catheter while it was pushed through a leaflet of the aortic valve into the left ventricle (**Figure 1B**). The resulting tear in the leaflet induced an acute AR. AR was considered moderate in the instance of following echocardiographic criteria at the time of surgery; color Doppler ratio of the regurgitation jet width to LVOT diameter was 50–70%, and pulsed-wave Doppler confirming reversed diastolic flow in the abdominal aorta.[14] Leaflet perfusion was repeated when the severity of the regurgitation jet in the abdominal aorta was considered insufficient by echocardiographic criteria (**Figures 2A**,**B**). When the generation of AR was completed, the proximal carotid artery was ligated with 4-0 nylon sutures.

Donor Graft Harvesting and Engineering

The harvesting of the donor graft was conducted as we have previously described.[15] In brief, donor rats (n=17) were euthanized by CO_2 insufflation. After thoracotomy, the heart and the

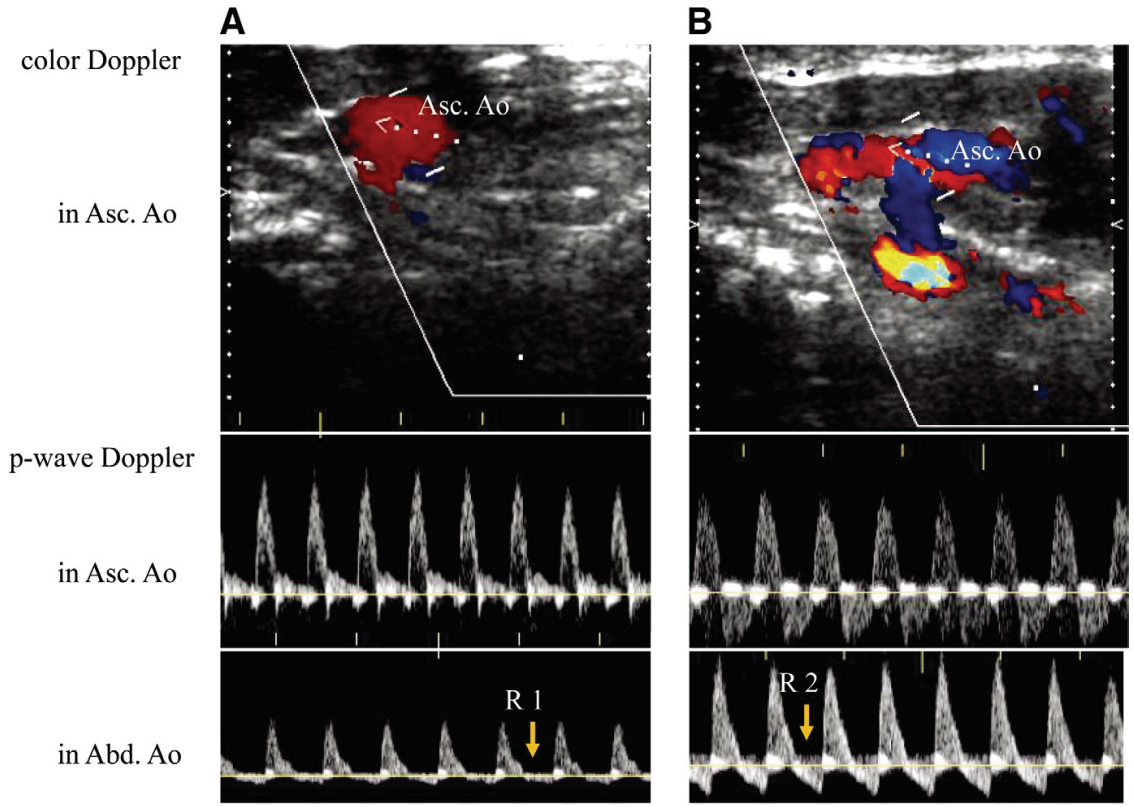

Figure 2. Control of the aortic regurgitation (AR) grade. Both images were taken during the operative generation of AR. (**Upper panel**) Color Doppler of the ascending aorta. (**Middle panel**) Pulsed-wave Doppler of the ascending aorta. (**Lower panel**) Pulsed-wave Doppler of the abdominal aorta. (**A**) After the insertion of the catheter through the left ventricular outflow tract (LVOT), the resulting tear in the leaflet induced an acute AR in the ascending aorta. But many cases did not reach moderate AR and sufficient reversed diastolic flow in the abdominal aorta by a single perforation (R1 arrow). (**B**) After repeated attempts for the creation of AR, we could confirm ample reversed diastolic flow in the abdominal aorta (R2 arrow). P-wave Doppler, pulsed-wave Doppler; Asc. Ao, ascending aorta; Abd. Ao, abdominal aorta.

thoracic aorta were dissected from surrounding tissue. Using a stereomicroscope (Nikon, Duesseldorf, Germany), a U-shaped aortic conduit with a small myocardial cuff was prepared. The coronary arteries were ligated by using a 8-0 monofilament (Ethicon, Norderstedt, Germany). Soon after the harvesting, the aortic graft conduits were decellularized according to a detergent-based protocol consisting of 4 cycles of 12 h incubation with 0.5% sodium dodecyl sulphate, 0.5% sodium deoxycholate and 0.05% (g/v) sodium azide (Sigma-Aldrich, Taufkirchen, Germany), followed by 24 h rinsing with distilled water containing 0.05% sodium azide, and 3 subsequent cycles of 24 h with PBS containing 1% penicillin/streptomycin.

Graft Implantation Procedure

Two weeks after the induction of AR, the recipient rats (n=17) were intubated, anesthetized with 2.0–2.5% isoflurane, and a central venous jugular vein catheter was inserted. The graft implantation procedure was performed as previously described.[15] All animals underwent a median laparotomy, lateralization of intestines, and dissection of the infrarenal aorta from the inferior vena cava. After systemic administration of 300 IU/kg heparin and aortic clamping, a U-shaped, decellularized aortic conduit was sutured to the infrarenal aorta in an end-to-side manner, using a 10-0 monofilament, non-absorbable polypropylene suture (Ethicon, Norderstedt, Germany). Intermittent reperfusion was used to keep limb ischemia times below 30 min. Following the release of blood flow through the conduit, the native aorta between the 2 anastomoses was ligated to improve perfusion of the implant.

Functional Evaluation of the Implant

Before recovery from the anesthesia and after completion of the implantation, the function of the implanted CV was examined by using a novel improved method by transabdominal aortic color- and pulsed-wave Doppler.[8,9] Proximally and distally to the CV position, the reversed diastolic flow color jet recording of the AR was analyzed. An intermittent disappearance of the reversed diastolic flow distal to the CV was regarded as proof for a complete diastolic closure of the valve; hence physiological function of the CV had been obtained (**Figures 3A,B Upper**). But during the follow-up times, appearance of the reversed diastolic flow distal to the CV was interpreted as a sign that the respective CV had developed a regurgitation (**Figure 3B Lower**). Therefore, we quantitatively analyzed the CV regurgitation at each follow-up time point. The CV regurgitation grade was defined as a RVTI in pre and post CV according to the following formula:

$$\text{CV regurgitation grade ratio} = \frac{(\text{RVTI in post-conduit})}{(\text{RVTI in pre-conduit})}$$

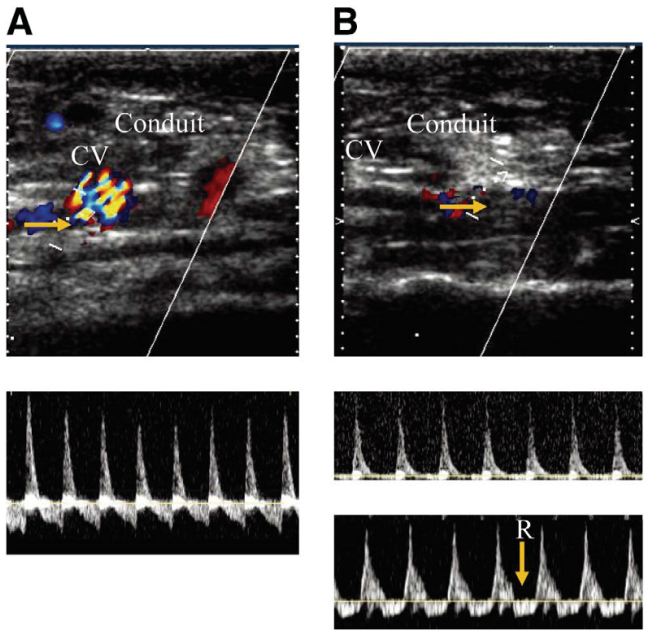

Figure 3. Conduit valve function analysis. We established a new method to prove the function of the conduit valve in vivo. All images were taken using transabdominal color and pulsed-wave Doppler. (**A**) The image positioned in the abdominal aorta before the conduit valve shows the reversed diastolic color jet flow because of the native aortic valve regurgitation. (**B**) Abdominal aorta distal to the conduit valve. (**Upper panel**) The reversed diastolic color jet flow disappeared in the position distal to the conduit valve. (**Lower panel**) At 12 weeks, reversed diastolic color jet flow appeared distal to the conduit valve (R arrow), indicating that this conduit valve had developed a new regurgitation. CV, position of the conduit valve; Arrows, position of the analysis.

Table 1. Physiological Characteristics of Rats After AR Induction

	Acute death (n=3)	Survival (n=17)	P value
Operation time (min)	34±9	41±17	0.39
LVDd (mm)	5.2±0.15	5.1±0.49	0.70
LVDs (mm)	2.5±0.11	2.5±0.36	0.92
EF (%)	86±2.5	85±4.2	0.73
AR jet/LVOT (%)	77±6.0	57±6.0	<0.001
AR severe, n (%)	3 (100)	1 (5.8)	<0.001
RVTI in Asc. Ao (%)	1.4±0.91	0.66±0.13	<0.01
RVTI in Abd. Ao (%)	0.60±0.17	0.53±0.13	0.16

Physiological characteristics of rats after AR induction. Based on the acute survival results, animals were divided into 2 groups: acute death group (n=3) and survival group (n=17). Values are mean±SD. AR, aortic regurgitation; LVDd, left ventricular diastolic diameter; LVDs, left ventricular systolic diameter; EF, ejection fraction; AR jet/LVOT, color Doppler ratio of aortic regurgitation jet width to left ventricular outflow tract diameter; AR severe, number of the severe aortic regurgitation grade; RVTI in Asc. Ao, ratio of time-velocity integral of reversed diastolic flow to forward systolic flow in the ascending aorta; RVTI in Abd. Ao, ratio of time-velocity integral of reversed diastolic flow to forward systolic flow in the abdominal aorta.

In addition to CV function, we analyzed CV stenosis under MSV in the Asc. Ao and the Abd. Ao according to the following formula:

$$\text{CV stenosis grade ratio} = \frac{(\text{MSV in post-conduit}) - (\text{MSV in pre-conduit})}{(\text{MSV in Asc. Ao})}$$

where post-conduit is the post-conduit abdominal aorta and pre-conduit is the pre-conduit abdominal aorta.

Chronic Follow up

Long-term follow up was carried out at 4 and 12 weeks after implantation. Animals were anesthetized, and then functional assessment of the CV and the left ventricle was performed using echocardiography. After the final functional evaluation at the 12 week time point, animals were sacrificed for molecular and histological analyses that will be subject to further investigation in a separate study.

Statistical Analysis

All statistical comparisons were performed using Stat View J-5.0 software (SAS Institute, Cary, NC). All values are expressed as the mean±standard deviation. Comparisons between the 2 groups were made using an unpaired t-test for parametric values. By simple linear regression analysis, the correlation of the color Doppler ratio of regurgitation jet width to LV outflow tract diameter was evaluated using these comparisons. Differences were considered statistically significant at $P<0.05$. Estimation of survival was performed with Kaplan-Meier's curves with a 95% confidence interval.

Results

Creation of AR in the Recipients

Catheter-induced aortic valve injury resulted in significant acute AR with a large volume of reversed diastolic flow in the abdominal aorta in all animals. AR was graded as moderate (in

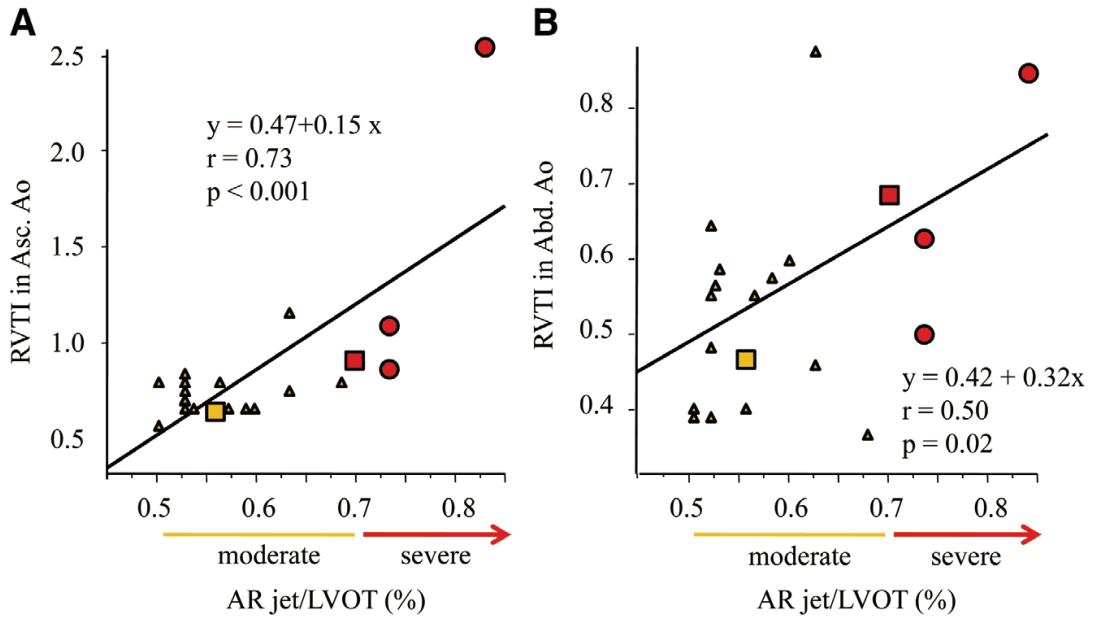

Figure 4. Correlation of color Doppler ratio of regurgitation jet width to left ventricular (LV) outflow tract diameter and ratio of time-velocity integral of reversed diastolic flow to forward systolic flow in the ascending aorta (**A**) or in the abdominal aorta (**B**) at the time of aortic regurgitation (AR) creation. RVTI in Asc. Ao correlated well (r=0.73) with the AR severity (**A**), but RVTI in Abd. Ao did not correlate (r=0.50) with the AR severity (**B**). ○, short-term dead rats; □, long-term dead rats. AR jet/LVOT, color Doppler ratio of aortic regurgitation jet width to LV outflow tract diameter; RVTI in Asc. Ao, ratio of time-velocity integral of reversed diastolic flow to forward systolic flow in the ascending aorta; RVTI in Abd. Ao, ratio of time-velocity integral of reversed diastolic flow to forward systolic flow in the abdominal aorta).

Table 2. Follow up Echocardiography Data

	AR (n=20)	Implantation (n=17)	4 weeks (n=17)	12 weeks (n=15)
Body weight (g)	223±15	252±31†	280±28†	270±60†
LVDd (mm)	5.1±0.49	7.5±0.75†	8.0±0.82†,*	8.2±0.83†,*
LVDs (mm)	2.5±0.36	4.3±0.55†	4.7±0.69†,*	5.1±0.46†,*
EF (%)	85±4.2	75±7.9†	75±4.2†	73±3.2†
AR jet/LVOT (%)	0.56±0.06	0.60±0.05	0.56±0.09	0.55±0.04
RVTI in Asc. Ao (%)	0.66±0.13	0.59±0.17	0.74±0.25	0.61±0.18
MSV in Asc. Ao (cm/s)	178±43	170±32	167±23	161±50
Conduit valve regurgitation				
Appearance of regurgitation	–	0	5	14
RVTI in pre-conduit (%)	0.53±0.13	0.62±0.26	0.51±0.14	0.53±0.13
RVTI in post-conduit (%)	–	0	0.07±0.12	0.37±0.14*,**
Conduit valve stenosis				
MSV in pre-conduit (cm/s)	–	160±49	127±28	81±21*,**
MSV in post-conduit (cm/s)	–	166±52	133±25	109±27*,**

Follow-up echocardiography data. All surviving rats showed movement of the conduit valve at all follow-up times, but 5 rats (29%) at 4 weeks and 14 rats (93%) at 12 weeks appeared with new conduit valve regurgitation.
MSV, maximum forward systolic flow velocity; pre-conduit, pre-conduit abdominal aorta; post-conduit, post-conduit abdominal aorta. All other abbreviations as per Table 1. Values are mean±SD.†P<0.05 vs. AR, *P<0.05 vs. implantation, **P<0.05 vs. 4 weeks.

n=16, 80%) to severe (in n=4, 20%) on the basis of the width of the AR jet. Three rats were subsequently euthanized (n=2 after 1 day, n=1 after 3 days) because of clinical deterioration caused by acute congestive heart failure (15% short-term mortality). Based on the acute survival result, animals were divided into 2 groups; the acute death group (n=3) and the surviving group (n=17). Serial measurements recorded are shown in **Table 1**.

No significant differences were observed regarding the operation time and LV echocardiography data between the 2 groups. With respect to AR, the animals in the death group showed a significantly greater severity than those in the surviving group (color Doppler ratio of regurgitation jet width to LV outflow tract diameter and number of rats with severe AR, P<0.001). There was a significant difference in the ratio of time-velocity

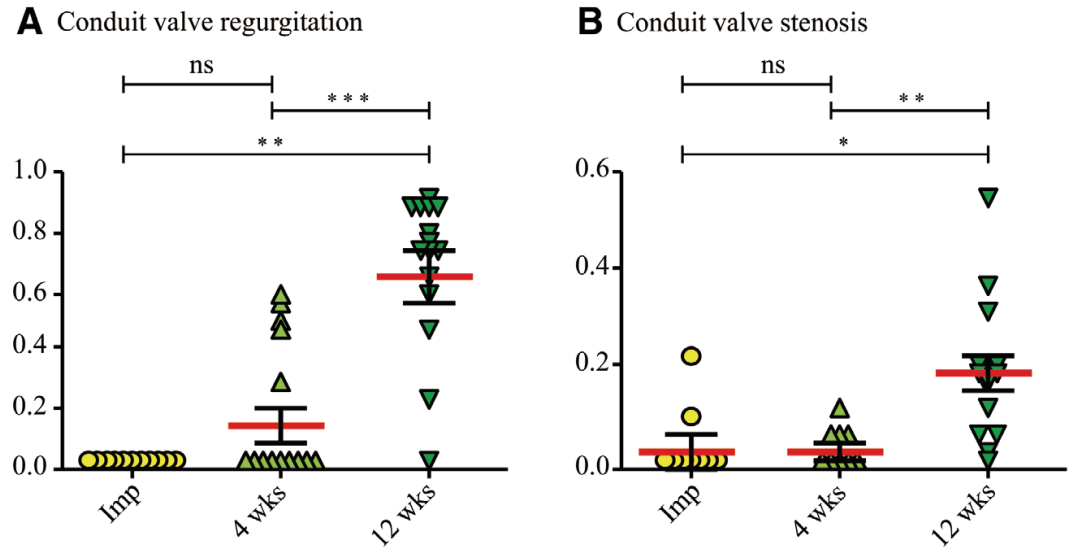

Figure 5. Evolution of conduit valve (CV) destruction. The function of the implanted CV was quantitatively examined using our new method of aortic color and pulsed-wave Doppler analyses. The left column depicts the results obtained at implantation (Imp); the middle column depicts the results obtained at 4 weeks after implantation (4wks); and the right column demonstrates results after 12 weeks (12wks). NS, no significant difference between these 2 groups. (**A**) At implantation, all CV showed complete functional competence and no regurgitation. However, 5 rats at 4 weeks and 14 rats at 12 weeks after implantation were revealed to have developed new CV regurgitation. At analysis of these regurgitation phenomena, there was a significant difference between the 2 follow-up points (**P<0.01, ***P<0.001). (**B**) In the first 4 weeks after implantation, the average CV stenosis grade remained stable, whereas at the time point of 12 weeks after implantation, there was a significant increase as compared to previous time points (*P<0.05, **P<0.01).

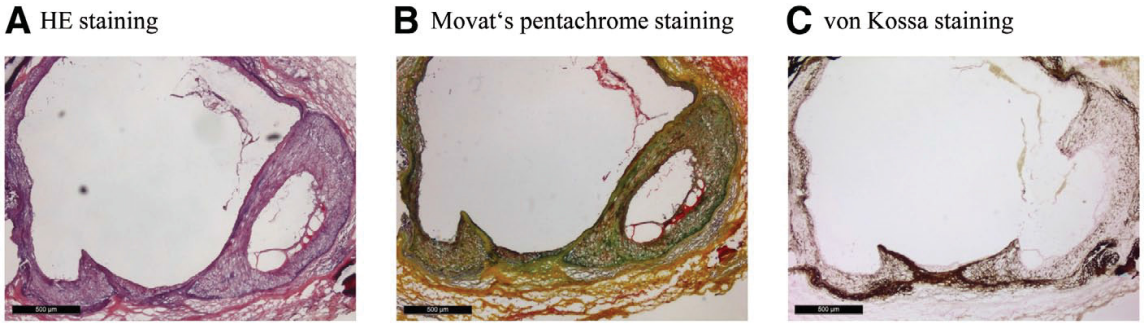

Figure 6. Hematoxylin/eosin (**A**), Movat's pentachrome (**B**) and von Kossa staining (**C**) of cross sections of decellularized aortic conduit valves 12 weeks after implantation. Calcification of the leaflets as well as the aortic sinus wall was observed.

integral of reversed diastolic flow to forward systolic flow in the ascending thoracic aorta between the 2 groups (P<0.01), whereas no significant difference was observed in the abdominal aorta (P=0.16).

Detection of Effective AR in Recipients' Abdominal Aorta

In order to analyze the relationship between AR severity and reversed flow in the abdominal aorta in the recipient rats, single line analysis was performed. We have established the correlation of color Doppler ratio of regurgitation jet width to LV outflow tract diameter and ratio of time-velocity integral of reversed diastolic flow to forward systolic flow in the ascending aorta (**Figure 4A**) or in the abdominal aorta (**Figure 4B**) at the time of AR creation. The reason for this observation might be that RVTI in the abdominal aorta does not correlate well (r=0.50) with the AR severity in the moderate AR group.

Implantation Operative Results

Seventeen surviving rats received an infrarenal decellularized CV implant. The implantation was performed with a mean operative duration of 128±15 min. Aortic cross-clamp times for the proximal anastomosis varied between 20 and 35 min (23±5 min), and aortic cross-clamp times for distal anastomosis ranged from 10 to 25 min (18±4 min). All animals recovered without signs of neurological problems and/or ischemic symptoms of the lower limbs.

Long-Term Survival

All rats survived the implantation of conduits for 4 weeks (100%). At 12 weeks, however, the survival rate decreased to 88%. A detailed investigation of the effect of controlled moderate AR on survival for short- and long-term periods was performed, comparing the subgroups with severe AR (Group S; n=4, 20%) and moderate AR (Group M; n=16, 80%) with Kaplan-Meier's curves (P<0.001). At both 4 and 12 week time points, the actual survival was significantly higher in the moderate AR group as compared to the severe AR group (Group S: 25% vs. Group M: 100% at 4 weeks and Group S: 0% vs. Group M: 90% at 12 weeks, P<0.001; **Figure S1**).

Evaluation of Long-Term LV and CV Function

Table 2 summarizes the long-term echocardiography data. EF was significantly different between the time point of the creation of AR and the 4 and 12 weeks follow-up time points, but there were no significant differences between implantation and the 2 follow-up time points.

After 4 and 12 weeks following implantation, all surviving rats showed movement of the CV leaflets. With regard to the CV function, 5 rats at 4 weeks and 14 rats at 12 weeks appeared to develop a new CV regurgitation with an average valve regurgitation of 0.14±0.22 at 4 weeks and 0.66±0.26 at 12 weeks according to the applied definition (P<0.05). Average CV stenosis was demonstrated to be 0.04±0.07, 0.03±0.04 and 0.19±0.15 at each follow-up point (P<0.05; **Figure 5**). Representative cross sections through the CV 12 weeks after implantation showed partially preserved and partially calcified leaflets (**Figure 6**). Moreover, due to the severely procalcific diet, the aortic wall of the conduits exhibited progressive calcification during follow up (**Figure S2**).

Discussion

In the present study, a standardized small animal model of heterotopic aortic conduit implantation allowing for preserved implant valve function was developed. This goal was achieved by echocardiography-controlled generation of moderate AR of the native aortic valve, additionally resulting in reduced short- and long-term mortality. The functional preservation of the implant valve makes our model suitable for small animal studies of native as well as tissue-engineered heart valve prostheses.

Aortic valve allografts (AVA) have been used for more than 50 years with satisfactory clinical outcome. Although cryopreservation is widely accepted as the gold standard method for processing and storage of AVA, novel technologies, such as decellularization and tissue engineering have been introduced to overcome the limitations of AVA.[16–18] Clinical feasibility and safety of decellularization as a method of improvement of aortic valve implantation have been demonstrated, but comparable results are scarce.[19] For this reason, in vivo scenarios for the preclinical analysis of decellularized AVA in well characterized small animal models present a valuable tool. Small animal models are favored in the biomedical research due to lower costs and a wide range of histological and molecular biological analytic tools.

Current rat models of infrarenal aortic valve implantation are well described and have provided important advances in our understanding of decellularized allograft failure. However, these previous studies have focused on the valve conduit rather than the leaflets, despite having leaflets present in the blood stream and despite the evidence of the leaflet movement. We consider, in many cases, these leaflets remaining not completely functional in the physiological manner. Because of this, the leaflets are prone to thrombosis against the adjacent aorta and fail usually rather early when compared to the preclinical and clinical experience with decellularized valves implanted in the orthotopic position.[5,19,20] Thus, the availability of a functional CV model is of critical importance.

Under these premises, Légaré et al[8] reported on an aortic conduit model involving native AR for allowing flow reversal in the abdominal aorta. We believe that this concept is the most suitable to analyze CV failure as it provides a functional valve to assess the interaction between immunological and mechanical injury in AVA failure. But this aortic conduit model involving native AR has a few drawbacks such as high mortality due to generated regurgitation and a lack of long-term evaluation. Moreover, previous reports did not evaluate complete CV function. In the present study, after analyzing the aforementioned drawbacks, we propose solutions to improve the involved problems.

One of the major limitations to the aortic conduit model with AR is the rather high mortality in the short term. The study by Légaré et al reported 3 deaths (33%) in the short term due to acute heart failure and 1 death (11%) due to sinus of valsalva aneurysm and right arterial fistula. We suspect that the outcome was due to the fact that AR in their study was created not under continuous echocardiographic guidance. Arsenault et al[13] reported aortic valve leaflet injury models using echocardiography for studying congestive heart failure in the presence of severe AR. Echocardiography was straightforward in the rat AR model during their procedure, as is the case in studies on the native (orthotopic) heart.[21] The perforating catheter was easily identified and controlled, thus the AR was clearly visible. This might explain why in their study a low acute mortality rate was demonstrated (17%). In our current series, we found a comparable outcome, confirming the observation of the latter study with an acute mortality rate of 15% in the present study. Moreover, a high rate of controlled AR generation (76% by this study for generating severe AR and 80% by our study to generate moderate AR) became feasible, when high quality live echocardiography imaging was used. Based on these results, we therefore suggest that echocardiography should be used during aortic valve leaflet injury via a catheter.

A second major limitation generally adherent to the presented model is its unsuitability for long-term follow-up studies because of the creation of AR, which often results in progressive congestive heart failure from volume overload. All severe AR rats in our study died during the follow-up period suggesting that possibly creating a lower degree of AR would have been a solution to avoid this problem, which then could enable long-term follow-up studies to be performed.

However, on the other hand, a lower AR grade could not preserve CV function in our study. Tani et al[14] reported in their study that the presence of reversed flow in the abdominal aorta suggested an AR greater than a moderate grade. In our study, single-line analysis was performed (**Figure 4**), which confirmed that if the rats demonstrated an AR greater than a moderate grade, we sometimes could not find an increased reversed flow in the abdominal aorta. Following this report and our analysis, we hypothesized that moderate AR is not only enough to obtain an acceptable result for implanted valves, but it might also be necessary to reduce the long-term mortality. Here we summarize our positive results for the approach of controlled moderate AR: (1) achievement of a fine 12 weeks' long-term survival (88%); and (2) successful accomplishment of CV function.

Regarding CV function, previous reports have demonstrated only the movement of CV leaflet by transabdominal M-Mode

echocardiography with direct imaging of the CV.[9,11] Otherwise, in these small animal models, one of the major limitations is the difficulty to perform measurements by directly targeting the CV for a quantitative analysis of the valve function, either by measuring the regurgitant fraction or the vena contracta. Our study is the first report involving a small animal model to evaluate CV regurgitation and stenosis via pulsed-wave Doppler measurements in the recipient abdominal aorta in positions post and pre CV. The goal of our study was to analyze CV function in a greater depth and in a longitudinal follow-up manner. We believe that these echocardiographic measurements should be used in aortic conduit studies because of their relatively easy and low invasive application, providing a highly valid and reproducible assessment of the valve function.

In most of the explants, calcification of the valve was observed after 12 weeks. The main underlying cause for the fast implant calcification is the application of a procalcific diet resulting in accelerated cardiovascular calcification, which is supposed to have contributed to the partial destruction of the implant valves after 12 weeks. However, the procalcific diet allows for examination of prosthesis degeneration in short time periods. Combined with the present small animal implantation model of echocardiography-controlled moderate AR of the native valve, we present a tool worthwhile to elucidate and influence pathophysiological mechanisms involved in the degeneration of aortic valve prostheses, which will be subject to future studies.

Study Limitations

There are several limitations to the present study. The findings of this study are based on a limited number of small animals and certainly need further validation in upcoming trials, ideally involving other animal species. From the clinical standpoint, the herein employed model of heterotopic valve implantation should be considered with caution as it does not entirely reflect the hemodynamic scenario of orthotopically implanted valve prostheses. Although this small animal model provides a number of advantages for the preclinical screening and in vivo evaluation of novel engineered heart valves, the results should be further validated in animal models of orthotopic valve implantation. Considering very recent technological developments, a further enhancement of the employed echocardiography instruments, for example, by using systems equipped with 30 or 35 MHz transducers, might provide superior imaging quality and thereby probably even further improve the study results, as it has been suggested for the clinical scenario.[22]

Conclusion

Generation of controlled moderate AR using echocardiography can effectively reduce short- and long-term mortality in our standardized combined AR and conduit implantation model. In addition, by assessing the reversed diastolic flow behind the implanted CV, a quantitative analysis of the CV function was demonstrated. Therefore, we conclude that this model might represent an ideal model for studying aortic CVs in small animal models.

References

1. New SEP, Aikawa E. Cardiovascular calcification: An inflammatory disease. *Circ J* 2011; **75:** 1305–1313.
2. Bussey H. An overview of anticoagulants, antiplatelet agents, and the combination in patients with mechanical heart valves. *J Heart Valve Dis* 2004; **13:** 319–324.
3. Mahesh B, Angelini G, Caputo M, Jin XY, Bryan A. Prosthetic valve endocarditis. *Ann Thorac Surg* 2005; **80:** 1151–1158.
4. Schoen FJ, Levy RJ. Calcification of tissue heart valve substitutes: Progress toward understanding and prevention. *Ann Thorac Surg* 2005; **79:** 1072–1080.
5. Akhyari P, Kamiya H, Gwanmesia P, Aubin H, Tschierschke R, Hoffmann S, et al. In vivo functional performance and structural maturation of decellularised allogenic aortic valves in the subcoronary position. *Eur J Cardiothorac Surg* 2010; **38:** 539–546.
6. Lichtenberg A, Cebotari S, Tudorache I, Hilfiker A, Haverich A. Biological scaffolds for heart valve tissue engineering. *Methods Mol Med* 2007; **140:** 309–317.
7. Meyer SR, Nagendran J, Desai LS, Rayat GR, Churchill TA. Decellularization reduces the immune response to aortic valve allografts in the rat. *J Thorac Cardiovasc Surg* 2005; **130:** 469–476.
8. Légaré JF, Nanton MA, Bryan P, Lee TD, Ross DB. Aortic valve graft implantation in rats: A new functional model. *J Thorac Cardiovasc Surg* 2000; **120:** 679–685.
9. Kallenbach K, Sorrentino S, Mertsching H, Kostin S, Pethig K, Haverich A, et al. A novel small-animal model for accelerated investigation of tissue-engineered aortic valve conduits. *Tissue Eng Part C Methods* 2010; **16:** 41–50.
10. Oei FB, Welters MJ, Bonthuis F, Vaessen LM, Marquet RL, Zondervan PE, et al. A size-matching heterotopic aortic valve implantation model in the rat. *J Surg Res* 1999; **87:** 239–244.
11. Légaré JF, Ross DB. Suggestion for functional model to test effects of decellularization of rat aortic valve allografts on leaflet destruction and extracellular matrix remodeling. *J Thorac Cardiovasc Surg* 2004; **128:** 155–156 [author reply 156].
12. Zendaoui A, Lachance D, Roussel E, Couet J, Arsenault M. Usefulness of carvedilol in the treatment of chronic aortic valve regurgitation. *Circ Heart Fail* 2011; **4:** 207–213.
13. Arsenault M, Plante E, Drolet MC, Couet J. Experimental aortic regurgitation in rats under echocardiographic guidance. *J Heart Valve Dis* 2002; **11:** 128–134.
14. Tani LY, Minich LL, Day RW, Orsmond GS, Shaddy RE. Doppler evaluation of aortic regurgitation in children. *Am J Cardiol* 1997; **80:** 927–931.
15. Assmann A, Akhyari P, Delfs C, Flögel U, Jacoby C, Kamiya H, et al. Development of a growing rat model for the in vivo assessment of engineered aortic conduits. *J Surg Res* 2012; **176:** 367–375.
16. O'Brien MF, Harrocks S, Stafford EG, Gardner MA, Pohlner PG, Tesar PJ, et al. The homograft aortic valve: A 29-year, 99.3% follow up of 1,022 valve replacements. *J Heart Valve Dis* 2001; **10:** 334–344; discussion 335.
17. Dignan R, O'Brien M, Hogan P, Thornton A, Fowler K, Byrne D, et al. Aortic valve allograft structural deterioration is associated with a subset of antibodies to human leukocyte antigens. *J Heart Valve Dis* 2003; **12:** 382–390; discussion 390–391.
18. Cebotari S, Tudorache I, Ciubotaru A, Boethig D, Sarikouch S, Goerler A, et al. Use of fresh decellularized allografts for pulmonary valve replacement may reduce the reoperation rate in children and young adults: Early report. *Circulation* 2011; **124:** S115–S123.
19. da Costa FD, Santos LR, Collatusso C, Matsuda CN, Lopes SA, Cauduro S, et al. Thirteen years' experience with the Ross Operation. *J Heart Valve Dis* 2009; **18:** 84–94.
20. Baraki H, Tudorache I, Braun M, Höffler K, Görler A, Lichtenberg A, et al. Orthotopic replacement of the aortic valve with decellularized allograft in a sheep model. *Biomaterials* 2009; **30:** 6240–6246.
21. Xu H, Yang YJ, Qian HY, Tang YD, Wang H, Zhang Q. Rosuvastatin treatment activates JAK-STAT pathway and increases efficacy of allogeneic mesenchymal stem cell transplantation in infarcted hearts. *Circ J* 2011; **75:** 1476–1485.
22. Okura H, Takada Y, Yamabe A, Ozaki T, Yamagishi H, Toda I, et al. Prevalence and correlates of physiological valvular regurgitation in healthy subjects. *Circ J* 2011; **75:** 2699–2704.

Supplementary Files

Supplementary File 1

Figure S1. Effects of controlled moderate aortic regurgitation (AR) on short- and long-term survival in a completely functional conduit valve implantation model.

Figure S2. von Kossa staining of cross sections of the aortic conduit wall 4 weeks (**A**) and 12 weeks (**B**) after implantation.

Please find supplementary file(s);
http://dx.doi.org/10.1253/circj.CJ-12-1439

3.1.3 **Accelerated cardiovascular calcification**

***Assmann A**, Zwirnmann K, Heidelberg F, Schiffer F, Horstkötter K, Munakata H, Gremse F, Barth M, Lichtenberg A, Akhyari P. The degeneration of biological cardiovascular prostheses under pro-calcific metabolic conditions in a small animal model. **Biomaterials**. 2014; 35:7416-7428.*

In order to examine the calcifying degeneration of cardiovascular implants in our rat model within reasonable time periods, we aimed at developing and characterizing a model of accelerated cardiovascular calcification. Thus, different regimens of pro-calcific diet containing combinations of VD, CH and PH were tested regarding their metabolic and arterio-degenerative effects in a total of 102 rats fed over up to 12 weeks.

Animals supplemented with high-dose VD (groups HIGH, $I_{\text{-CH}}$ and $II_{\text{-PH}}$) exhibited significantly increased levels of MMP activity measured by *in situ* zymography and hydroxyapatite deposition in the aortic wall, while low-dose VD (group LOW) resulted in less MMP activity and calcium deposition, and a lack of VD feeding (group $III_{\text{-VD}}$) led to data similar to those in the control group without pro-calcific supplements. Corresponding results for MMP activity and calcification were observed on the level of the aortic wall of the rats. Micro-computed tomography confirmed the enhanced calcium burden in high-dose VD animals and revealed an aortic calcification pattern similar to human atherosclerosis, whereas the infrarenal aorta of rats was less diseased as typically occurring in humans. However, enhanced MMP activity and hydroxyapatite deposition as observed in our rat model are known features of calcifying areas in human aortic valves and arteries [65-68].

At the major sites of aortic valve calcification, the commissures, clusters of lipid vacuoles and chondroid cells as well as signs of nitrosative stress and apoptosis were found. Extensive aortic sinus calcification was accompanied by intimal hyperplasia of fibroblastoid cells. All these observations parallel the adverse valve remodeling in human calcific disease [69].

Real-time polymerase chain reaction (PCR) of aortic wall samples revealed significantly increased gene expression of the osteogenic transformation markers osteopontin and runt-related transcription factor-2 in rats with full-dose VD, which was in accordance

with the observed severe wall calcification. In terms of inflammation, only CD39 and CD73, involved in controlling inflammatory processes [70], were increased. Particularly, there was relevant infiltration with inflammatory cells neither in the aortic valves nor in the aortic walls, as shown by hematoxylin/eosin and Movat's pentachrome staining as well as immunostaining against CD3 and CD68.

Twelve weeks of full-dose VD feeding were also associated with progressive inappetance, loss of body weight and physical impairment. Thus, longer observational studies should be condcucted with half-dose VD supplementation, the more so as extensive calcification under full-dose VD diet may mask non-calcific degenerative effects or even beneficial effects of therapeutic approaches.

The combination of the models of functional heterotopic aortic conduit implantation and accelerated cardiovascular degeneration in rats provides a unique platform to profoundly analyze the *in vivo* fate of valvular as well as vascular prostheses within reasonable time periods. The species rat allows for comparative studies with large group numbers and extensive readout methodology to examine basic mechanisms and interventional strategies in the context of bioprosthesis degeneration.

Biomaterials 35 (2014) 7416–7428

Contents lists available at ScienceDirect

Biomaterials

journal homepage: www.elsevier.com/locate/biomaterials

The degeneration of biological cardiovascular prostheses under pro-calcific metabolic conditions in a small animal model

Alexander Assmann [a, 1, 2], Kai Zwirnmann [a], Friederike Heidelberg [a], Franziska Schiffer [a], Kim Horstkötter [a], Hiroshi Munakata [a], Felix Gremse [b], Mareike Barth [a], Artur Lichtenberg [a, *], Payam Akhyari [a]

[a] Department of Cardiovascular Surgery and Research Group for Experimental Surgery, Heinrich Heine University, Medical Faculty, Moorenstrasse 5, Duesseldorf 40225, Germany
[b] Department of Experimental Molecular Imaging, RWTH-Aachen University, Medical Faculty, Pauwelsstr. 30, Aachen D-52074, Germany

ARTICLE INFO

Article history:
Received 2 April 2014
Accepted 14 May 2014
Available online 7 June 2014

Keywords:
Animal model
Aortic valve sclerosis
Atherosclerosis
Heart valve prosthesis
Decellularization
Vitamin D

ABSTRACT

In order to allow for a comparative evaluation of the *in vivo* degeneration of biological and tissue-engineered heart valves and vascular grafts, a small animal model of accelerated cardiovascular calcification is desired. Wistar rats ($n = 102$; 6 groups) were fed *ad libitum* with regular chow and 5 different regimens of pro-calcific diet supplemented with combinations of vitamin D (VD), cholesterol (CH) and dicalcium phosphate (PH). Moreover, cryopreserved ($n = 7$) or detergent-decellularized rat aortic conduit grafts ($n = 6$) were infrarenally implanted in Wistar rats under severely pro-calcific conditions. The follow-up lasted up to 12 weeks. High-dose application of VD (300,000 IU/kg), CH (2%) and PH (1.5%) resulted in elevated serum calcium and cholesterol levels as well as LDL/HDL ratio. It increased the tissue MMP activity visualized by *in situ* zymography and caused significantly aggravated calcification of the native aortic valve as well as the aortic wall as assessed by histology and micro-computed tomography. (Immuno)histology and quantitative real-time PCR revealed chondro-osteogenic cell transformation, lipid deposition, nitrosative stress and low-level inflammation to be involved in the formation of calcific lesions. Despite pro-calcific *in vivo* conditions, decellularization significantly reduced calcification, inflammation and intimal hyperplasia in aortic conduit implants. A well balanced dietary trigger for pathologic metabolic conditions may represent an appropriate mid-term treatment to induce calcifying degeneration of aortic valves as well as vascular structures in the systemic circulation in rats. With respect to experimental investigation focusing on calcifying degeneration of native or prosthetic tissue, this regimen may serve as a valuable tool with a rapid onset and multi-facetted character of cardiovascular degeneration.

1. Introduction

All currently available heart valve bioprostheses undergo progressive calcifying degeneration that terminally results in implant failure requiring a redo procedure with an elevated risk for the recipient patient [1]. In order to solve this problem, decellularized and tissue-engineered aortic valve implants have become an alternative with promising results in preclinical as well as clinical studies [2–5]. However, central aspects of engineering these prostheses are controversially discussed, e.g. biological versus artificial scaffolds, preoperative *in vitro* cell seeding versus spontaneous implant repopulation *in vivo*, the method of decellularization or the need for surface coating strategies to enhance the biocompatibility of the implants [6].

* Corresponding author. Department of Cardiovascular Surgery, Heinrich Heine University, Medical Faculty, Moorenstrasse 5, D-40225 Duesseldorf, Germany. Tel.: +49 (0) 211 81 18331; fax: +49 (0) 211 81 18333.
E-mail addresses: alexander.assmann@med.uni-duesseldorf.de (A. Assmann), artur.lichtenberg@med.uni-duesseldorf.de (A. Lichtenberg).
[1] Present address: Center for Biomedical Engineering, Department of Medicine, Brigham and Women's Hospital, Harvard Medical School, 75 Francis St, Boston, MA 02115, USA.
[2] Present address: Harvard-MIT Division of Health Sciences and Technology, Massachusetts Institute of Technology, 65 Landsdowne St, Cambridge, MA 02139, USA.

http://dx.doi.org/10.1016/j.biomaterials.2014.05.034
0142-9612/

In terms of optimizing the properties of tissue-engineered heart valves, it is widely accepted that the prosthesis-surrounding milieu, e.g. recipient-inherent comorbidities and risk factors, may have an impact on the durability and long-term function of biological heart valves, and this impact may be just as crucial as the material characteristics of the prosthesis are. Data from clinical cohorts confirm renal insufficiency and lipid disorders as independent risk factors for the degeneration of bioprosthetic heart valves. Although the complexity of comorbidities found in patients is hardly to mimic by standardized animal models, yet there is a need for animal models in the preclinical graft testing allowing for an accelerated degeneration of cardiovascular implants. Since they enable large-scale comparative studies and because of the availability of a broader range of molecular-biological readout modalities, small animal models are preferred for the examination of fundamental strategies of engineering cardiovascular implants. Recently, we reported on the development and functional optimization of a standardized rat implantation model facilitating the comparative evaluation of the fate of biological and tissue-engineered aortic conduit grafts in the systemic circulation [7–9]. In order to further optimize our model by allowing for implant degeneration within short observation periods, the present study was designed to develop a reliable model of accelerated cardiovascular calcification in rats.

Dietary vitamin D (VD) and cholesterol (CH) supplementation have been reported to enhance the calcium deposition in the arterial vessel wall of rodents [10]. In rabbits, the combination of VD and CH has been observed to induce histological as well as functional signs of aortic valve sclerosis [11,12]. The effect of VD and CH on the calcifying degeneration of rat aortic valves has not been subject to a systematic and in-depth investigation, yet. Moreover, increased phosphate (PH) serum levels are supposed to contribute to the progression of aortic valve sclerosis in humans [13,14].

The primary aim of the present study was to develop a standardized model of accelerated aortic valve as well as arterial calcification in rats by evaluating different chow regimens supplemented with VD, CH and PH [Table 1]. Furthermore, the suitability of this model to examine the degeneration of cardiovascular prostheses was tested *in vivo* by comparing cryopreserved and decellularized aortic conduit implants.

2. Materials and methods

2.1. Animals

Male Wistar ($n = 115$) and Sprague–Dawley ($n = 13$) rats weighing 200–250 g were obtained from the local animal care facility, received chow *ad libitum* and were exposed to constant temperature, humidity and circadian daylight rhythm. All experiments were conducted according to the national animal welfare act, and approved by the state animal care committee (reference number 87-51.04.2010.A068).

2.2. In vivo examination of different dietary regimens

A Wistar rat population of 102 animals was randomly divided into six groups receiving different regimens of pro-calcific diet containing VD, CH and PH [Table 1]. The follow-up periods were 4, 8 and 12 weeks in each group. Body weight and the amount of fed chow were continuously monitored on a weekly base.

Blood was drawn after 4, 8 and 12 weeks, and the serum levels of calcium, phosphate, urea and cholesterol (including HDL and LDL fractions) were measured according to routine procedures employing standard assays for rats by the Institute of Clinical Chemistry and Laboratory Diagnostics, Heinrich Heine University, Medical Faculty, Duesseldorf, Germany.

Global cardiac function as well as relevant parameters for the detection of valvular stenosis of the aortic valve were assessed by transthoracic echocardiography using a Philips HDX11 ultrasonography system equipped with a 15 MHz probe (Philips, Amsterdam, Netherlands). Following parameters were analyzed: Left ventricular enddiastolic and endsystolic diameter (LVEDD, LVESD), left ventricular ejection fraction (LVEF) and transvalvular pressure gradient at the aortic valve (dp_{AV}).

At the end of the follow-up, echocardiography was performed in rats under inhalative anesthetization with isoflurane (2.0–2.5%) and analgesia with intraperitoneal carprofen (5 mg/kg). After combined thoracotomy, laparotomy and systemic heparinization (1000 IU i.v.), the circulatory system was perfused with PBS, and the aortic valve as well as the whole aorta were excised and further processed for histology, immunohistology, *in situ* zymography, quantitative real-time polymerase chain reaction (RT-PCR), and micro-computed tomography (μCT). Moreover, the heart weight was determined after thorough drying.

2.3. In vivo testing of aortic conduit implants

Aortic conduit grafts from Sprague–Dawley rats were either cryopreserved (group CRYO; $n = 7$) or detergent-decellularized (group DC; $n = 6$) and implanted in male Wistar rats ($n = 13$). Fourteen days before the grafting procedure (d-14), all recipient rats underwent an interventional generation of native aortic valve insufficiency (AI). Controlled generation of native aortic valve insufficiency was conducted as recently published [9]. Under general anesthesia and echocardiographic guidance, the aortic valve leaflets were interventionally perforated to induce an AI grade II–III. Animals with AI grade I or grade IV in the postoperative echocardiography assessment were excluded from the study. At day 0, cryopreserved or decellularized aortic conduits were infrarenally implanted into the systemic circulation according to a recently published standardized small animal model [7,9]. Four or 12 weeks after implantation, conduit grafts were explanted and the animals euthanized. The grafts were rinsed with heparinized PBS via abdominal cannulation and further processed for histology, immunohistology, or *in situ* zymography (each with $n = 3$ per group at days 28 and 84). For μCT, the whole native aorta including the implant was excised ($n = 1$). Graft perfusion was controlled by Doppler sonography at implantation and pre-explantation.

All recipients received a pro-calcifying diet (+300,000 IU/kg vitamin D + 2% cholesterol + 1.5% calcium phosphate) from day −14 until the final explantation of the prostheses.

2.4. Graft harvesting and engineering

Rat aortic conduit grafts were explanted and either cryopreserved or decellularized as recently described [7]. Grafts in group CRYO were transferred into conservation medium (Dulbecco's modified Eagle's medium + 10% dimethylsulfoxide +20% fetal calf serum at 5°C) immediately after preparation. Afterwards, the conduits were frozen to −80°C under controlled cooling (1°C per minute in a propan-2-ol box). Four weeks later, the cryopreserved grafts were thawed, washed three times in heparinized PBS and implanted. Prostheses in group DC were decellularized within four cycles (12 h) with 0.5% sodium dodecyl sulfate + 0.5% deoxycholate, followed by 24 h rinsing with distilled water and three further rinsing cycles (24 h) with PBS supplemented with 1% penicillin/streptomycin and 0.05% sodium azide.

2.5. Histology

Explanted tissue was embedded in TissueTek cryo-mounting medium and tissue sections of 4 and 6 μm were prepared (cryostat CM 1950; Leica Biosystems, Wetzlar, Germany). Histological stainings were performed according to previously published protocols, including hematoxylin/eosin (H&E) staining, Movat's pentachrome staining, von Kossa staining, and Oil Red O staining [11]. Images were acquired on a microscope system DM2000 equipped with a digital camera DFC 425C (Leica

Table 1
Chow regimens.

	Group N Normal $n = 19$	Group HIGH High-dose $n = 19$	Group LOW Low-dose $n = 19$	Group I_{-CH} w/o cholesterol $n = 15$	Group II_{-PH} w/o phosphate $n = 15$	Group III_{-VD} w/o vitamin D $n = 15$
Vitamin D	–	300,000 IU/kg	150,000 IU/kg	300,000 IU/kg	300,000 IU/kg	–
Cholesterol	–	2% (w/w)	1% (w/w)	–	2% (w/w)	2% (w/w)
Dicalcium phosphate	–	1.5% (w/w)	0.75% (w/w)	1.5% (w/w)	–	1.5% (w/w)

A male Wistar rat population ($n = 102$) was randomly divided into six groups receiving different regimens of pro-calcific chow supplementation. Group N received normal chow without any supplementation. In each group, the follow-up periods were 4, 8 and 12 weeks ($n = 5–7$ per time point).

Microsystems, Wetzlar, Germany), applying Leica Application Suite V3.7 software. Morphometric analyses for the detection of inter-group differences were conducted using Image J v1.46 (Wayne Rasband, National Institutes of Health, USA).

In order to quantify the calcification of the aortic valve and the ascending aorta, 6 μm cross-sections in a distance of 200 μm to each other underwent von Kossa staining and histomorphological analysis. Separate semi-quantitative scoring systems for the aortic valve and the aorta were developed: Aortic wall cross-sections were divided into four radially orientated segments, which were independently assessed according to a pre-defined scoring system. For analysis of the aortic valve, cross-sections were divided into six segments, consisting of three commissural and three sinus segments. The applied scoring range comprised values of 0–3 (0 = no calcification; 1 = micro-calcification; 2 = macro-calcification <50% of the tissue area; 3 = macro-calcification >50% of the tissue area), resulting in maximum values of 12 and 18 for the ascending aorta and the aortic valve, respectively. For validation of both von Kossa scoring systems, cross-sections of each animal at 12 weeks were analyzed by applying the scoring systems as well as automatic measurements of the calcified area, which resulted in a confirmation of the blinded-observer-derived data.

In the aortic conduit explants, standardized comparative quantification of neointimal hyperplasia was executed by dividing each conduit into four regions: aortic valve (region A1), ascending aorta (region A2), descending aorta (region B1) and distal anastomosis with the native recipient aorta (region B2). In each region, three cross-sections in a distance of 200 μm to each other were histomorphologically analyzed, and the median intima-to-media ratio was determined.

Quantification of the graft calcification was conducted based on von Kossa-stained cross-sections of each conduit region (A1-B2) by applying the above described scoring system with a value range of 0–3 (0 = no calcification; 1 = micro-calcification; 2 = macro-calcification <50% of the conduit wall; 3 = macro-calcification >50% of the conduit wall), resulting in a maximum value of 12.

2.6. Immunohistology

Immunohistology was conducted as recently described [11]. Cryo-sections (4 μm) were stained with primary antibodies for anti-vonWillebrand factor (vWF) (DAKO, Hamburg, Germany), anti-alpha-smooth muscle actin (aSMA), anti-CD3 (both from Sigma–Aldrich, Taufkirchen, Germany), anti-syndecan-3, anti-CD68, anti-desmin and anti-3-nitrotyrosine (all from Abcam, Cambridge, UK). Secondary antibodies were conjugated to the fluorophores Alexa488 and Alexa546 (Invitrogen, Carlsbad, USA). Sections were covered with Vectashield mounting medium containing DAPI (Vector Labs, Peterborough, United Kingdom), and image acquisition was performed with a microscope system DM2000, equipped with a digital camera DFC 425C (Leica, Wetzlar, Germany) and the Leica Application Suite V3.7 software.

2.7. In situ zymography

In situ zymography was performed as recently published to determine the matrix metalloproteinase (MMP) activity in the explants [11]. Briefly, 4 μm cryo-sections were incubated with 40 μg/ml fluorescein-labeled gelatin (Invitrogen, Carlsbad, USA) in 50 mM Tris–HCl supplemented with 10 mM $CaCl_2$, 150 mM NaCl and 5% Triton-X-100 for 24 h at 37 °C. Finally, sections were mounted with Vectashield medium containing DAPI, and MMP gelatinase activity was visualized by excitation at 488 nm. Specificity of gelatinase activity was confirmed in control specimens undergoing identical treatment with the additional supplementation of 20 mM EDTA. Quantitative analysis of the MMP activity was performed by measuring the fluorescence intensity using Image J software.

2.8. Semi-quantitative RNA analysis

By means of semi-quantitative RT-PCR, expression of specific genes in the aortic wall was analyzed. Total RNA was isolated using a combination of a standard TRIzol method and a commercially available kit (RNeasy Mini Kit; Qiagen, Hilden, Germany). In brief, tissue was homogenized in TRIzol (Invitrogen, Carlsbad, USA), and RNA was precipitated by isopropanol. After passaging through a DNA-removing column (Qiagen, Hilden, Germany), the RNA sample was collected and the following quality analyses were performed. Purity and quantity of isolated RNA were determined spectrophotometrically (BioPhotometer plus, Eppendorf, Hamburg, Germany), and optical density values at 230, 260 and 280 nm were recorded. Additionally, the Agilent RNA 6000 Nano Kit (Agilent Technologies, Santa Clara, USA) was utilized to examine the level of RNA degradation as a measure of overall RNA quality. cDNA was generated with the QuantiTect Reverse Transcription Kit (Qiagen, Hilden, Germany) according to the manufacturer's protocol. Semi-quantitative RT-PCR was conducted on a StepOnePlus cycler (Applied Biosystems, Foster City, USA) using the Platinum SYBR Green PCR Master Mix (Invitrogen, Carlsbad, USA). Relative gene expression was calculated using the ddCt method. Primers for the following genes were obtained from Invitrogen (Carlsbad, USA): Genes associated with inflammation, hypoxia and thrombogenicity (CD39; CD73; RAGE, receptor for advanced glycation end products; HIF1a, hypoxia-inducible factor-1-alpha) and genes associated with chondro-osteogenic transformation (OPN, osteopontin; OCN, osteocalcin; RUNX2, runt-related transcription factor-2). All primer sequences are displayed in [online Table 1].

2.9. Micro-computed tomography

Whole aortic explants were filled with low melting point agarose (5% in aqua dest.) for maintaining the aortic geometry. Subsequently, the explants were transferred into a gelatin solution (15% in aqua dest. +2% lipids). After curing, the gelatin blocks were scanned in a high-resolution dual-energy small animal μCT (Tomoscope DUO; CT Imaging, Erlangen, Germany) using a multimodal imaging cassette [15]. Using a modified Feldkamp algorithm with a smooth reconstruction kernel, Cupping correction and ring artifact reduction, 3D volume data sets were reconstructed with an isotropic voxel size of 35 μm. A water phantom was used to calibrate the μCT scanning protocol to generate reproducible and quantitative image intensities in Hounsfield Units [16]. Image analysis was performed using the Imalytics Preclinical Software (Philips, Aachen, Germany). Calcified regions were determined by applying a fixed threshold above the gelatin intensity and assigned to anatomical regions by the operator. Subsequently, the volume of these lesions was determined as a representative score for the amount of calcification.

2.10. Statistics

Continuous variables are expressed as mean values ± standard errors of the mean. For comparisons between multiple groups, one-way-ANOVA, and in case of multiple time points, two-way-ANOVA, each with Bonferroni post-hoc tests, were applied. Statistical significance was assumed if p-values were lower than 0.05. Data analysis was conducted with GraphPad Prism v5.04 (GraphPad Software, San Diego, USA).

3. Results

3.1. In vivo examination of different dietary regimens

3.1.1. Clinical outcome and hemodynamics

All animals included into the study and receiving a combination of diet supplemented with VD, CH and PH survived the scheduled period of time. The somatic growth of the animals receiving different diets was mainly dependent on the dose of supplemented VD, whereas the other two experimentally varied components had no impact on the observed weight gain. Rats with low-dose VD or without supplemented VD presented constant food intake and continuous gain in body weight, whereas high-dose VD-supplemented chow caused impaired food intake and loss of body weight during the later follow-up [online Fig. S1]. After 12 weeks, the gain in body weight in each of the groups N (226 ± 19.9 g), LOW (202 ± 37.1 g) and III_{-VD} (210 ± 20.0 g) was significantly increased (each with $p < 0.01$ or $p < 0.001$) versus respective mean values observed for the groups HIGH (50 ± 16.1 g), I_{-CH} (28 ± 27.1 g) and II_{-PH} (50 ± 21.7 g). High-dose VD feeding also resulted in evident physical impairment after 8–12 weeks, including spinal ankylosis.

Echocardiography at explantation time point revealed constant values for LVEDD, LVESD and LVEF without significant inter-group differences [online Fig. S2A]. After 12 weeks, the dp_{AV} values were significantly enhanced in the groups LOW (10.7 ± 1.29 mmHg with $p < 0.001$ vs. group N and $p < 0.01$ vs. group I_{-CH} and $p < 0.05$ vs. group II_{-PH}) and III_{-VD} (8.8 ± 0.80 mmHg with $p < 0.05$ vs. group N) [online Fig. S2B].

In accordance with the somatic growth, the myocardial mass, as evaluated by measuring the heart weight at explantation after 12 weeks, was significantly increased in the groups LOW and III_{-VD} versus each of the groups N, HIGH, I_{-CH} and II_{-PH}.

3.2. Metabolic effects of different dietary regimens

Blood serum level analyses after 4, 8 and 12 weeks revealed chow-dependent metabolic effects. In all groups with VD supplementation (HIGH, LOW, I_{-CH}, II_{-PH}), the serum calcium levels were significantly increased as compared to the groups receiving no VD supplementation (N and III_{-VD}) after 4 weeks. This significant elevation of serum calcium levels was also present after 12 weeks [online Fig. S3A]. The total cholesterol serum levels of all groups with any combination of supplemental diet components were enhanced throughout the entire study when compared to animals

receiving regular chow (group N), whereas the differences to this control group were reduced during the later follow-up. Only values of the group receiving high-dose of all supplements (group HIGH) differed significantly at all time points. Analyzing the LDL/HDL ratio resulted in significantly increased values in the groups HIGH and LOW throughout the whole follow-up [online Fig. S3B]. The levels of phosphate and urea were not significantly different between the groups [online Fig. S3C and D].

3.3. Extent of induced cardiovascular calcification

By means of von Kossa staining of cross-sections through the aortic valves, the local hydroxyapatite deposition was determined. In all groups with VD supplementation, progressive calcification occurred, which was more evident in the commissural region and appeared at earlier time points than in the sinus wall [Fig. 1A–F]. After 12 weeks, the onset of calcium deposition was also observed in the aortic valve leaflets [Fig. 1B, D and E] [online Fig. S4]. Semi-quantitative evaluation resulted in significantly increased calcification in the high-dose VD groups (HIGH, I_{-CH}, II_{-PH}), as compared to animals with reduced or without any additional VD supplementation (groups N, LOW and III_{-VD}) [Fig. 1G–I]. However, also animals receiving a reduced level of supplemented VD exhibited a strong trend towards increased calcification when compared to groups without any additional dietary VD, although this difference was not statistically significant at any time point.

Von Kossa staining of aortic cross-sections revealed extensive hydroxyapatite deposition predominantly in the aortic media of all animals supplemented with high-dose VD, whereas low-dose VD in group LOW resulted in slowly progressing micro-calcification [Fig. 2A–F]. By means of a von Kossa staining score system, the increase of calcification in the groups HIGH, I_{-CH} and II_{-PH} was shown to reach significance versus each of the groups with reduced or without VD supplementation after 12 weeks [Fig. 2G–I].

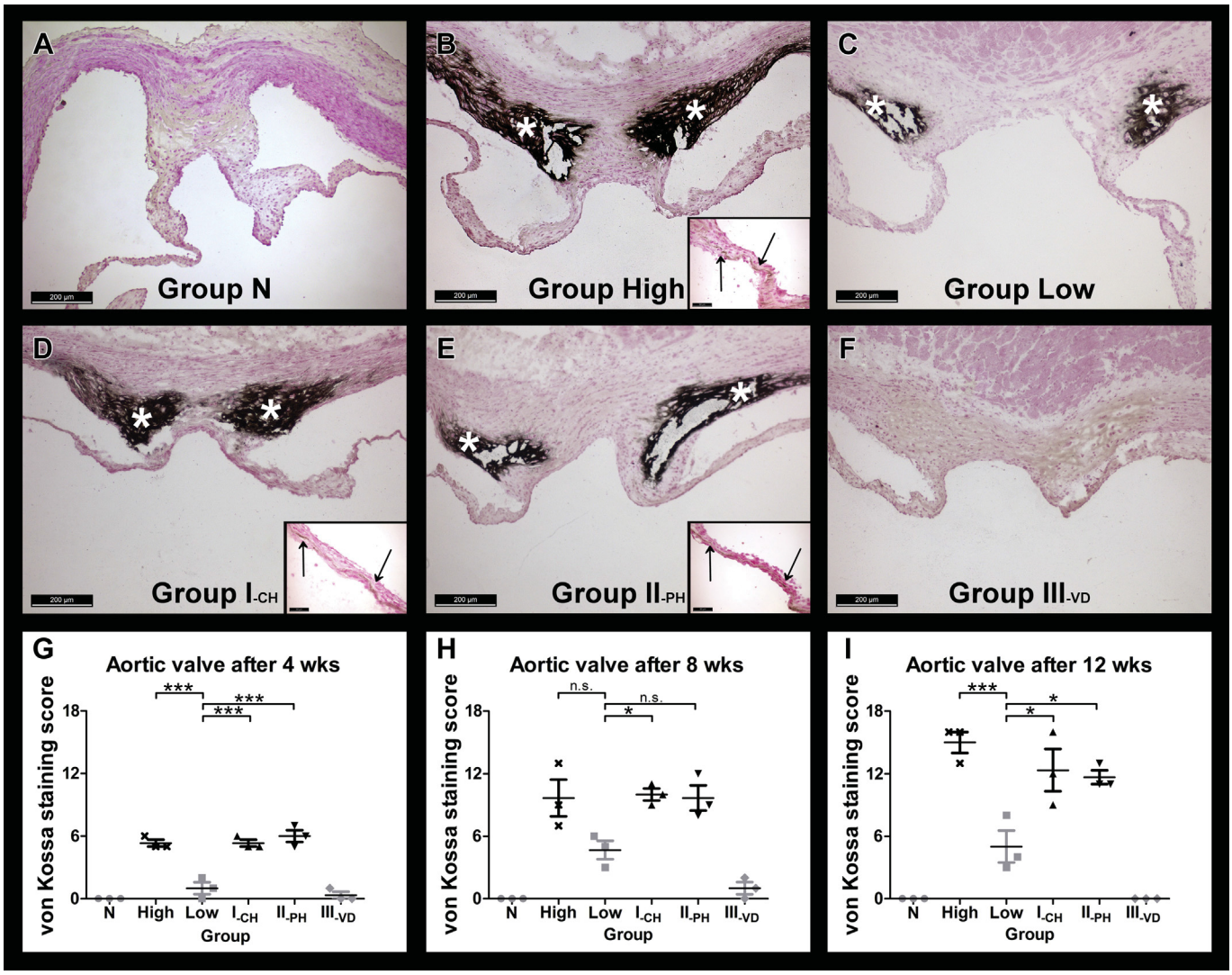

Fig. 1. Calcification of the aortic valve. Representative cross-sections through the aortic valve after 12 weeks of diet showed extensive hydroxyapatite deposition (brown; white asterisks) in all animals receiving VD supplementation, particularly in the commissural region (A: group N; B: group HIGH; C: group LOW; D: group I_{-CH}; E: group II_{-PH}; F: group III_{-VD}). A semi-quantitative scoring system based on von Kossa staining revealed a progressive hydroxyapatite deposition with significantly increased calcium burden in the high-dose VD groups (HIGH, I_{-CH}, II_{-PH}), as compared to animals with reduced or without VD supplementation in the groups N, LOW and III_{-VD} (G–I). In the leaflets of VD-supplemented rats, micro-calcification (arrows) occurred after 12 weeks (small pictures in B, D and E); high magnification pictures of the leaflets are available in [online Fig. S4]. Von Kossa staining; scale bars = 200 μm (50 μm in the small pictures); n.s., statistically not significant; $^{*}p < 0.05$; $^{***}p < 0.001$ (For interpretation of the references to color in this figure legend, the reader is referred to the web version of this article.).

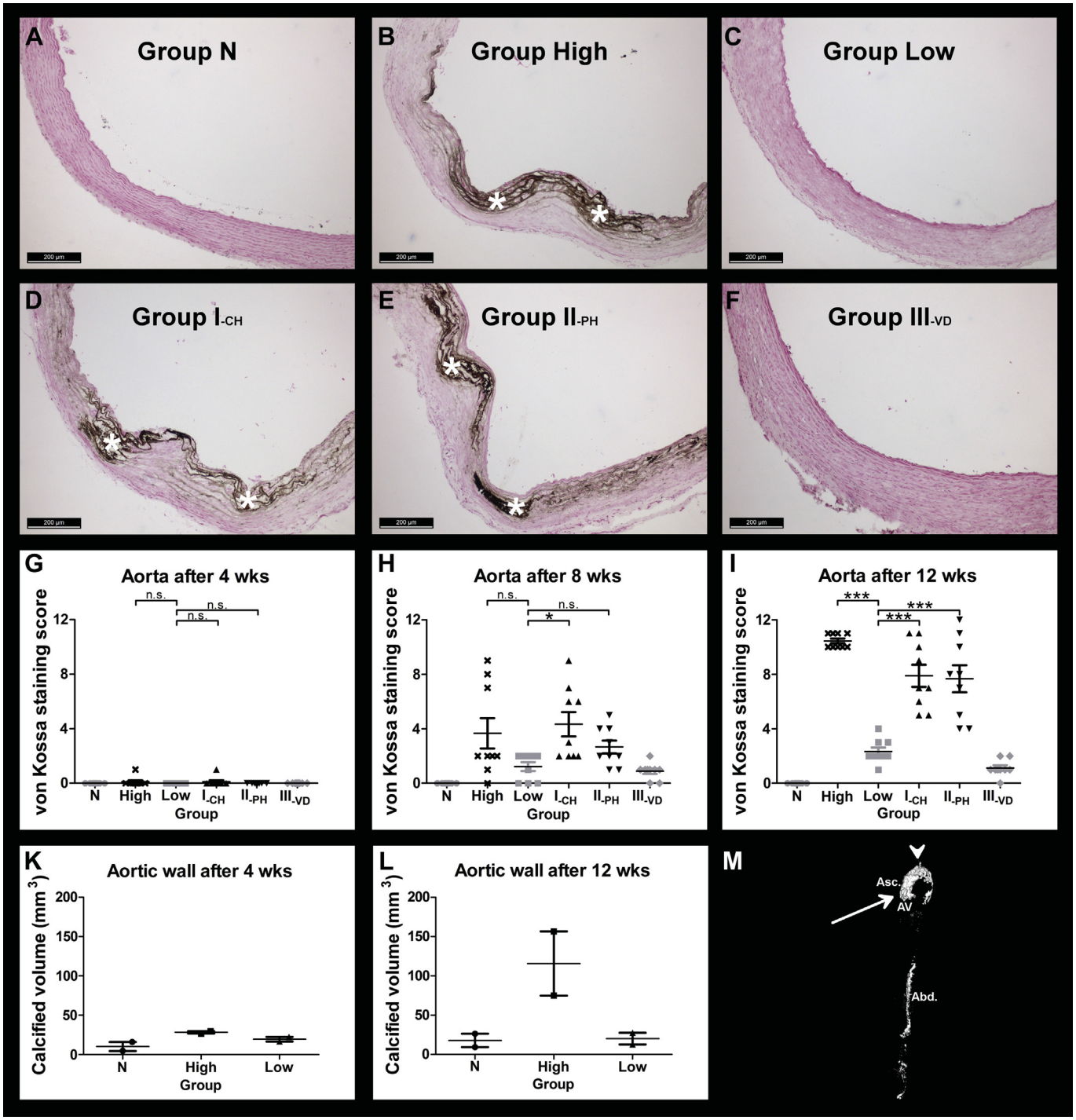

Fig. 2. Calcification of the aorta. Representative cross-sections through the aortic wall after 12 weeks of dietary supplementation showed extensive hydroxyapatite deposition (brown; white asterisks) in all animals receiving high-dose VD supplementation (B: group HIGH; D: group I_{-CH}; E: group II_{-PH}). A semi-quantitative von Kossa staining scoring system revealed a progressive hydroxyapatite deposition with significantly increased calcium burden in the high-dose VD groups (HIGH, I_{-CH}, II_{-PH}) at 12 weeks, as compared to animals with reduced or without VD supplementation in the groups N, LOW and III_{-VD} (G–I). Von Kossa staining; A, group N; C, group LOW; F, group III_{-VD}; scale bars = 200 μm; n.s., statistically not significant; $^{*}p < 0.05$; $^{***}p < 0.001$. μCT-based quantification of the total amount of calcium in the aortic wall revealed generally low values after 4 weeks in all groups (K), while after 12 weeks, the calcium burden in group HIGH was remarkably enhanced versus the groups N and LOW (L). Representative 3D rendering of the μCT data set showing the spatial distribution of calcium deposition in the aorta of an animal in group HIGH after 12 weeks of pro-calcific diet: The main calcium burden was located in the aortic valve annulus (arrow), the ascending aorta, the aortic arch (arrow head) and, to a lesser extent, in the proximal abdominal aorta (M). AV, aortic valve; Asc., ascending aorta; Abd., abdominal aorta (For interpretation of the references to color in this figure legend, the reader is referred to the web version of this article.).

The spatial distribution as well as the total volume of calcium deposition in the whole aorta were determined by *ex vivo* μCT. After 4 weeks, the calcium burden in the groups N, HIGH and LOW was generally low with a slight enhancement in group HIGH [Fig. 2K]. After 12 weeks, the aortic calcification in group HIGH was remarkably augmented, while the groups N and LOW did not exhibit relevant calcification assessable by μCT [Fig. 2L]. The main calcium burden of group HIGH was found in the aortic annulus, the

ascending aorta and the proximal aortic arch, while the proximal abdominal aorta was less calcified and the descending thoracic as well as the distal abdominal aorta did not show any relevant calcification [Fig. 2M].

3.4. Mechanisms of induced cardiovascular degeneration

In order to examine the MMP activity in the native aortic valves, *in situ* zymography was conducted. Generally, increased MMP activity was co-localized with the calcium deposition in the aortic tissue, particularly the commissural wall [Fig. 3A and B]. Similarly to the results for calcification, the MMP activity was significantly increased in the high-dose VD groups (HIGH, I_{-CH}, II_{-PH} vs. groups N, LOW and III_{-VD}) after 12 weeks, indicating enhanced tissue remodeling activity [Fig. 3C].

The MMP activity in the aortic wall was generally higher than the activity in the aortic valve tissue. In the high-dose VD groups, it was enhanced as compared to other groups, whereas only the following differences were statistically significant [Fig. 3D]: Groups HIGH and II_{-PH} versus group N with $p < 0.01$ and $p < 0.001$, respectively; group II_{-PH} versus group LOW with $p < 0.05$; groups HIGH, I_{-CH} and II_{-PH} versus group III_{-VD} with $p < 0.01$, $p < 0.05$ and $p < 0.001$, respectively. Peak activity values were located in areas of progressive wall calcification.

After 4 weeks of feeding with supplemented diet compositions, we found lipid vacuoles in the commissural and sinus wall of aortic valves in all groups, whereas the groups with high-dose VD and CH (HIGH and II_{-PH}) showed more vacuoles per cross-section. After 12 weeks, the vacuole content in the groups HIGH and II_{-PH} was unchanged, while the valves of all other groups did not contain vacuoles any more [Fig. 4A–C]. Areas with remaining lipid vacuoles were co-localized with calcification at later follow-up. In these regions, the early chondrocyte marker syndecan-3 was detected [Fig. 4D], cells with a chondrogenic phenotype occurred [Fig. 5A and B], and staining against 3-nitrotyrosine, a marker for reactive nitrogen species-induced nitrosative stress and apoptosis, was positive [Fig. 5C]. In areas of extensive calcification in the groups HIGH and I_{-CH}, hyperplastic neointima formation involving spindle-shaped cells occurred at the commissural and sinus walls after 12 weeks [Fig. 5E and F].

Cells in the aortic media were characterized by means of immunohistology. While after 4 weeks, all cells stained positive for aSMA, the calcified areas after 12 weeks contained cells staining negative for aSMA and desmin.

H&E staining did not reveal relevant invasion of inflammatory cells into the aortic valve region or the aortic wall, and staining against the inflammatory cell markers CD3 and CD68 was negative throughout all groups [data not shown].

3.5. Quantitative gene expression analysis in the diet study

In order to elucidate changes in gene expression profiles triggered by dietary treatment, quantitative RT-PCR for different marker genes of inflammation and thrombogenicity (CD39, CD73,

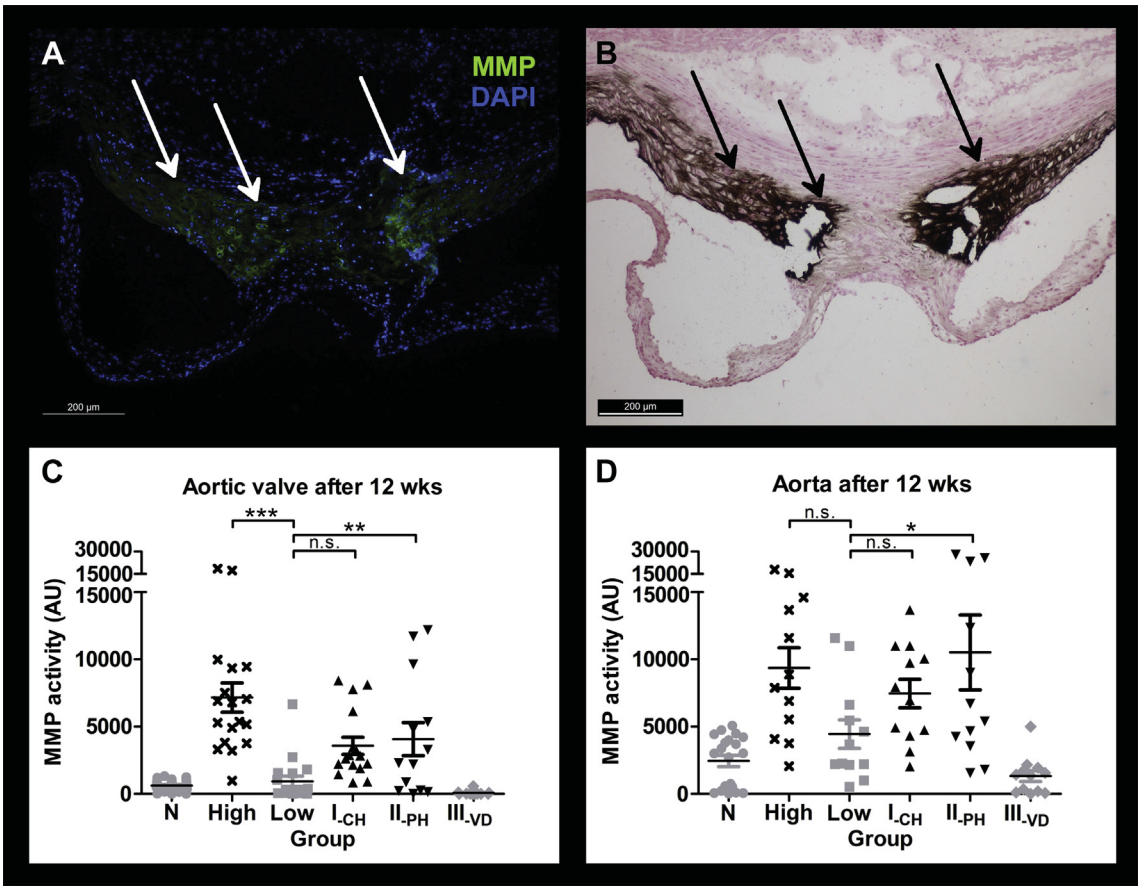

Fig. 3. Chow-dependent MMP activity. A representative cross-section through the aortic valve (group HIGH at 12 wks) shows the typical pattern of enhanced MMP gelatinase activity in the commissural wall (white arrows in A), co-localized with extensive hydroxyapatite deposition (black arrows in B). After 12 weeks, the MMP activity in the aortic valve of the high-dose VD groups (HIGH, I_{-CH}, II_{-PH}) was increased as compared to all other groups (C). The MMP activity in the aortic wall was generally higher than in the aortic valve, again with enhanced values in the high-dose VD groups (D). A, *in situ* zymography; B, von Kossa staining; scale bars = 200 µm; AU, arbitrary units; n.s., statistically not significant; $^{*}p < 0.05$; $^{**}p < 0.01$; $^{***}p < 0.001$.

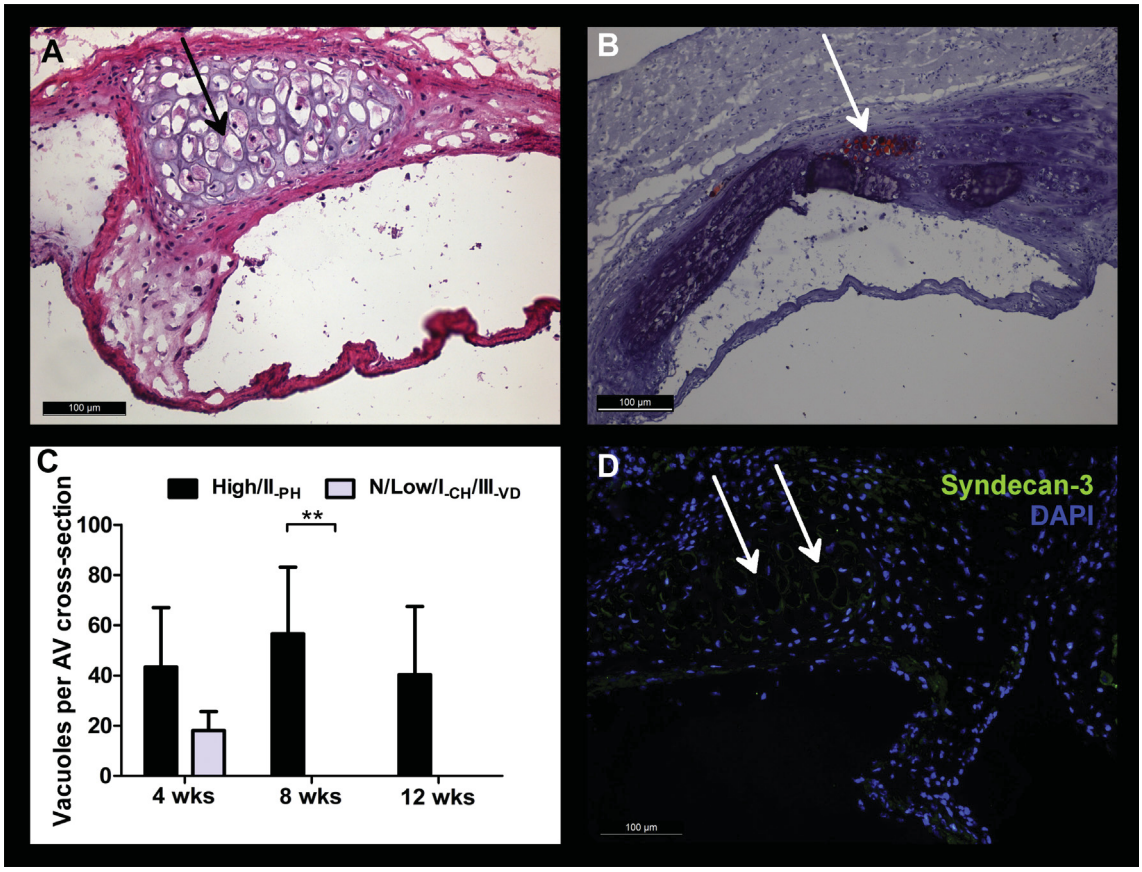

Fig. 4. Lipid vacuoles at calcification sites. Representative aortic valve cross-sections demonstrate lipid vacuoles (arrows) next to chondrogenic cells in group HIGH after 12 weeks (A, B). After 4 weeks, islets of lipid vacuoles were observed in the aortic valve of all groups, particularly in the sinus wall. At later time points, only the groups receiving high-dose VD and CH (HIGH and II_{-PH}) exhibited vacuoles (C). Areas with lipid deposition and chondrogenic cells stained positive for the early chondrocyte marker syndecan-3 (D). A, H&E staining; B, Oil Red O staining; C, total vacuole count per cross-section as mean value of the indicated groups; D, immunohistological staining for syndecan-3 (green) with nuclear counterstaining (DAPI, blue); scale bars = 100 µm; $^{**}p < 0.01$ (For interpretation of the references to color in this figure legend, the reader is referred to the web version of this article.).

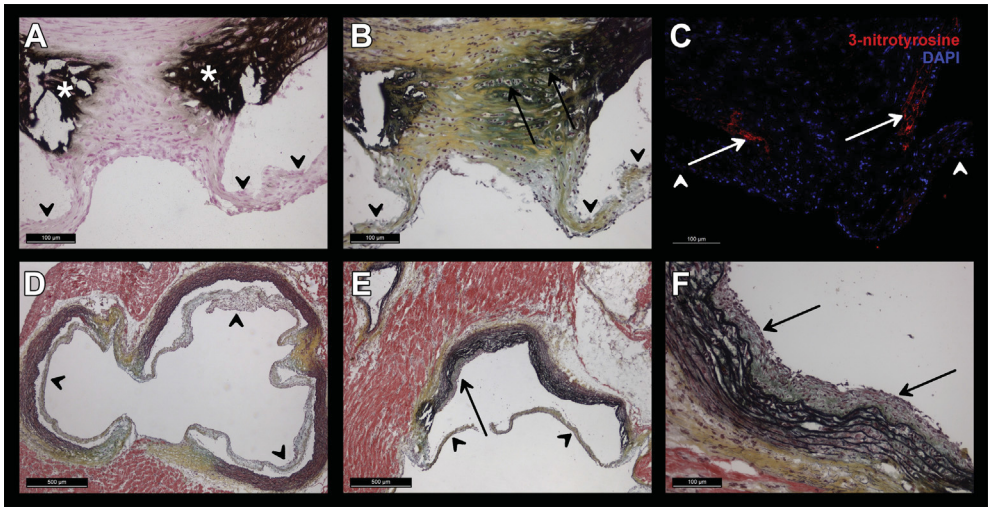

Fig. 5. Adverse remodeling at calcification sites. Representative cross-sections through aortic valves in group HIGH after 12 weeks showing sites of extensive calcification (white asterisks in A) with co-localized chondroid cells (black arrows in B) and 3-nitrotyrosine production (white arrows in C). In contrast to non-calcified aortic valves (D: group III_{-VD}), these calcified areas exhibited hyperplastic neointima formation (black arrows in E, F). A, von Kossa staining; B, D–F, Movat's pentachrome staining; C, immunohistological staining for 3-nitrotyrosine (red) with nuclear counterstaining (DAPI, blue); arrow heads point to aortic valve leaflets; scale bars = 200 µm (A–C, F) or 500 µm (D, E), respectively.

RAGE and HIF1a) as well as chondro-osteogenic transformation (OPN, OCN and RUNX2) was conducted. We observed a significant up-regulation of genes encoding for CD39, CD73 and OPN, as well as the transcription factor RUNX2 in animals receiving a pro-calcific diet [Fig. 6]. Especially the OPN values in group HIGH were remarkably elevated as compared to the groups N and LOW.

3.6. *In vivo outcome of aortic conduit implants under pro-calcific metabolic conditions*

3.6.1. *Operative outcome and implant function*

Overall survival after implantation of the aortic conduits amounted for 100%. Six weeks after onset of the severely pro-calcific diet, the body weight of the recipient rats reached a peak value in both groups and decreased afterwards [online Fig. S5]. All rats fed with pro-calcific chow for a total of 14 weeks showed signs of physical impairment at the end of the study.

Doppler sonography at the time of graft implantation and explantation revealed unimpaired perfusion of the aortic conduits in all animals.

3.7. *Adverse graft remodeling*

The luminal surface of the decellularized aortic conduits (group DC) underwent fast cellular repopulation. After 4 weeks, approximately half of the inner surface was covered with neointima, and after 12 weeks, the recellularized area amounted for nearly 100%. The luminal cell layer of the intima stained positive for vWF, indicating endothelial cells. However, a progressive formation of hyperplastic neointima, involving predominantly aSMA positive cells, was also observed [online Fig. S6A]. This phenomenon of adverse graft remodeling was even more distinct in the cryopreserved aortic conduit allografts (group CRYO) [online Fig. S6B]. While the neointima in group DC predominantly consisted of cells with a spindle-shaped phenotype [online Fig. S6C], large areas with chondroid cells and extensive intercellular substance occurred in the hyperplastic neointima of group CRYO [online Fig. S6D]. Comparative quantification of the neointima hyperplasia by determining the intima-to-media ratio revealed a significant time-dependent progression ($p < 0.0001$) with decreased values in group DC versus group CRYO (d28: 0.1 ± 0.04 vs. 0.7 ± 0.14 with $p < 0.001$; d84: 0.8 ± 0.10 vs. 1.0 ± 0.09 (n.s.)) [Fig. 7].

In group CRYO, large clusters of inflammatory cell infiltration occurred at both time points [Fig. 7B and D]. After 4 weeks, immunohistology staining showed intensive accumulation of CD3 in the neointima of group CRYO [online Fig. S7D], while the grafts of group DC did not exhibit CD3 positive inflammatory cells at all [online Fig. S7C].

By means of *in situ* zymography, the MMP gelatinase activity in the aortic conduit grafts was measured. Four weeks after implantation, the MMP activities of both groups did not differ, however, after 12 weeks, the MMP activity was increased ($p < 0.0001$ vs. d28)

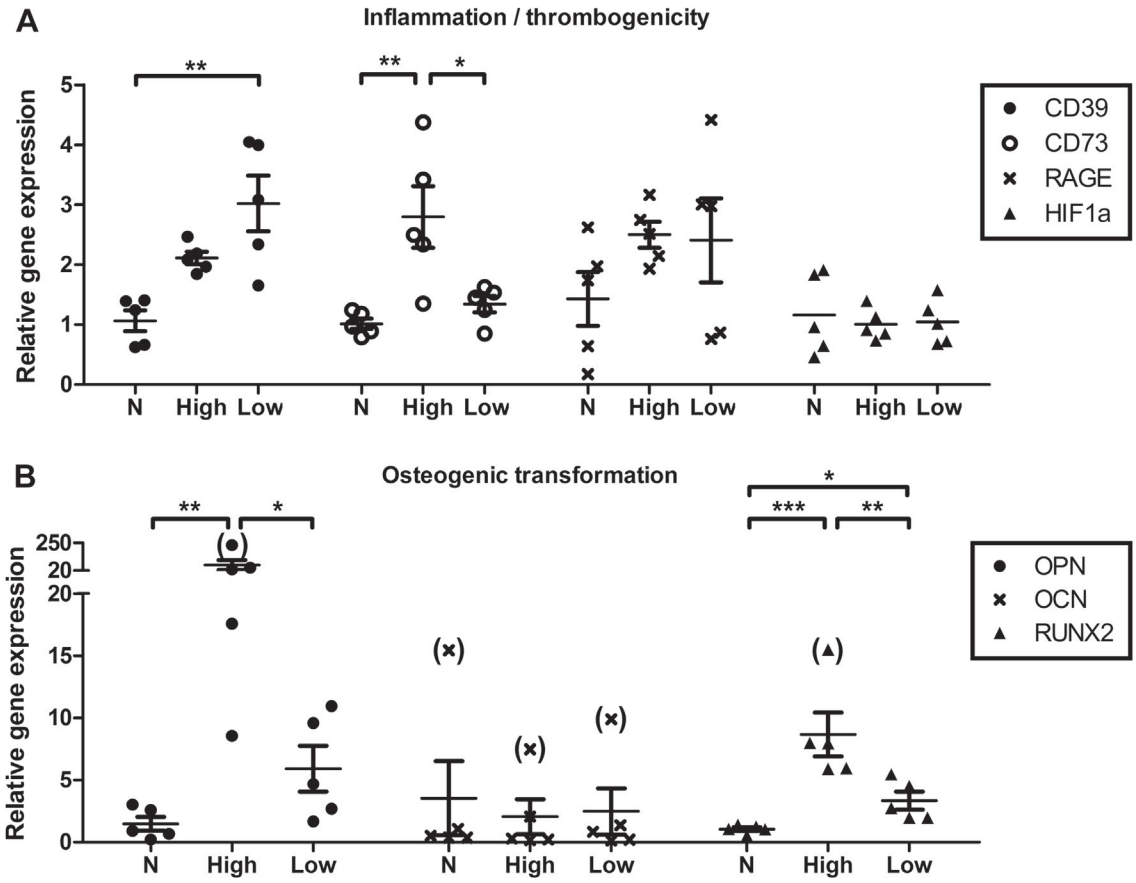

Fig. 6. Pro-calcific diet leads to altered gene expression in the aortic wall. Relative gene expression analysis in the aortic wall tissue after 12 weeks was performed in three groups receiving normal chow (group N), high-dose pro-calcific diet (group HIGH) and low-dose pro-calcific diet (group LOW) by means of quantitative RT-PCR (ddCt method). Different markers of inflammation and thrombogenicity (A) as well as chondro-osteogenic transformation (B) were analyzed. Gene expression of CD39, CD73, OPN and RUNX2 was significantly up-regulated by pro-calcific diet, indicating a profound pro-inflammatory and pro-degenerative change induced by the applied dietary treatment. RAGE, receptor for advanced glycation end products; HIF1a, hypoxia-inducible factor-1-alpha; OPN, osteopontin; OCN, osteocalcin; RUNX2, runt-related transcription factor-2; $^{*}p < 0.05$; $^{**}p < 0.01$; $^{***}p < 0.001$; values in brackets excluded from statistical group comparison.

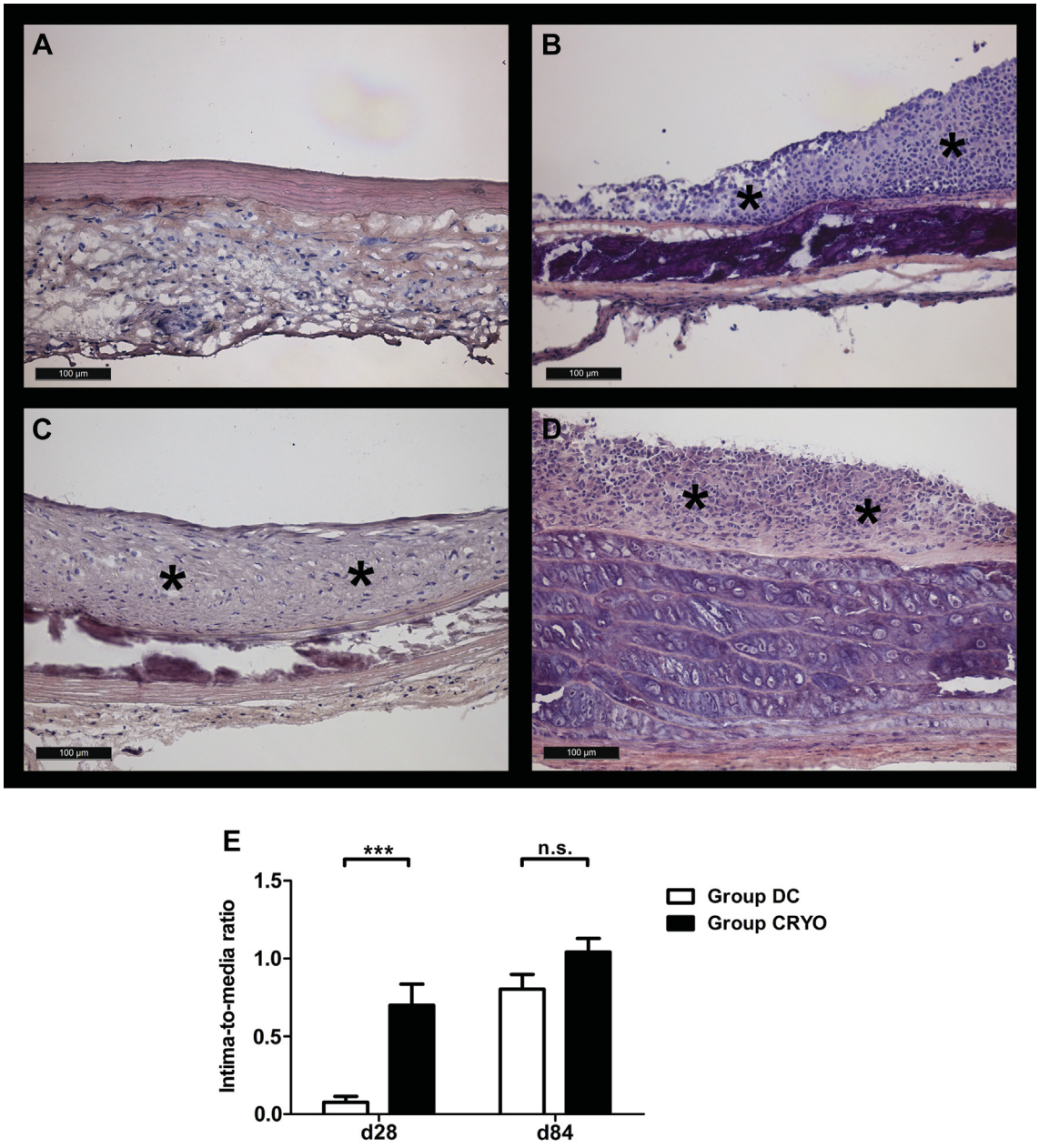

Fig. 7. Quantity of hyperplastic neointima in the aortic conduit grafts. After 4 weeks *in vivo* under pro-calcific metabolic conditions, hyperplastic neointima formation (black asterisks) was a rare event in decellularized aortic conduit grafts (A: group DC), while cryopreserved counterparts showed extensive early hyperplasia (B: group CRYO). After 12 weeks, adverse graft remodeling had proceeded in both groups (C: group DC, D: group CRYO). In group CRYO, the neointima contained multiple cellular clusters with inflammatory cells (asterisks). The intima-to-media ratio in the whole aortic conduit grafts was significantly increased in group CRYO after 4 weeks (E). Hematoxylin/eosin staining; scale bars = 100 µm; ***$p < 0.001$; n.s., statistically not significantly different.

with significantly higher values in group DC as compared to group CRYO ($p < 0.001$ at d84) [online Fig. S8].

3.8. Graft calcification

In order to visualize the calcification of the implants, von Kossa staining was performed, and the calcium burden was semi-quantitatively evaluated. The analyses revealed a progressive hydroxyapatite deposition (with $p < 0.001$ at d84 vs. d28) predominantly in the graft media. Statistical group comparisons resulted in increased early calcification in group CRYO after 4 weeks ($p < 0.01$) [Fig. 8A–E]. Micro-CT imaging showed severe calcification of the whole aorta and the implant [Fig. 8F].

In the severely calcified areas of the media of group CRYO, large clusters of cells with a chondroid phenotype occurred after 12 weeks [online Fig. S9A and B]. These cells partially stained positive for the chondrocyte differentiation marker syndecan-3 [online Fig. S9C].

4. Discussion

In the present study, we sought to develop and characterize a standardized and reliable small animal model of accelerated aortic valve as well as arterial calcification by dietary supplementation with VD, CH and PH. The optimal dietary regimen was then applied to an *in vivo* model of heterotopic aortic conduit implantation to

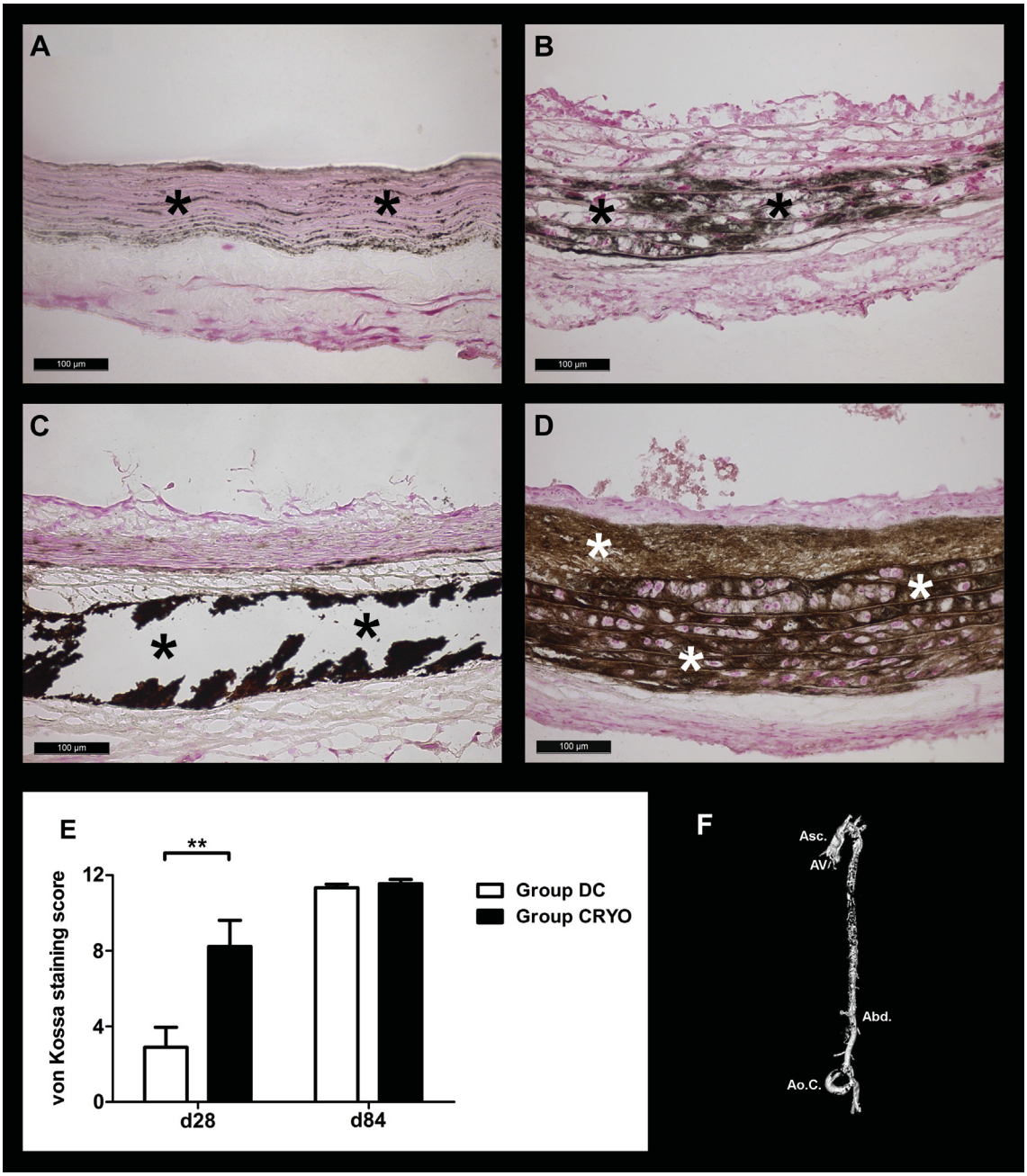

Fig. 8. Implant calcification under pro-calcific metabolic conditions *in vivo*. Representative cross-sections through the ascending aorta of decellularized (A, C: group DC) and cryopreserved (B, D: group CRYO) conduit grafts showed a progressive hydroxyapatite deposition (brown; asterisks) after 4 weeks (A, B) and 12 weeks (C, D) under pro-calcific conditions. Calcification was predominantly present in group CRYO with early onset in the media. von Kossa staining; scale bars = 100 µm. By means of a semi-quantitative von Kossa staining scoring system, a time-dependent progression of calcification was shown in both groups ($p < 0.0001$ for week 4 vs. week 12). Moreover, at 4 weeks, the calcium burden was significantly increased in group CRYO vs. DC (E). $^{**}p < 0.01$. Three-D rendering of the µCT data set showing the spatial distribution of calcium deposition in the aorta and the aortic conduit implant (Ao.C.) of an animal in group CRYO after 12 weeks. AV, recipient aortic valve; Asc., recipient ascending aorta; Abd., recipient abdominal aorta (For interpretation of the references to color in this figure legend, the reader is referred to the web version of this article.).

evaluate the effect of pro-calcific metabolic conditions on the aortic conduit graft remodeling *in vivo*.

VD and CH have been previously used to induce aortic valve sclerosis in rabbits and atherosclerosis in rats, respectively [10–12]. However, the majority of previous work has been largely focused on the calcifying degeneration of the aorta, whereas systematic exploration of the diet-mediated calcific degeneration of the aortic valve has not been previously reported in rats. Even more interestingly, in combination with a recently introduced standardized model of aortic conduit implantation, the present model facilitates comparative evaluation of the *in vivo* degeneration of biological and tissue-engineered cardiovascular grafts within short periods of time.

4.1. Dietary induction of degeneration of the aortic valve

The MMP activity has been suggested as a general marker for enhanced tissue remodeling activity, which has been described to be a consistent feature of cardiovascular degeneration in the course of atherosclerosis as well as aortic valve degeneration [17–22].

Moreover, the participation of migrating and tissue-invading cells, e.g. monocytes and macrophages, in the progression of aortic stenosis has been demonstrated to be partially MMP-dependent [23]. Determining the MMP activity in the native aortic valve after 12 weeks of feeding, we found enhanced tissue remodeling predominantly in the commissural region of the aortic root in all experimental groups receiving high-dose VD supplementation. These results are in line with data derived from studies in other species showing the association of MMP activity with aortic valve degeneration, and specifically with fragmentation of elastin fibers [20,21]. In particular, MMP-2 and MMP-9 were shown to be actively involved in early calcium deposition in elastin fiber constructs which had been subcutaneously implanted in rats [24,25].

In the present study, calcification was predominantly co-localized with increased MMP activity at the commissural walls. The amount of deposited calcium was directly associated with the applied dose of VD and subsequently increased calcium serum levels. It has been previously reported that dietary regimens consisting of VD and CH or VD alone induce calcification and functional impairment of aortic valves in rabbits, whereas CH supplementation alone did not lead to relevant calcifying degeneration [11,12]. Similarly, we found VD supplementation alone to be sufficient to enhance aortic valve sclerosis, independently on CH supplementation, although in the present rat model, higher VD doses were necessary to induce extensive calcification after 8–12 weeks, as compared to the rabbit models mentioned above (approximately 240,000 vs. 150,000 [11] or 45,000 [12] IU/kg BW/week).

In our experiments, animals kept on a dietary CH-containing regimen showed enhanced LDL/HDL ratios. In animals receiving high-dose VD and CH, we observed multiple lipid vacuoles in the commissural walls at all time points, while the vacuoles in all other groups disappeared during the follow-up. These vacuoles at the predestined sites of calcification stained positive for the early chondrocyte differentiation marker syndecan-3. At advanced stages of degeneration after 8 and 12 weeks, cells with a chondrogenic phenotype occurred. We regard these changes to be partly comparable to those observed in human aortic valve degeneration. It has been previously hypothesized that lipid deposition in the interfibrillar spaces and chondro-osteogenic transformation of interstitial cells with subsequent biomineralization are key mechanisms in the development of aortic valve sclerosis [26,27]. However, it remains unclear whether these processes are independent events in the course of aortic valve degeneration or interactive features of one biological program activated by a yet unknown pathophysiological trigger.

As a further feature of calcific degeneration, we observed nitrosative stress and apoptosis as induced by reactive nitrogen species. These findings parallel previous studies which suggested nitric oxide donors to act in a protective manner against chondro-osteogenic transformation, and enhanced tissue resistance to nitric oxide to be associated with the progression of human aortic valve sclerosis [28,29].

At sites of advanced lesions including the endothelial layer of the commissural and sinus wall at the level of the aortic root, hyperplastic neointima formation involving spindle-shaped cells was observed. Intimal hyperplasia by proliferation of aSMA positive cells is known to occur at advanced stages of atherosclerosis in humans or at sites of endothelial injury [30,31].

Recently, inflammation, particularly by macrophage invasion, has been shifted into the focus of research on calcific aortic valve as well as arterial degeneration [32,33]. However, inflammation is only one of a number of different aspects of calcifying aortic valve degeneration in humans, and the extent of inflammatory infiltration has been reported to be only marginally correlated with the severity of the disease [34,35]. In the present rat model of accelerated calcifying degeneration, we did not observe relevant inflammation in the aortic valve cusp tissue. In rats developing aortic valve calcification after high-dose PH feeding, only a few macrophages have been observed by others [36]. However, taking into account the chronic process of low-level inflammatory tissue remodeling, this yet very modest level of inflammation may ultimately exert a sufficiently negative impact in the sense of a vicious circle that has been previously described for the development and progression of aortic valve degeneration [23,26].

The value of dietary regimens with supplementation of VD and CH in rabbits has been recently questioned, since in some reports, the authors could not observe any change of aortic valve pressure gradients after 3 months of feeding, and the detected calcification has affected the ascending aorta only [37]. However, there are conflicting data, and other studies with a similar chow regimen have resulted in enhanced pressure gradients after 12 weeks [11]. In the present study, the increase of the pressure gradients in rats after 12 weeks was even higher than the values observed in the aforementioned rabbit model. Moreover, we detected extensive calcification not only in the ascending aorta, but also at the basis of the aortic valve leaflets, and micro-calcification in the region of the free edge of the aortic valve leaflets. A calcification focus at the leaflet basis parallels the pathological changes observed in patients undergoing aortic valve replacement due to stenotic degeneration. This pattern of plaque location can be explained by low shear stress and high flow disturbance at these sites, favoring the development of atherosclerotic lesions [38–40].

Collectively, we regard the presented dietary regimen to be a well suited model for the creation of extreme pro-degenerative conditions *in vivo*, providing a platform to study the involved biological events in native tissues and organs or in biological implants. In the second line, further elaboration of the presented regimens appears as a meaningful next step to expand the functional character of aortic valve stenosis, which in turn may be used for a wide range of studies on preventive and therapeutic strategies against cardiovascular calcific degeneration.

4.2. Chow-induced degeneration of the aorta

The histological and molecular-biological findings on the aortic wall as induced by the different chow regimens are discussed in the online supplementary data.

4.3. Selection of the chow regimen for observational studies

The presented data show pro-calcific diets containing high-dose VD (300,000 IU/kg) to induce significant calcification at the level of the aortic valve as well as the great arterial vessels. Dietary compositions including VD and CH may be rather preferable, since they elevate the LDL/HDL ratio, which is an important aspect of calcific degeneration of the cardiovascular system in humans. Moreover, the content of lipid vacuoles was increased when high-dose VD and CH were fed at the same time. The additional application of PH further enhanced the LDL/HDL ratio as well as the calcium deposition in the aortic valve and the aorta to an even larger extent.

However, high-dose VD administration affected not only the cardiovascular system, but also resulted in physical impairment and loss of body weight after 8–12 weeks. Therefore, these dietary regimens should not be used in projects with longer follow-up. For studies with observational periods >12 weeks or experiments not primarily focusing on calcifying aspects of arterial degeneration or implant degeneration, a regimen with lower dose VD (150,000 IU/kg), CH and PH seems to be suitable. The current data suggest that the latter treatment features a slower progression of calcium deposition allowing for physiological somatic growth, while yet

leading to increased transvalvular pressure gradients of the aortic valve, which in our study, even exceeded the values obtained by the high-dose chow regimen.

4.4. Decellularized versus cryopreserved cardiovascular grafts

The suitability of the present model to examine the *in vivo* degeneration of different types of cardiovascular implants was tested by implanting decellularized and cryopreserved aortic conduits, which were followed up for 12 weeks.

Fast endoluminal cellular repopulation is an important process enhancing the biocompatibility and reducing the thrombogenicity of acellular cardiovascular implants. Autologous recellularization of the decellularized prostheses reached 100% of the luminal surface area within 12 weeks. This result conforms to the findings of a previous study in our small animal model showing early and complete recellularization of decellularized aortic conduit grafts [8]. However, cellular population of implant surfaces is regularly accompanied by hyperplastic intima formation. In the systemic circulation, aortic allografts experience progressive intima hyperplasia in the first 3–5 months, as demonstrated in different small and large animal models [41,42]. Decellularization has been shown to inhibit this process of bio-implant degeneration, as confirmed in different implantation models and different species [3,43,44]. Histologically, areas of intimal hyperplasia have repeatedly been characterized by containing proliferating spindle-shaped fibroblast-like cells expressing aSMA as major cellular component and an endoluminal layer of endothelial cells [45]. These findings confirm the observations of the present study. Moreover, we did not observe inflammatory infiltration in the decellularized group. In contrast, the cryopreserved control implants showed extensive CD3(+) cellular infiltration after 4 and 12 weeks. Similarly, cryopreserved rat allografts have been reported to show increased infiltration of mononuclear cells and T-lymphocytes 7 days after heterotopic implantation, while syngeneity and the lack of cryopreservation reduced the inflammation in the implants [46].

In cryopreserved allografts of the present study, particularly in the conduit parts with expanded hyperplasia, inflammatory infiltration was accompanied by chondro-osteogeneic cell differentiation. Both processes represent early stages of adverse remodeling which ultimately results in calcifying degeneration and deterioration of the allogeneic prostheses. Fast and progressive calcification of heart valve allografts has been reported to be detectable histologically as well as radiographically already 6 months after implantation in the pulmonary position in a sheep model, even though the extent of calcification in this model has been lower [47]. In the present standardized model of aortic conduit allografting into the systemic circulation of rats, detergent-based decellularization decreased the calcium deposition when compared to cryopreserved cellular grafts, adding further evidence to the advantageous outcome of decellularized arterial grafts.

4.5. Correlation with clinical data

Grafting of cryopreserved allogeneic heart valves is known to induce a donor-specific immune response by the recipient, particularly against human leukocyte antigens (HLA) class I and II, which are presented at the surface of the donor cells [48,49]. Implantation of decellularized grafts not exhibiting HLA may solve the main issue regarding immunogenicity and subsequent deterioration of the prostheses.

In a study on 38 patients with pulmonary valve replacement, fresh decellularized allografts showed reduced rates of necessity for operative graft revision and lower mean transvalvular gradients after 5 years, when compared to matched controls receiving glutaraldehyde-fixed bovine jugular vein grafts or cryopreserved homografts [50]. Retrospective analyses on decellularized and subsequently cryopreserved pulmonary allografts versus cryopreserved allogeneic control prostheses revealed a strong trend towards enhanced freedom from reoperation and major insufficiency, and reduced transvalvular gradients [51–53]. The reported reoperation rates after 5 years reach up to 25% for cryopreserved pulmonary valve implants, while they do not exceed 15% in case of decellularized grafts [50,52]. With regard to fresh as well as cryopreserved decellularized prostheses in the aortic valve position, promising early functional results have been recently published [4,5]. However, further randomized controlled trials including long-term studies are required to evaluate the impact of decellularization on the degeneration of aortic heart valve implants in humans.

4.6. Study limitations

The model of accelerated cardiovascular calcification is limited due to the anatomy and the physiology of small rodents. Rats are known to be less prone to atherosclerosis than humans. Since they do not develop the disease morphology spontaneously, high doses of pro-calcific supplements are necessary, which in turn limits the extent to which the resulting changes exactly mimic the metabolic conditions in human cardiovascular diseases and direct conclusions can be derived thereof.

5. Conclusions

In the present study, a standardized rat model of calcifying degeneration of the aortic valve as well as the arterial vessels was developed by supplementation with varying combinations of VD, CH and PH. For studies with observational periods >12 weeks, the application of low-dose VD, CH and PH is suitable to induce pro-degenerative metabolic conditions *in vivo*. In combination with surgical models of functional aortic valve implantation available in rats, the presented dietary induction of pro-calcific metabolic conditions allows for an in-depth evaluation of the *in vivo* fate of biological and tissue-engineered aortic conduits within short time periods. Applying this combined model, decellularization was shown to decelerate inflammation, neointimal hyperplasia and destructive calcification in cardiovascular implants. Thereby, decellularized aortic allograft conduits are promising alternatives to cryopreserved allografts routinely used in cardiac surgery.

Acknowledgments

The authors gratefully acknowledge the blood serum analyses conducted by the Institute of Clinical Chemistry and Laboratory Diagnostics, Heinrich Heine University, Medical Faculty, Duesseldorf, Germany. Moreover, the authors gratefully thank Christofer Delfs and Marc Struβ (Department of Cardiovascular Surgery and Research Group for Experimental Surgery, Medical Faculty, Heinrich Heine University Duesseldorf, Germany) for their support during the animal experiments, and Gisela Müller (Department of Cardiovascular Surgery and Research Group for Experimental Surgery, Medical Faculty, Heinrich Heine University Duesseldorf, Germany) for her help in the PCR experiments.

Appendix A. Supplementary data

Supplementary data related to this article can be found at http://dx.doi.org/10.1016/j.biomaterials.2014.05.034.

References

[1] Schoen FJ, Levy RJ. Calcification of tissue heart valve substitutes: progress toward understanding and prevention. Ann Thorac Surg 2005;79:1072–80.
[2] Akhyari P, Kamiya H, Gwanmesia P, Aubin H, Tschierschke R, Hoffmann S, et al. In vivo functional performance and structural maturation of decellularised allogenic aortic valves in the subcoronary position. Eur J Cardiothorac Surg 2010;38:539–46.
[3] Baraki H, Tudorache I, Braun M, Höffler K, Görler A, Lichtenberg A, et al. Orthotopic replacement of the aortic valve with decellularized allograft in a sheep model. Biomaterials 2009;30:6240–6.
[4] da Costa FD, Costa AC, Prestes R, Domanski AC, Balbi EM, Ferreira AD, et al. The early and midterm function of decellularized aortic valve allografts. Ann Thorac Surg 2010;90:1854–60.
[5] Zehr KJ, Yagubyan M, Connolly HM, Nelson SM, Schaff HV. Aortic root replacement with a novel decellularized cryopreserved aortic homograft: postoperative immunoreactivity and early results. J Thorac Cardiovasc Surg 2005;130:1010–5.
[6] Schoen FJ. Evolving concepts of cardiac valve dynamics: the continuum of development, functional structure, pathobiology, and tissue engineering. Circulation 2008;118:1864–80.
[7] Assmann A, Akhyari P, Delfs C, Flögel U, Jacoby C, Kamiya H, et al. Development of a growing rat model for the in vivo assessment of engineered aortic conduits. J Surg Res 2012;176:367–75.
[8] Assmann A, Delfs C, Munakata H, Schiffer F, Horstkötter K, Huynh K, et al. Acceleration of autologous in vivo recellularization of decellularized aortic conduits by fibronectin surface coating. Biomaterials 2013;34:6015–26.
[9] Munakata H, Assmann A, Poudel-Bochmann B, Horstkötter K, Kamiya H, Okita Y, et al. Aortic conduit valve-model with controlled moderate aortic regurgitation in rats: a technical modification to improve short- and long-term outcome and to increase the functional results. Circ J 2013;77:2295–302.
[10] Tang FT, Chen SR, Wu XQ, Wang TQ, Chen JW, Li J, et al. Hypercholesterolemia accelerates vascular calcification induced by excessive vitamin D via oxidative stress. Calcif Tissue Int 2006;79:326–39.
[11] Drolet MC, Couet J, Arsenault M. Development of aortic valve sclerosis or stenosis in rabbits: role of cholesterol and calcium. J Heart Valve Dis 2008;17:381–7.
[12] Ngo DT, Stafford I, Kelly DJ, Sverdlov AL, Wuttke RD, Weedon H, et al. Vitamin D(2) supplementation induces the development of aortic stenosis in rabbits: interactions with endothelial function and thioredoxin-interacting protein. Eur J Pharmacol 2008;590:290–6.
[13] Hoshina M, Wada H, Sakakura K, Kubo N, Ikeda N, Sugawara Y, et al. Determinants of progression of aortic valve stenosis and outcome of adverse events in hemodialysis patients. J Cardiol 2012;59:78–83.
[14] Linefsky JP, O'Brien KD, Katz R, de Boer IH, Barasch E, Jenny NS, et al. Association of serum phosphate levels with aortic valve sclerosis and annular calcification: the cardiovascular health study. J Am Coll Cardiol 2011;58:291–7.
[15] Kunjachan S, Gremse F, Theek B, Koczera P, Pola R, Pechar M, et al. Noninvasive optical imaging of nanomedicine biodistribution. ACS Nano 2013;7:252–62.
[16] Gremse F, Schulz V. Qualitative and quantitative data analysis. In: Kiessling F, Pichler BJ, editors. Small animal imaging. Berlin: Springer; 2011. pp. 363–78.
[17] Wang H, Liu C, Song Y, Gordon D, Alavi MZ, Moore S. Expression of metalloproteinases and its inhibitor in later stage of rabbit neointima development. Int J Mol Med 2001;7:105–12.
[18] Li Z, Li L, Zielke R, Cheng L, Xiao R, Crow M, et al. Increased expression of 72-kD type IV collagenase (MMP2) in human aortic atherosclerotic lesions. Am J Pathol 1996;148:121–8.
[19] Loftus IM, Naylor AR, Goodall S, Crowther M, Jones L, Bell PR, et al. Increased matrix metalloproteinase-9 activity in unstable carotid plaques. A potential role in acute plaque disruption. Stroke 2000;31:40–7.
[20] Krishnamurthy VK, Opoka AM, Kern CB, Guilak F, Narmoneva DA, Hinton RB. Maladaptive matrix remodeling and regional biomechanical dysfunction in a mouse model of aortic valve disease. Matrix Biol 2012;31:197–205.
[21] Perrotta I, Russo E, Camastra C, Filice G, Di Mizio G, Colosimo F, et al. New evidence for a critical role of elastin in calcification of native heart valves: immunohistochemical and ultrastructural study with literature review. Histopathology 2011;59:504–13.
[22] Hakuno D, Kimura N, Yoshioka M, Mukai M, Kimura T, Okada Y, et al. Periostin advances atherosclerotic and rheumatic cardiac valve degeneration by inducing angiogenesis and MMP production in humans and rodents. J Clin Invest 2010;120:2292–306.
[23] Joghetaei N, Akhyari P, Rauch BH, Cullen P, Lichtenberg A, Rudelius M, et al. Extracellular matrix metalloproteinase inducer (CD147) and membrane type 1-matrix metalloproteinase are expressed on tissue macrophages in calcific aortic stenosis and induce transmigration in an artificial valve model. J Thorac Cardiovasc Surg 2011;142:191–8.
[24] Vyavahare N, Jones PL, Tallapragada S, Levy RJ. Inhibition of matrix metalloproteinase activity attenuates tenascin-C production and calcification of implanted purified elastin in rats. Am J Pathol 2000;157:885–93.
[25] Bailey M, Pillarisetti S, Jones P, Xiao H, Simionescu D, Vyavahare N. Involvement of matrix metalloproteinases and tenascin-C in elastin calcification. Cardiovasc Pathol 2004;13:146–55.
[26] Rajamannan NM. Mechanisms of aortic valve calcification: the LDL-density-radius theory: a translation from cell signaling to physiology. Am J Physiol Heart Circ Physiol 2010;298:H5–15.
[27] Togashi M, Tamura K, Masuda Y, Fukuda Y. Comparative study of calcified changes in aortic valvular diseases. J Nippon Med Sch 2008;75:138–45.
[28] Kennedy JA, Hua X, Mishra K, Murphy GA, Rosenkranz AC, Horowitz JD. Inhibition of calcifying nodule formation in cultured porcine aortic valve cells by nitric oxide donors. Eur J Pharmacol 2009;602:28–35.
[29] Sverdlov AL, Ngo DT, Chan WP, Chirkov YY, Gersh BJ, McNeil JJ, et al. Determinants of aortic sclerosis progression: implications regarding impairment of nitric oxide signalling and potential therapeutics. Eur Heart J 2012;33:2419–25.
[30] Ross R. Atherosclerosis–an inflammatory disease. N Engl J Med 1999;340:115–26.
[31] Zhang LN, Parkinson JF, Haskell C, Wang YX. Mechanisms of intimal hyperplasia learned from a murine carotid artery ligation model. Curr Vasc Pharmacol 2008;6:37–43.
[32] New SE, Goettsch C, Aikawa M, Marchini JF, Shibasaki M, Yabusaki K, et al. Macrophage-derived matrix vesicles: an alternative novel mechanism for microcalcification in atherosclerotic plaques. Circ Res 2013;113:72–7.
[33] Hjortnaes J, Butcher J, Figueiredo JL, Riccio M, Kohler RH, Kozloff KM, et al. Arterial and aortic valve calcification inversely correlates with osteoporotic bone remodelling: a role for inflammation. Eur Heart J 2010;31:1975–84.
[34] Coté N, Mahmut A, Bosse Y, Couture C, Pagé S, Trahan S, et al. Inflammation is associated with the remodeling of calcific aortic valve disease. Inflammation 2013;36:573–81.
[35] O'Brien KD, Reichenbach DD, Marcovina SM, Kuusisto J, Alpers CE, Otto CM. Apolipoproteins B, and E accumulate in the morphologically early lesion of 'degenerative' valvular aortic stenosis. Arterioscler Thromb Vasc Biol 1996;16:523–32.
[36] Shuvy M, Abedat S, Beeri R, Danenberg HD, Planer D, Ben-Dov IZ, et al. Uraemic hyperparathyroidism causes a reversible inflammatory process of aortic valve calcification in rats. Cardiovasc Res 2008;79:492–9.
[37] Hekimian G, Passefort S, Louedec L, Houard X, Jacob MP, Vahanian A, et al. High-cholesterol + vitamin D2 regimen: a questionable in-vivo experimental model of aortic valve stenosis. J Heart Valve Dis 2009;18:152–8.
[38] Butcher JT, Simmons CA, Warnock JN. Mechanobiology of the aortic heart valve. J Heart Valve Dis 2008;17:62–73.
[39] Gould ST, Srigunapalan S, Simmons CA, Anseth KS. Hemodynamic and cellular response feedback in calcific aortic valve disease. Circ Res 2013;113:186–97.
[40] Lehoux S, Castier Y, Tedgui A. Molecular mechanisms of the vascular responses to haemodynamic forces. J Intern Med 2006;259:381–92.
[41] Brockbank KG, Song YC. Morphological analyses of ice-free and frozen cryopreserved heart valve explants. J Heart Valve Dis 2004;13:297–301.
[42] Ikonen TS, Briffa N, Gummert JF, Honda Y, Hayase M, Hausen B, et al. Multidimensional assessment of graft vascular disease (GVD) in aortic grafts by serial intravascular ultrasound in rhesus monkeys. Transplantation 2000;70:420–9.
[43] Hopkins RA, Jones AL, Wolfinbarger L, Moore MA, Bert AA, Lofland GK. Decellularization reduces calcification while improving both durability and 1-year functional results of pulmonary homograft valves in juvenile sheep. J Thorac Cardiovasc Surg 2009;137:907–13.
[44] Martin ND, Schaner PJ, Tulenko TN, Shapiro IM, Dimatteo CA, Williams TK, et al. In vivo behavior of decellularized vein allograft. J Surg Res 2005;129:17–23.
[45] Takagi K, Fukunaga S, Nishi A, Shojima T, Yoshikawa K, Hori H, et al. In vivo recellularization of plain decellularized xenografts with specific cell characterization in the systemic circulation: histological and immunohistochemical study. Artif Organs 2006;30:233–41.
[46] Legare JF, Lee TD, Ross DB. Cryopreservation of rat aortic valves results in increased structural failure. Circulation 2000;102:III75–8.
[47] Flameng W, Jashari R, De Visscher G, Mesure L, Meuris B. Calcification of allograft and stentless xenograft valves for right ventricular outflow tract reconstruction: an experimental study in adolescent sheep. J Thorac Cardiovasc Surg 2011;141:1513–21.
[48] Hoekstra FM, Witvliet M, Knoop CY, Wassenaar C, Bogers AJ, Weimar W, et al. Immunogenic human leukocyte antigen class II antigens on human cardiac valves induce specific alloantibodies. Ann Thorac Surg 1998;66:2022–6.
[49] Hogan P, Duplock L, Green M, Smith S, Gall KL, Frazer IH, et al. Human aortic valve allografts elicit a donor-specific immune response. J Thorac Cardiovasc Surg 1996;112:1260–6.
[50] Cebotari S, Tudorache I, Ciubotaru A, Boethig D, Sarikouch S, Goerler A, et al. Use of fresh decellularized allografts for pulmonary valve replacement may reduce the reoperation rate in children and young adults: early report. Circulation 2011;124:S115–23.
[51] Burch PT, Kaza AK, Lambert LM, Holubkov R, Shaddy RE, Hawkins JA. Clinical performance of decellularized cryopreserved valved allografts compared with standard allografts in the right ventricular outflow tract. Ann Thorac Surg 2010;90:1301–5.
[52] Ruzmetov M, Shah JJ, Geiss DM, Fortuna RS. Decellularized versus standard cryopreserved valve allografts for right ventricular outflow tract reconstruction: a single-institution comparison. J Thorac Cardiovasc Surg 2012;143:543–9.
[53] Tavakkol Z, Gelehrter S, Goldberg CS, Bove EL, Devaney EJ, Ohye RG. Superior durability of SynerGraft pulmonary allografts compared with standard cryopreserved allografts. Ann Thorac Surg 2005;80:1610–4.

3.2 **Decreased *in vivo* degeneration of aortic conduit grafts by decellularization versus cryopreservation**

***Assmann A**, Zwirnmann K, Heidelberg F, Schiffer F, Horstkötter K, Munakata H, Gremse F, Barth M, Lichtenberg A, Akhyari P. The degeneration of biological cardiovascular prostheses under pro-calcific metabolic conditions in a small animal model. **Biomaterials**. 2014; 35:7416-7428.*

The full text article is presented in section 3.1.3.

In our rat model of accelerated cardiovascular calcification, the degeneration of decellularized aortic conduit implants (group DC; n=6) was evaluated in comparison to cryopreserved non-decellularized control grafts (group CRYO; n=7) up to 12 weeks after implantation.

Under severely pro-degenerative conditions, decellularized implants showed slow non-inflammatory neointima formation with hyperplastic pannus areas not before week 12 after implantation, whereas severe infiltration with inflammatory cells and pannus formation occurred early in cryopreserved grafts resulting in increased intima-to-media ratios. Immunostaining against CD3 confirmed the histological observation that decellularization had abolished the cellular inflammation in the implants. These findings are in line with previous reports on the inflammatory intima destruction of heart valve and vessel allografts, as well as on the potential of implant decellularization to diminish this process [52,71-73].

In all prostheses, we found progressive hydroxyapatite deposition in the media and at later stages also in the intima, whereas the calcium burden in the cryopreserved grafts was increased. After 12 weeks, all parts of the cryopreserved prostheses contained chondroid cells staining positive for the chondrocyte differentiation marker syndecan-3.

The anti-degenerative effect of decellularization of biological grafts seems to be confirmed by first clinical trials. These reports imply improved short- and mid-term functionality as well as freedom from reoperation for decellularized versus cryopreserved grafts in the pulmonary and aortic position [74-77]. Studies on the long-term performance and final calcification are underway.

In summary, decellularization has been shown to decelerate different adverse processes ultimately resulting in the deterioration of cardiovascular implants. Not only does it abrogate the early inflammation in the allografts, but also it reduces the pannus formation and decreases the destructive implant calcification in a standardized rat implantation model of accelerated cardiovascular calcification. Thereby, decellularized aortic allograft conduits are promising alternatives to cryopreserved allografts routinely used in cardiac surgery.

3.3 Increased autologous *in vivo* recellularization of decellularized aortic conduit grafts by fibronectin surface coating

***Assmann A**, Delfs C, Munakata H, Schiffer F, Horstkötter K, Huynh K, Barth M, Stoldt VR, Kamiya H, Boeken U, Lichtenberg A, Akhyari P. Acceleration of autologous in vivo recellularization of decellularized aortic conduits by fibronectin surface coating. **Biomaterials**. 2013; 34:6015-6026.*

In order to improve the biocompatibility of decellularized cardiovascular implants by accelerating the autologous *in vivo* recellularization, aortic conduit grafts were surface-coated with FN (group FN; n=18), and the results within the first 8 postoperative weeks were compared to non-coated (group C; n=18) controls.

The fluorophore-labeled FN was shown to persist as surface coating for at least up to 8 weeks, whereas the signal decreased during the follow-up, presumably also due to degradation or uncoupling of the fluorophore. While the loss kinetics of FN surface coating have been studied before *in vitro* for the first hours after the coating procedure, this is the first *in vivo* examination of FN persistence on cardiovascular implants [78].

Histological analyses of the luminal recellularization revealed that FN-coated conduits were repopulated faster than uncoated controls, whereas the major portion of cells seems to have migrated from the anastomoses into the grafts and was not blood flow-derived. Unfortunately, FN also aggravated intimal pannus formation. Immunofluorescence staining revealed most of the cells in the hyperplastic pannus areas of both groups to contain alpha-smooth muscle actin, while the luminal endothelial layer stained positive for von Willebrand factor. By means of Movat's pentachrome staining, we found areas of neointima with spindle-shaped cells. However, in regions of extensive hyperplasia, also clusters of cells with a chondroid phenotype occurred, which proved positive for the early chondrocyte differentiation marker syndecan-3. Moreover, these clusters were shown to be partially surrounded by hydroxyapatite. This indicates that future approaches should focus on the prevention of pannus formation, which is also known to occur on human artificial and bioimplants. In contrast to the clinically applied artificial and cellular biografts, decellularized prostheses in our model did not induce cellular inflammation

(hematoxylin/eosin and Movat's Pentachrome staining; CD3 and CD68 immunofluorescence), which is a major driving force of bioprosthesis deterioration.

Interestingly, repopulation of the aortic media originated from the adventitial and not from the luminal side in both groups, suggesting the basal membrane to be a preserved barrier for cell migration. While the media of control grafts was recellularized only sparsely, FN coating increased the repopulation speed significantly. Areas of cellular repopulation were marked by increased MMP activity with peak values in the FN group, which may be due to direct MMP stimulation by FN [79].The media-repopulating cells stained positive for alpha-smooth muscle actin and desmin, a combination that is regarded to indicate smooth muscle cells as opposed to myofibroblasts in the neointima staining negative for desmin.

Quantitative real-time PCR revealed no inter-group differences for several markers of cell activation, inflammation and osteogenic transformation, except for the osteogenicity marker osteocalcin, which was increased in the control group. The lack of inflammation and relevant calcification marker levels in both groups is consistent with the histological results and underlines the potential of decellularized grafts to improve clinical implant standards.

In summary, a fluorophore-based labeling approach enabled the *in vivo* tracking of FN coating and proved its persistence for up to 8 weeks in the systemic circulation. FN improved the cell adhesion capacity and the biocompatibility of the decellularized grafts resulting in a significantly accelerated endothelialization at the cost of aggravated hyperplastic pannus formation. Remarkably, FN coating induced medial graft repopulation in the absence of an inflammatory reaction or adverse gene expression, indicating the feasibility and potential of this strategy in terms of improvement of current clinically applied bioprostheses.

Biomaterials 34 (2013) 6015–6026

Contents lists available at SciVerse ScienceDirect

Biomaterials

journal homepage: www.elsevier.com/locate/biomaterials

Acceleration of autologous *in vivo* recellularization of decellularized aortic conduits by fibronectin surface coating☆

Alexander Assmann [a], Christofer Delfs [a], Hiroshi Munakata [a], Franziska Schiffer [a], Kim Horstkötter [a], Khon Huynh [b], Mareike Barth [a], Volker R. Stoldt [b], Hiroyuki Kamiya [a], Udo Boeken [a], Artur Lichtenberg [a], Payam Akhyari [a,*]

[a] Department of Cardiovascular Surgery and Research Group for Experimental Surgery, Heinrich Heine University, Medical Faculty, Moorenstrasse 5, Duesseldorf D-40225, Germany
[b] Institute of Haemostaseology and Transfusion Medicine, Heinrich Heine University, Medical Faculty, Duesseldorf D-40225, Germany

ARTICLE INFO

Article history:
Received 5 March 2013
Accepted 13 April 2013
Available online 15 May 2013

Keywords:
Endothelialisation
Fibronectin
Heart valve
Biocompatibility
Extracellular matrix
Vascular grafts

ABSTRACT

Decellularization is a promising option to diminish immune and inflammatory response against donor grafts. In order to accelerate the autologous *in vivo* recellularization of aortic conduits for an enhanced biocompatibility, we tested fibronectin surface coating in a standardized rat implantation model. Detergent-decellularized rat aortic conduits ($n = 36$) were surface-coated with covalently Alexa488-labeled fibronectin (50 μg/ml, 24 h) and implanted into the systemic circulation of Wistar rats for up to 8 weeks (group FN; $n = 18$). Uncoated implants served as controls (group C; $n = 18$). Fibronectin-bound fluorescence on both surfaces of the aortic conduits was persistent for at least 8 weeks. Cellular repopulation was examined by histology and immunofluorescence ($n = 24$). Luminal endothelialization was significantly accelerated in group FN ($p = 0.006$ after 8 weeks), however, local myofibroblast hyperplasia with significantly increased ratio of intima-to-media thickness occurred ($p = 0.0002$ after 8 weeks). Originating from the adventitial surface, alpha-smooth muscle actin and desmin positive cell invasion into the media of fibronectin-coated conduits was significantly increased as compared to group C ($p < 0.0001$). In these medial areas, *in situ* zymography revealed enhanced matrix metalloproteinase activity. In both groups, inflammatory cell markers (CD3 and CD68) and signs of thrombosis proved negative. With regard to several markers of cell adhesion, inflammation and calcification, quantitative real-time PCR ($n = 12$) revealed no significant inter-group differences. Fibronectin surface coating of decellularized cardiovascular implants proved feasible and persistent for at least 8 weeks in the systemic circulation. Biofunctional protein coating accelerated the autologous *in vivo* endothelialization and induced a significantly increased medial recellularization. Therefore, this strategy may contribute to the improvement of current clinically applied bioprostheses.

1. Introduction

Nowadays, aortic valve allografts are the standard implants in cardiac surgery providing good long-term results in adults [1]. Nevertheless, especially in younger patients, an accelerated calcific degeneration results in implant failure and warrants a redo operation with increased risk of morbidity and mortality [2].

Decellularized cardiovascular implants are a promising alternative to common prostheses, since the lack of major cell bound antigens, e.g. human leukocyte antigens or alpha-Gal-epitopes, diminishes the recipient's adaptive immune response, which triggers degeneration and implant failure in both, animals and humans [3,4]. Moreover, experimental evidence suggests a reduction of the risk of thromboembolic events by decellularization, e.g. reducing retrovalvular thrombus formation after heterotopic aortic conduit implantation in rats [5]. Recent studies reported on the successful implantation of tissue-engineered pulmonary and aortic heart valves with encouraging short- to mid-term functional outcome in preclinical models [6,7]. More interesting, these results have now been confirmed in the first clinical series of decellularized allogenic valve implantation in the pulmonary as well as in the aortic position [8,9].

☆ The content of this paper was presented at the AHA Scientific Sessions on November 5th, 2012, Los Angeles.

* Corresponding author. Tel.: +49 (0)211 81 18331; fax: +49 (0)211 81 18333.
E-mail addresses: payam.akhyari@med.uni-duesseldorf.de, payam.akhyari@gmx.de (P. Akhyari).

0142-9612/$ – see front matter © 2013 Elsevier Ltd. All rights reserved.
http://dx.doi.org/10.1016/j.biomaterials.2013.04.037

However, after implantation of decellularized porcine heart valves ("SYNERGRAFT") in pediatric patients, serious calcification and early graft failure occurred, which may be attributed to thrombogenesis and immune response against donor cell remnants [10,11]. Besides incompletely removed cell fragments, that necessitate improved decellularization protocols, non-autologous extracellular matrix proteins on the luminal graft surfaces may also trigger inflammation, immune response and thrombus formation [12,13].

Therefore, and in order to prevent intimal hyperplasia in the absence of intact endothelium, it is crucial that decellularized cardiovascular prostheses undergo autologous luminal endothelialization within a short time period after implantation. Surface coating of artificial and biological vascular grafts with biofunctional proteins, such as fibronectin, fibrin or vascular endothelial growth factor, has been shown to accelerate the *in vivo* adhesion of recipient cells, thereby improving the *in vivo* performance of the implants [14,15].

In order to accelerate the autologous *in vivo* recellularization of decellularized aortic conduits for enhanced biocompatibility, the present study aimed at examining a) the *in vivo* persistence and b) the functional relevance of fibronectin surface coating of decellularized aortic conduits in a standardized small animal model [16].

2. Materials and methods

2.1. Animals

Male Wistar rats ($n = 72$; 200–250 g) were purchased from the in-house breed of the local animal care facility and fed *ad libitum* with standard rat chow. All experiments were conducted according to the national animal welfare act, and approved by the state animal care committee (reference number 87-51.04.2010.A068).

2.2. Graft harvesting and engineering

Aortic conduit grafts ($n = 36$) were harvested and detergent-decellularized as recently published [16]. In brief, after euthanasia of the donor rats with CO_2, the heart and the thoracic aorta were explanted en bloc and thoroughly rinsed with heparinized phosphate buffered saline (PBS). A U-shaped aortic conduit with a small myocardial cuff was prepared. Coronary arteries were ligated and supraaortal arteries were clipped. All harvested grafts were decellularized according to a detergent-based protocol, which started with four cycles of 12 h with 0.5% sodium dodecyl sulfate + 0.5% deoxycholate, followed by 24 h rinsing with distilled water and three cycles of 24 h with PBS + 1% penicillin/streptomycin, in the presence of 0.05% sodium azide. All steps were conducted in 250 ml bottles, filled with 25 ml per conduit, containing a maximum of four grafts.

2.3. Graft surface coating with fibronectin

The covalent binding of the fluorochrome Alexa488 (Invitrogen, Carlsbad, USA) to fibronectin isolated from human blood plasma was conducted according to Huynh et al., unpublished data, 2013. In brief, fibronectin solution (1 mg/ml fibronectin in PBS, pH 7.3) was mixed with sodium bicarbonate at the final concentration of 0.1 M (pH 8.7) for amine labeling according to the user's manual. Labeling was done by adding 80-fold molar excess of Alexa488 to the fibronectin solution and incubating for 1 h in dark at room temperature with gentle rotation. Free dyes were removed by dialysis with PBS (pH 7.3) overnight. Concentrations and ratios of dye/fibronectin molecule conjugation were determined by reading the absorption at 280 nm, 496 nm and calculated according to the user's manual. Batches of Alexa488-labeled fibronectin with ratios between six and nine were chosen for further experiments.

In order to reveal the optimal fibronectin coating conditions for decellularized rat aortic conduits, different concentrations of the fibronectin coating solution (20, 50, 100 and 200 μg/ml) as well as different coating conditions, including different temperatures (20 and 37 °C) and static versus slightly agitated incubation, were tested prior to the experiments. With regard to the coating efficiency as well as to economic aspects, all decellularized rat aortic conduits intended for implantation ($n = 18$) were incubated with covalently Alexa488-labeled fibronectin under the following conditions: fibronectin concentration 50 μg/ml in PBS, incubation time 24 h and incubation temperature 37 °C.

After resection of a distal ring of the conduit for decellularization quality assurance and for confirmation of the coating efficiency, the grafts were instantaneously implanted avoiding prolonged exposure to light to prevent bleaching of the fluorophore.

2.4. Heterotopic graft implantation procedure

Heterotopic implantation of the engineered aortic conduit grafts into the systemic circulation of recipient rats was conducted as recently described [16]. Briefly, recipient rats were inhalatively anesthetized with 2.0–2.5% isoflurane, orally intubated, and a central venous jugular vein catheter was inserted. After median laparotomy and dissection of the infrarenal aorta from the inferior vena cava, heparin (300 IU/kg) was systemically administered. The abdominal aorta was clamped, and a U-shaped, engineered aortic conduit was anastomosed to the infrarenal aorta in an

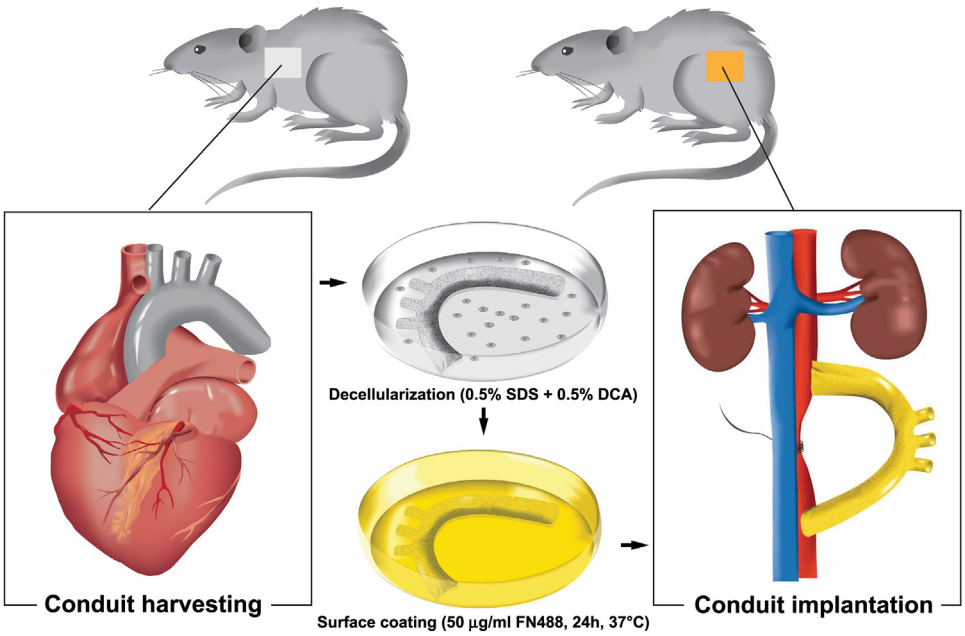

Fig. 1. Experimental design of implanting fibronectin-coated aortic conduits. SDS, sodium dodecyl sulfate; DCA, deoxycholic acid; FN488, fibronectin labeled by covalent binding of Alexa488.

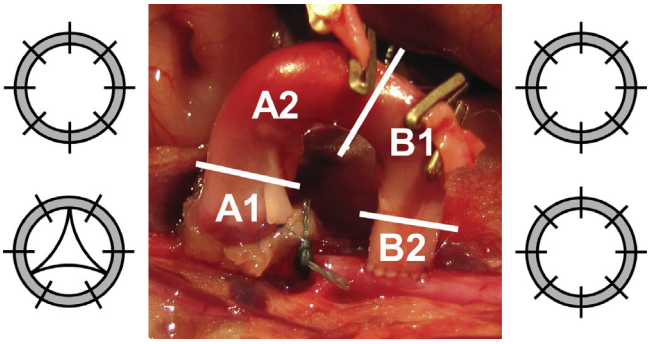

Fig. 2. Intraoperative image depicting the anatomic mapping of the explant grafts for subsequent histo-topographic analysis. Explanted conduits were subdivided in four regions: aortic valve (region A1), ascending aorta (region A2), descending aorta (region B1) and distal anastomosis with the native recipient aorta (region B2). The schematic drawings represent cross-sections through each region of the conduit, and display the subdivision into nine pieces (region A1) and eight pieces (regions A2, B1, and B2), respectively.

end-to-side manner, using a 10–0 monofilament, non-absorbable polypropylene suture (Ethicon, Norderstedt, Germany). Finally, the native aorta between the two anastomoses was ligated to improve the perfusion of the implant, the abdomen was closed, and after sonographic confirmation of unimpaired conduit perfusion with a Philips HDX11 ultrasonography system equipped with a 15 MHz probe (Philips, Amsterdam, Netherlands), the recipients were allowed to recover from anesthesia.

Recipients were divided in two groups: Group FN ($n = 18$) received aortic conduits coated with fibronectin [Fig. 1], while uncoated implants in group C ($n = 18$) served as controls.

2.5. Graft explantation

At the postoperative days 1, 7, 28 and 56, recipient rats were anesthetized as described above, and Doppler sonography was conducted to control the perfusion of the prostheses. After laparotomy, the implanted conduits were rinsed with heparinized PBS via abdominal cannulation, thoroughly excised and further processed for histology, immunofluorescence (each with $n = 3$ per group at each time point), *in situ* zymography ($n = 3$ per group at days 28 and 56) and quantitative real-time polymerase chain reaction (PCR) ($n = 6$ per group at day 56).

2.6. Explant histology

Cryo-sections of explanted grafts were subjected to histology (hematoxylin/eosin staining, Movat's pentachrome staining, von Kossa staining). Morphometric analyses for the detection of inter-group differences were performed using Image J v1.46 (Wayne Rasband, National Institutes of Health, USA).

In order to comparatively quantify the amount of luminal neointima in hematoxylin/eosin stained cross-sections, a standardized protocol was established: Each conduit was divided into four regions: aortic valve (region A1), ascending aorta (region A2), descending aorta (region B1) and distal anastomosis with the native recipient aorta (region B2) [Fig. 2]. In each region of the conduit, three representative cross-sections in a distance of 200 μm to each other underwent detailed histomorphological analysis to assess the cellular content and repopulation pattern of the implants. In the regions A2, B1 and B2, each cross-section was divided into eight segments by radial lines (angle: 45°) originating from the center of the aortic lumen [Fig. 2]. In each of these segments of the conduit wall, the percentage of recellularized surface was determined. For region A1, the cross-section of the aortic valve was divided into nine segments: three segments containing the aortic sinuses, three aortic commissures and three segments containing the aortic leaflets [Fig. 2]. In each segment, the percentage of recellularized tissue surface was determined. Finally, for each of the four regions of a conduit (A1-B2), the percentage of recellularized surface was calculated.

Moreover, with regard to intimal hyperplasia, the intima-to-media ratio was determined in predefined areas of the conduits: In brief, the division of the conduits into four regions with three representative cross-sections and the subdivision of each cross-section into eight pieces (aortic wall) or nine pieces (aortic valve), respectively, were conducted as described above. In each segment, the media thickness and the thickness of the neointima were measured to determine an intima-to-media ratio. Finally, for each of the four regions of a conduit, the median intima-to-media ratio was calculated.

Similarly, the repopulation of the media of the conduits was evaluated. Therefore, in each cross-section, the total number of cells invading into the medial part of the decellularized implants was counted.

2.7. Explant immunofluorescence

Cryo-embedding, sectioning and fixation were performed as described above. Afterwards, cryo-sections were incubated sequentially for 10 min with 0.25% Triton-X-100 (Sigma–Aldrich, Taufkirchen, Germany) and for 1 h with 5% bovine serum albumin (Sigma–Aldrich, Taufkirchen, Germany) + 0.1% Tween-20 (Merck Millipore Calbiochem, Darmstadt, Germany), in each case at room temperature. Incubation with primary antibodies (anti-vonWillebrand factor (vWF), DAKO, Hamburg, Germany; anti-alpha-smooth muscle actin (aSMA), Sigma–Aldrich, Taufkirchen, Germany; anti-desmin, Abcam, Cambridge, UK; anti-vimentin, Progen, Heidelberg, Germany; anti-syndecan-3, Abcam, Cambridge, UK; anti-CD3, Sigma–Aldrich, Taufkirchen, Germany; anti-CD68, Abcam, Cambridge, UK) + 1% bovine serum albumin + 0.1% Tween-20 lasted 1 h at 37 °C. All secondary antibodies were conjugated to the fluorophore Alexa546 (Invitrogen, Carlsbad, USA), and were applied (+1% bovine serum albumin + 0.1% Tween-20) for 45 min in a dark and humid chamber at 37 °C. Sections were covered with Vectashield mounting medium containing DAPI (Vector Labs, Peterborough, United Kingdom), and image acquisition was conducted utilizing the microscope system DM2000, equipped with a digital camera DFC 425C (Leica, Wetzlar, Germany) and the Leica Application Suite V3.7 software.

Fibronectin coating was detected by direct visualization of the conjugated fluorophore Alexa488.

2.8. In situ zymography

To determine the MMP activity in the grafted conduit tissue, *in situ* zymography was performed as recently published [17]. In brief, cryo-sections (6 μm) of explanted aortic conduits were incubated with 40 μg/ml fluorescein-labeled gelatin (Invitrogen, Carlsbad, USA) in 50 mM Tris–HCl, 10 mM $CaCl_2$, 150 mM NaCl and 5% Triton-X-100 for 24 h at 37 °C. Finally, sections were mounted with Vectashield medium containing DAPI, and the MMP gelatinase activity was visualized by fluorescence microscopy as described above. Specificity of gelatinase activity was confirmed by incubation with gelatin in the presence of 20 mM EDTA. Comparative quantification of the MMP activity was performed with Image J by measuring the mean fluorescence intensity of the aortic conduit wall.

2.9. Quantitative RNA analysis

Gene expression analysis of whole aortic conduit explants was performed by quantitative real-time PCR: Total RNA was isolated using the RNeasy Mini Kit (Qiagen, Hilden, Germany): In brief, tissue was homogenized in TRIzol (Invitrogen, Carlsbad, USA), and RNA was precipitated by isopropanol. After having passed a

Table 1
Sequences of the primers used for real-time PCR.

Primer	Forward sequence	Reverse sequence
Beta-actin	5′-CCGCGAGTACAACCTTCTTG-3′	5′-GCAGCGATATCGTCATCCA-3′
Alpha-smooth muscle actin	5′-GCTCTGGTGTGTGACAATGG-3′	5′-CCCCACATAGCTGTCCTTTT-3′
Vascular cell adhesion molecule-1	5′-TGGGAAACTGGAAAGAGGAA-3′	5′-CAGGAGCCAAACACTTGACC-3′
Intercellular adhesion molecule-1	5′-GTCAAACGGGAGATGAATGG-3′	5′-CCGCAATGATCAGTACCAAC-3′
Transforming growth factor-beta-1	5′-TGGAGCCTGGACACACAGTA-3′	5′-GCTTGCGACCCACGTAGTAG-3′
CD39	5′-GGGCCTATGGGTGGATTACT-3′	5′-CAAAGGTTGCCTGTTTCTGG-3′
CD73	5′-ACGTGTCCATGTGCATTGTAA-3′	5′-GGTTCTCCCAGGTGATGGTA-3′
Osteopontin	5′-AAGCCTGACCCATCTCAGAA-3′	5′-ATGGCTTTCATTGGAGTTGC-3′
Osteocalcin	5′-AAGCAGGAGGGCAGTAAGGT-3′	5′-GTCCGCTAGCTCGTCACAAT-3′
Alkaline phosphatase	5′-GCACTCCCACTATGTCTGGAA-3′	5′-AGGGAAGGGTCAGTCAGGTT-3′
Integrin-alpha-4	5′-GCCCCCTGTTACCAAGATTT-3′	5′-GCCGGTCCAGTACGATGAT-3′
Integrin-alpha-5	5′-CCCAAAGGAAACCTCACCTA-3′	5′-ACGGCATAGCCAAAATAGGA-3′

DNA-removing column, the RNA sample was collected and quality analyses were performed: Purity and quantity of isolated RNA were determined spectrophotometrically (BioPhotometer plus, Eppendorf, Hamburg, Germany), and optical density values at 230, 260 and 280 nm were recorded. Moreover, the level of RNA degradation was examined by usage of the Agilent RNA 6000 Nano Kit (Agilent Technologies, Santa Clara, USA). cDNA was generated with the QuantiTect Reverse Transcription Kit (Qiagen, Hilden, Germany) according to the manufacturer's protocol. Quantitative real-time PCR was performed on a StepOnePlus cycler (Applied Biosystems, Foster City, USA) using the Platinum SYBR Green PCR Master Mix (Invitrogen, Carlsbad, USA), a reaction volume of 20 μl and the following protocol: 50 °C for 2 min, 95 °C for 2 min, 95 °C for 15 s + 60 °C for 30 s (40 cycles), 95 °C for 15 s, 60 °C for 1 min, 95 °C for 15 s and 60 °C for 15 s.

Sample quantifications in both groups were normalized to the beta-actin expression (dCt method), and subsequently to the mean dCt value of the gene in the control group (ddCt method). The resulting relative gene expression values of both groups were statistically compared to each other.

Primers were obtained from Invitrogen (Carlsbad, USA), and their sequences were as displayed in [Table 1].

2.10. Statistics

Data is presented as mean values ± standard errors of the mean for all continuous variables. For direct group comparisons at one time point, Student's *t*-tests with or without Welch's correction or Mann-Whitney-U tests were performed, as indicated (Kolmogorov–Smirnov test, F-test). For group comparisons at multiple time-points, two-way-ANOVA analyses with Bonferroni post-hoc tests were performed. Significance was assumed if *p*-values were lower than 0.05. Data analysis was conducted with GraphPad Prism v5.04 (GraphPad Software, San Diego, USA).

3. Results

3.1. Operative outcome and implant function

For graft implantation, the mean cut-suture times were 85.6 ± 3.66 min in group FN versus 86.5 ± 4.75 min in group C ($p = 0.879$), while the single infrarenal aortic clamping times amounted to 20.7 ± 0.80 min versus 21.8 ± 1.25 min ($p = 0.784$). All recipient rats survived the study without clinical or sonographic signs of lower body malperfusion. Eight weeks after surgery, the body weight had increased adequately from 223.1 ± 5.19 g to 358.3 ± 9.54 g in group FN versus 223.2 ± 3.93 g to 342.2 ± 8.82 g in group C ($p = 0.226$).

3.2. Fibronectin coating persistence

Covalently Alexa488 bound fibronectin coating resulted in a brightly green fluorescent and continuous fibronectin coating on both surfaces of the aortic conduits [Fig. 3A]. After implantation, a continuous decrease of the fluorescence intensity was noted *in vivo* [Fig. 3B, C]. Surprisingly, we found a persisting fluorescence signal still present after 4 and 8 weeks [Fig. 3D, E], although the signal was substantially weaker.

3.3. Quantity and quality of neointima formation

In both groups and at all time points, the neointima consisted of areas with single-layer endothelium [Fig. 4A, C] and areas with multi-layer hyperplastic intima [Fig. 4B, D].

In group FN, the luminal endothelialization was significantly accelerated as compared to group C (89.9 ± 5.45% vs. 73.6 ± 13.14% with $p = 0.006$ after 8 weeks). In order to reveal local differences in neointima formation, a structured segmental analysis of the conduits was performed. On the level of the implanted aortic valve (region A1), the recellularized luminal conduit surface in group FN was significantly increased than in group C after 4 weeks (98.6 ± 1.39% vs. 77.8 ± 10.37%, $p < 0.05$). After 8 weeks, there was a complete luminal repopulation in the fibronectin-coated grafts, but still incomplete in group C (100.0 ± 0.00% vs. 88.9 ± 4.39%, $p =$ n.s.) [Fig. 5A]. In the ascending aorta (region A2), the recellularized luminal conduit surface in group FN amounted to 22.2 ± 8.78% after 4 weeks as compared to 6.9 ± 4.71% in group C ($p =$ n.s.), and at 8 weeks, this trend became statistically significant, favoring the fibronectin-coated group with an enhanced luminal repopulation (81.9 ± 9.34% vs. 34.7 ± 10.58%, $p < 0.01$) [Fig. 5B]. In the caudal regions B1 and B2, the differences between the two groups were less pronounced and did not reach significance.

In the conduit parts distant from the anastomoses (regions A2 and B1 in both groups), the extent of luminal repopulation increased significantly from week 4 to week 8 ($p < 0.0001$ for A2; $p < 0.01$ for B1), while in areas close to the anastomoses, the luminal surface was almost completely recellularized already after 4 weeks.

For analysis of neointima formation, the intima-to-media ratio was calculated in both groups. After 8 weeks *in vivo*, the overall intima-to-media ratio in group FN was significantly increased as compared to group C (1.1 ± 0.10 vs. 0.7 ± 0.07, $p = 0.0002$). With regard to the implant aortic valve, the intima-to-media ratio of the fibronectin-coated grafts was already increased after 4 weeks (1.3 ± 0.13 vs. 0.6 ± 0.10, $p < 0.01$). After 8 weeks, in three of the

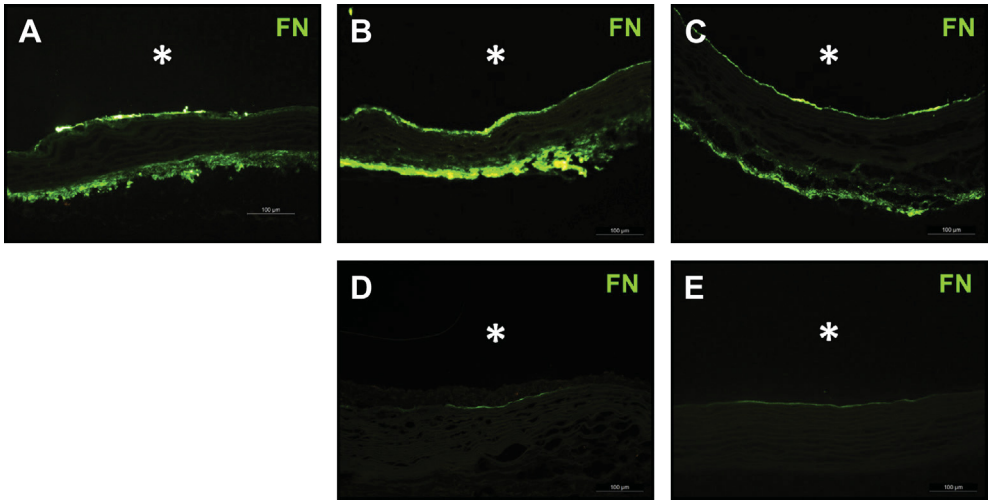

Fig. 3. Fibronectin coating efficiency and *in vivo* persistence. After coating, aortic conduits showed an intense layer of Alexa488-labeled fibronectin (A). When coated aortic conduits were explanted, a gradual loss of intensity was observed after 24 h (B), 7 days (C) And 28 days (D), respectively. However, fibronectin was still present at the latest follow-up time point at 8 weeks after implantation in the systemic circulation of the recipient rats (E). FN, fibronectin; green, Alexa488-labeled fibronectin; asterisks, vessel lumina. Scale bars = 100 μm.

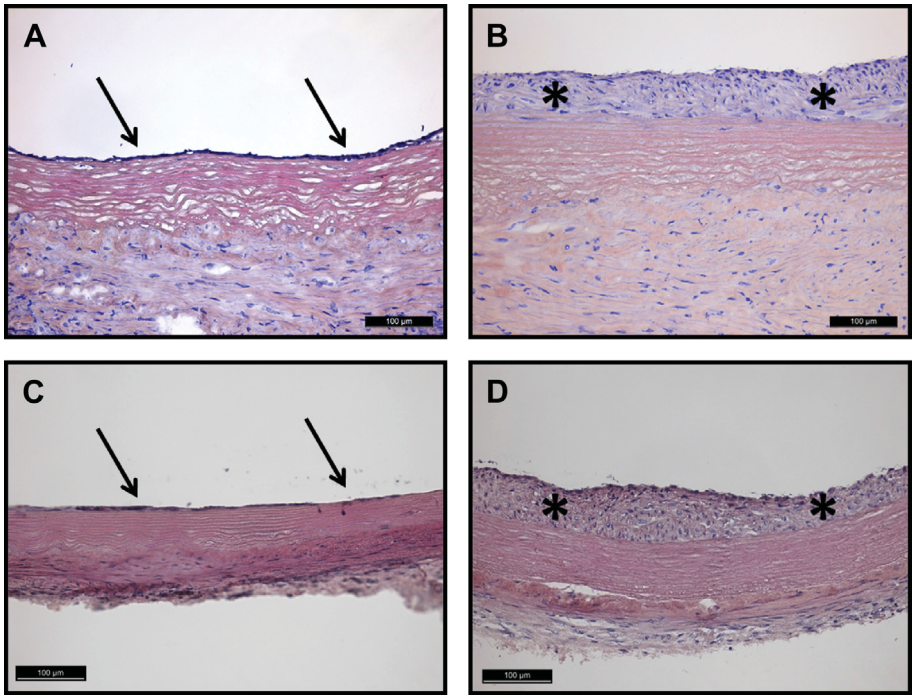

Fig. 4. Representative cross-sections through the ascending aorta of conduit grafts after 8 weeks *in vivo*. In both groups (group FN: A,B; group C: C,D), the neointima consisted of areas with single-layer endothelium (arrows in A and C) and areas with multi-layer hyperplasia (asterisks in B and D). Hematoxylin/eosin staining. Scale bars = 100 µm.

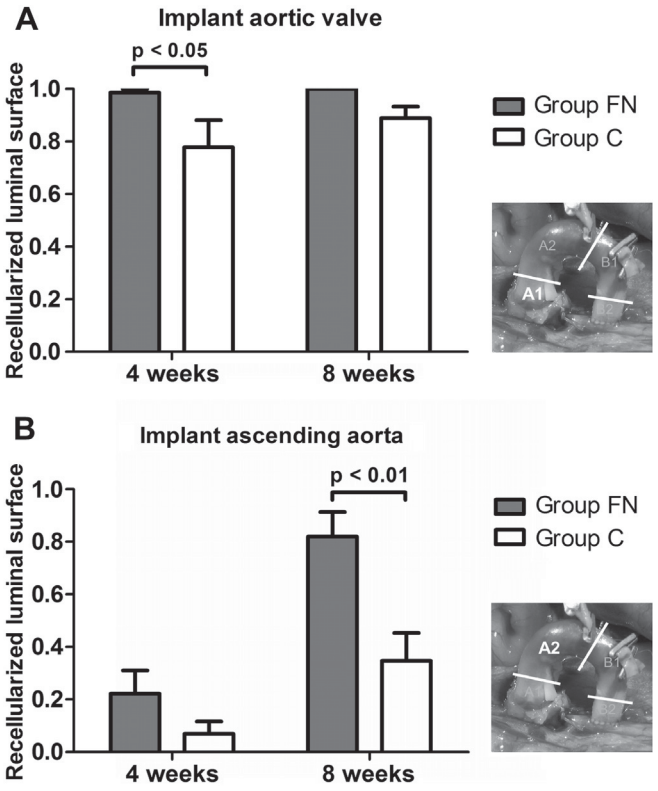

Fig. 5. Semiquantitative analysis of neointima formation, displayed as fractional recellularized luminal surface of the conduits. Fibronectin coating (group FN) accelerated the luminal recellularization as compared to controls (group C) at all time points. This difference was statistically significant at 4 weeks for the proximal region close to the implanted aortic valve (region A1, $p < 0.05$) (A). Similarly, at the distal part of the implanted ascending aorta, fibronectin accelerated the repopulation (region A2, $p < 0.01$ at 8 weeks) (B).

four evaluated regions of the implants, there was a significantly higher intima-to-media ratio (region A1: 1.7 ± 0.14 vs. 0.9 ± 0.15, $p < 0.001$; region A2: 0.9 ± 0.20 vs. 0.2 ± 0.10, $p < 0.001$; region B1: 0.7 ± 0.09 vs. 0.7 ± 0.14, $p =$ n.s.; region B2: 1.2 ± 0.10 vs. 0.9 ± 0.07, $p < 0.05$) [Fig. 6A–D]. In all parts of the conduits of both groups, there were signs of progressive neointima formation with intima-to-media ratios increasing significantly from week 4 to week 8 ($p < 0.05$ for A1, $p < 0.001$ for A2, $p < 0.0001$ for B1, and $p < 0.0001$ for B2).

Immunofluorescence staining revealed most of the cells in the hyperplastic areas of both groups to contain aSMA [Fig. 7B,D], while the luminal endothelial layer stained positive for vWF [Fig. 7A, C]. By means of Movat's pentachrome staining, we found areas of neointima with spindle-shaped cells. However, in regions of extensive hyperplasia, also clusters of cells with a chondroid phenotype occurred [Fig. 8] which proved positive for the early chondrocyte differentiation marker syndecan-3 [Fig. 9A]. Moreover, these clusters were shown to be partially surrounded by hydroxyapatite [Fig. 9B]. In both groups, inflammatory cell markers (CD3 and CD68) proved negative at all time points [Fig. 10].

3.4. Medial graft repopulation

In group FN, the absolute count of cells repopulating the media was significantly increased after 8 weeks as compared to group C ($p < 0.0001$) [Fig. 11A]. Interestingly, these cells invaded the conduits predominantly from the adventitial and not from the luminal surface [Fig. 11B, C]. The invaded cells stained positive for aSMA [Fig. 12B] and desmin [Fig. 12C], whereas vimentin was only sparsely detected [Fig. 12D].

In situ zymography revealed remarkable matrix metalloproteinase (MMP) activity around the media-repopulating cells as well as in the neointima [Fig. 13A, B]. Areas of increased cell density exhibited a marked MMP activity. After 4 and 8 weeks, the MMP activity was significantly increased in group FN as compared to group C ($p < 0.0001$ and $p = 0.029$) [Fig. 13C]. However, there was

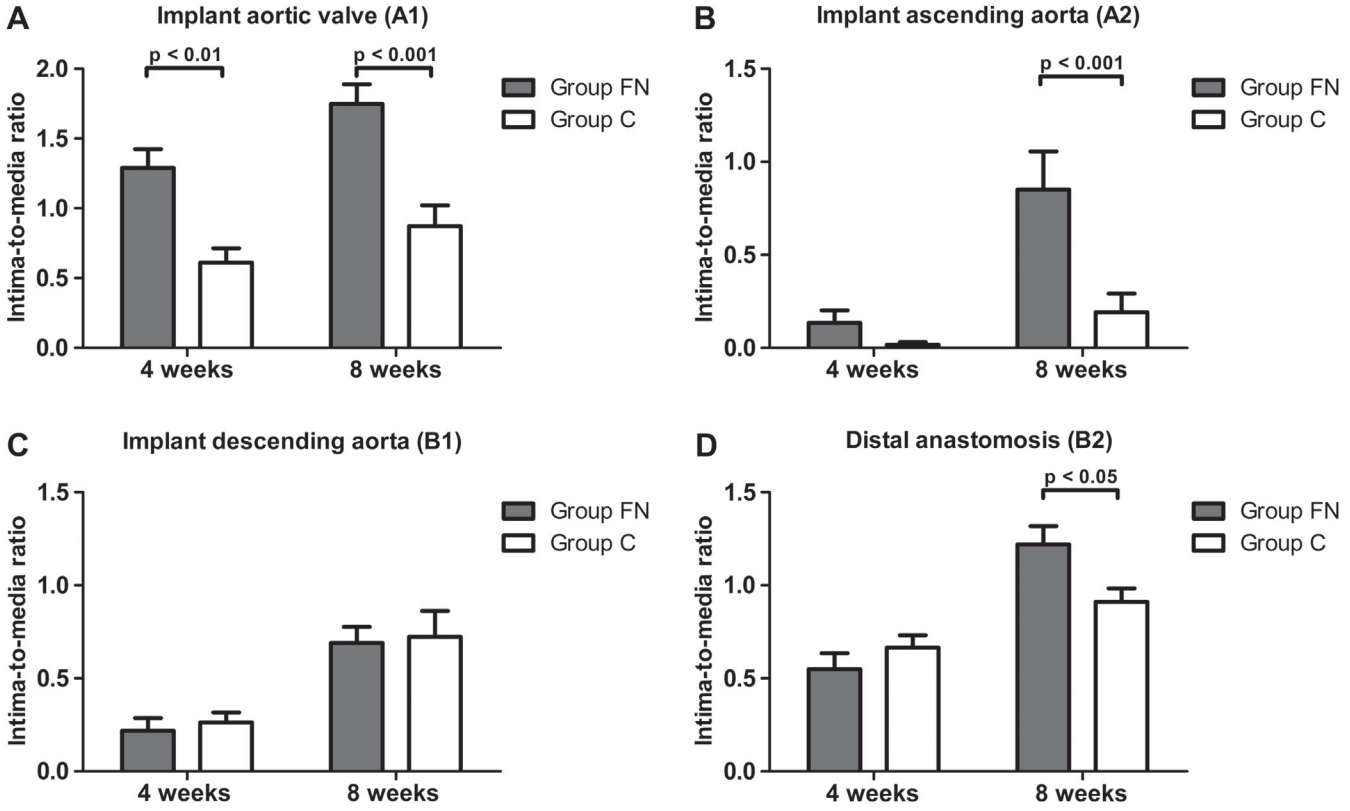

Fig. 6. Semiquantitative analysis of the intima-to-media ratio in different regions of the conduit explants. In all regions of the conduits, except region B1 (C), the intima-to-media ratio of group FN was significantly increased after 8 weeks as compared to group C (A,B,D).

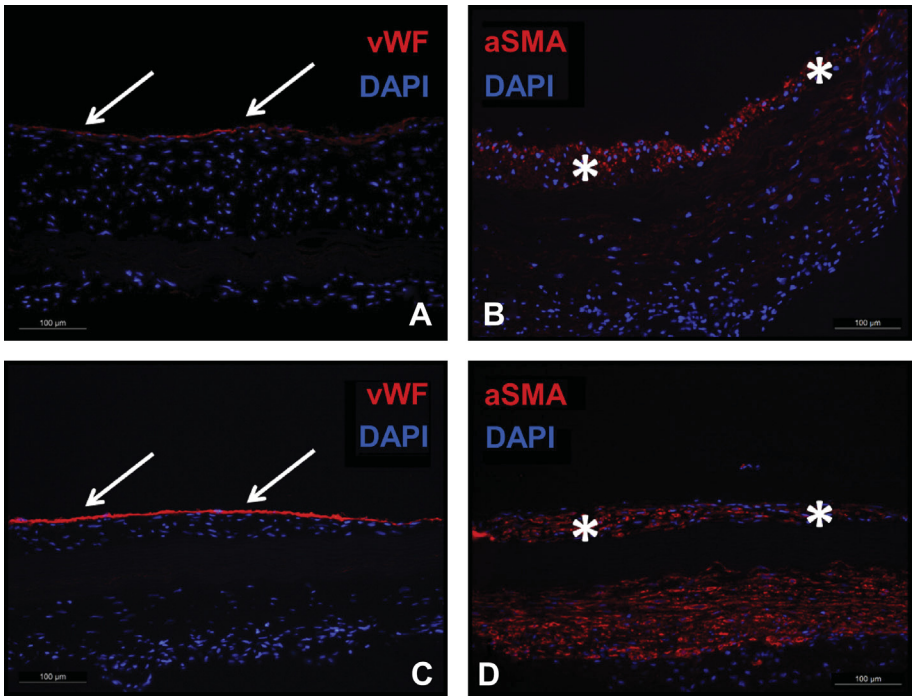

Fig. 7. Representative cross-sections through the ascending aorta of conduit grafts after 8 weeks *in vivo*. In both groups (group FN: A,B; group C: C,D), hyperplastic neointima was formed by aSMA(+) cells (red; asterisks in B and D), and vWF(+) endothelial cells covered the luminal border (red; arrows in A and C). Blue, DAPI. Scale bars = 100 μm.

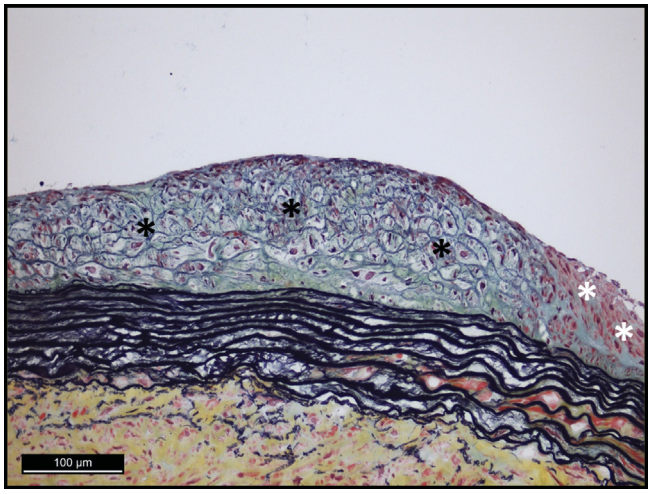

Fig. 8. Cross-sections through the ascending aorta of a conduit graft of group FN after 8 weeks *in vivo*. Hyperplastic neointima consisted of spindle-shaped cells (white asterisks) and chondroid cells in areas of extensive hyperplasia (black asterisks). Movat's pentachrome staining. Scale bar = 100 µm.

a significant drop in the MMP activity values from 4 weeks to 8 weeks in the group FN ($p < 0.0001$). As already demonstrated for the neointima regions, inflammatory cell markers (CD3 and CD68) were not present in the media at any time point [Fig. 10].

3.5. Quantitative RNA analysis

By analyzing gene expression, we sought to elaborate inter-group differences regarding relevant biological events. Therefore, we examined aSMA, VCAM1 and ICAM1 to assess interstitial cell activation, TGFb1, CD39 and CD73 for the evaluation of inflammatory and pro-thrombogenic state of the grafts and OPN, OCN and ALP as markers of chondro-osteogenic transformation of interstitial cells, which may promote calcifying degeneration in cardiovascular grafts. Moreover, integrins (ITNa4 and ITNa5) as key receptors for fibronectin were analyzed.

Osteocalcin was the only examined gene with a significantly different relative expression in group FN versus group C (0.2 ± 0.02 vs. 0.7 ± 0.24, $p = 0.045$) [Fig. 14]. Neither for the other markers of chondro-osteogenic transformation of interstitial cells (OPN: 0.9 ± 0.38 vs. 1.0 ± 0.12; ALP: 1.0 ± 0.22 vs. 1.2 ± 0.34), interstitial cell activation (aSMA: 0.8 ± 0.13 vs. 1.1 ± 0.22; VCAM1: 1.1 ± 0.07 vs. 1.0 ± 0.13; ICAM1: 1.0 ± 0.13 vs. 1.0 ± 0.13), and inflammatory markers (TGFb1: 1.1 ± 0.18 vs. 1.1 ± 0.18; CD39: 1.0 ± 0.20 vs. 1.1 ± 0.18; CD73: 0.8 ± 0.17 vs. 1.1 ± 0.22), nor with regard to the integrins (ITNa4: 0.9 ± 0.23 vs. 1.2 ± 0.28; ITNa5: 0.8 ± 0.18 vs. 1.1 ± 0.17), a significant inter-group difference was observed.

4. Discussion

To the best of the authors' knowledge, this is the first *in vivo* study on biofunctional protein coating of decellularized aortic conduits. Using a previously described small animal model of heterotopic aortic conduit implantation, we demonstrate fibronectin surface coating of cardiovascular implants to be feasible and persistent for at least 8 weeks in the systemic circulation. Moreover, fibronectin accelerated the autologous cellular repopulation of the implanted grafts optimizing their biocompatibility.

4.1. Fibronectin coating persistence

A couple of former studies referred to fibronectin coating of artificial vascular prostheses. Using polytetrafluoroethylene (PTFE) or Dacron® vascular grafts incubated with 10–500 µg/ml radiolabeled fibronectin, the loss kinetics during the first 24 h after implantation have been described *in vitro* [18]. Higher concentrations of fibronectin resulted in increased binding to the graft surface. However, with increasing concentrations, the effect of dosage augmentation was reduced. The present study revealed a concentration of 50 µg/ml fibronectin to result in an intensive surface coating of decellularized aortic conduits, with higher fibronectin concentrations failing to result in significantly improved coating results (data not shown). When coated aortic conduits were implanted, the use of fluorescence activity enabled the longest so far reported *in vivo* observation of protein coating persistence on cardiovascular implants.

4.2. Fibronectin as luminal coating agent

In the present study, biofunctional protein coating of decellularized aortic conduits by fibronectin accelerated the autologous *in vivo* reendothelialization of decellularized grafts. Previous reports have described similar positive effects of fibronectin coating on the seeding and integration of endothelial cells (EC) *in vitro* as well as *in vivo*, when artificial and biological vessel grafts were coated. Fibronectin incubation (20 µg/ml) of PTFE scaffolds prior to endothelial cell seeding has been reported to significantly increase the number of attached cells after 10–120 min [19]. After 7 days in a pulsatile bioreactor, EC on Dacron®/collagen scaffolds coated with fibronectin were more resistant to the applied physiological shear stress as determined by measurement of the loss of radiolabeled

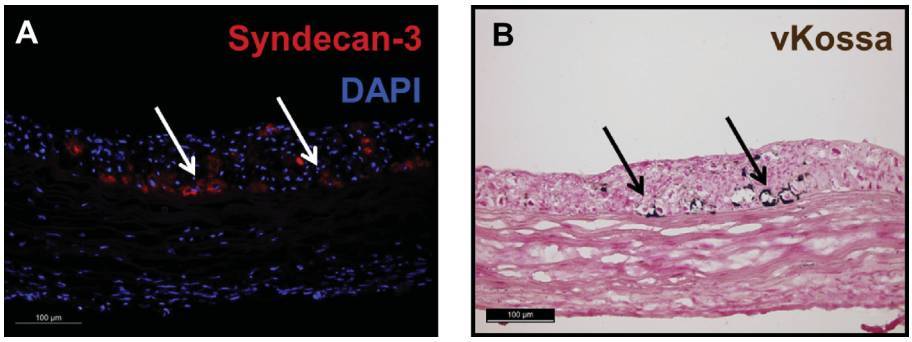

Fig. 9. Cross-sections through the ascending aorta of a conduit graft of group FN after 8 weeks *in vivo*. Chondroid cells in the hyperplastic neointima stained positive for syndecan-3 (red; arrows in A), indicating early chondrogenic differentiation, and were partially surrounded by hydroxyapatite (brown; arrows in B; von Kossa staining). Blue, DAPI. Scale bars = 100 µm. (For interpretation of the references to color in this figure legend, the reader is referred to the web version of this article.)

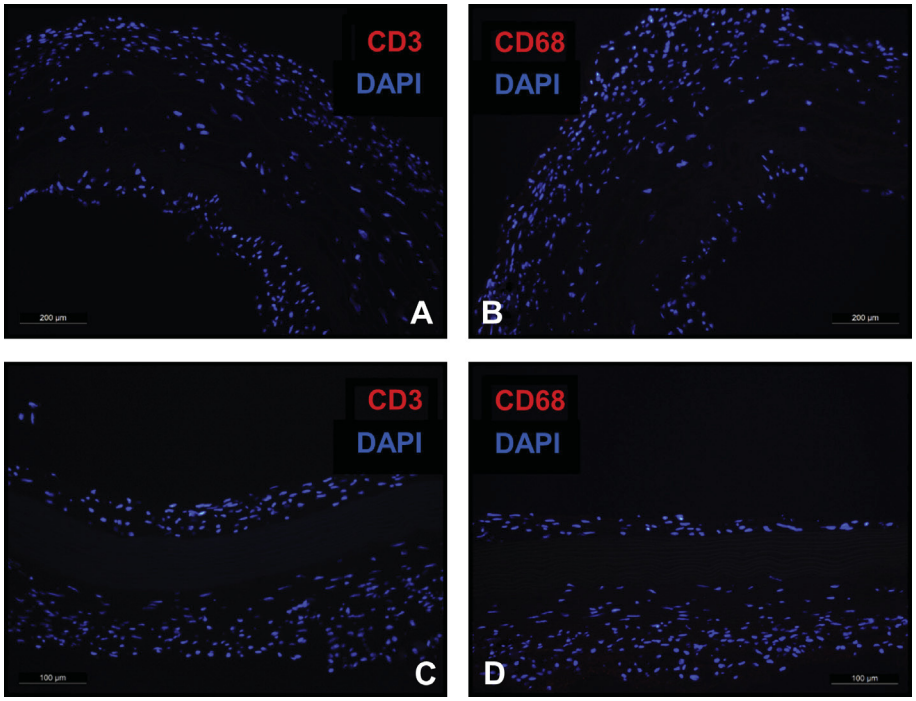

Fig. 10. Representative cross-sections through the ascending aorta of conduit grafts, exemplary after 8 weeks *in vivo*. In both groups (group FN: A,B; group C: C,D), staining against CD3 (red; A,C) and CD68 (red; B,D) was negative. Blue, DAPI. Scale bars = 200 μm in A,B and 100 μm in C,D. (For interpretation of the references to color in this figure legend, the reader is referred to the web version of this article.)

cells over time [20]. In a previous study, we revealed that fibronectin coating may serve as a protective factor preserving the morphology and function of valvular interstitial cells, and further inhibiting their calcifying degeneration in the presence of TGF-beta [21].

EC seeding prior to implantation is an alternative approach to enhance the biocompatibility of cardiovascular prostheses. However, while initially 60–70% of the luminal PTFE graft surface was covered with EC, only 5–15% of the graft surface remained endothelialized after 1–2 weeks, which represents a major drawback of

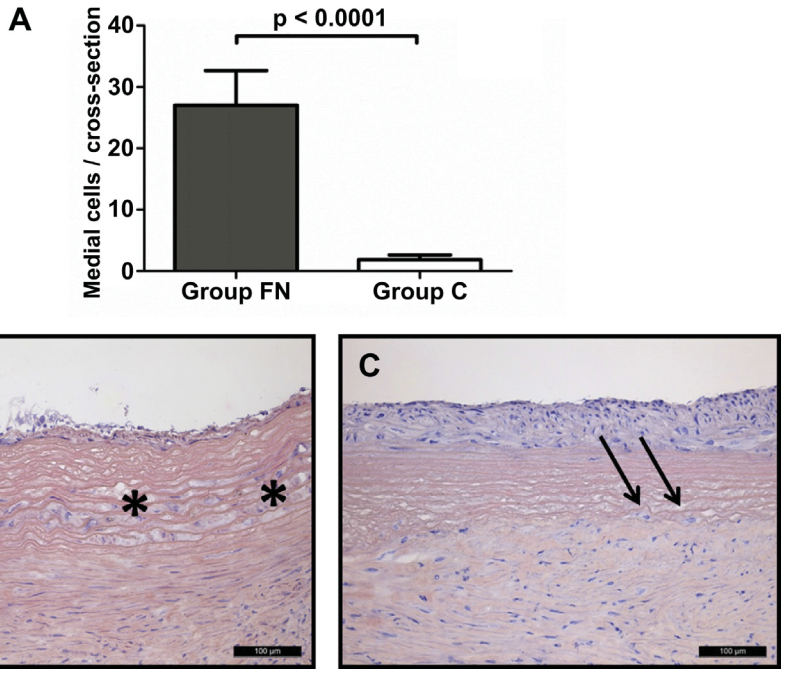

Fig. 11. Repopulation of the aortic conduit media after 8 weeks *in vivo*. The absolute count of media-repopulating cells was significantly increased in group FN versus group C (A). In both groups (group FN: B; group C: C), media-repopulating cells invaded the conduits from the adventitial surface (asterisks in B and arrows in C). Hematoxylin/eosin staining. Scale bars = 100 μm.

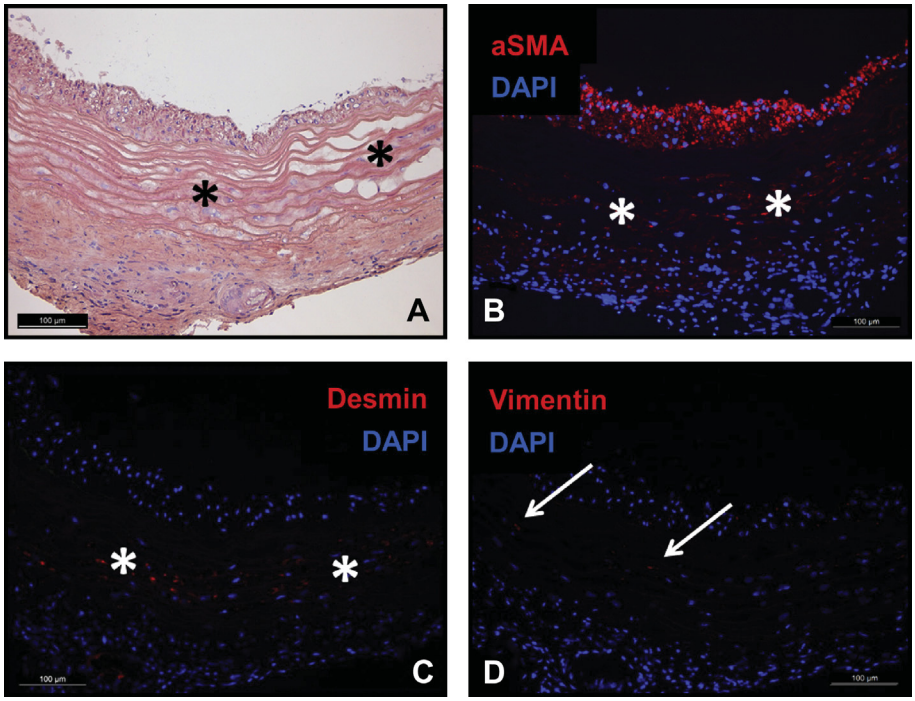

Fig. 12. Cross-sections through the ascending aorta of a conduit graft of group FN after 8 weeks *in vivo*. Media-repopulating cells (asterisks in A; hematoxylin/eosin staining) stained positive predominantly for aSMA (red; asterisks in B), partially for desmin (red, asterisks in C), and sparsely for vimentin (red, asterisks in D). In the neointima, desmin did not occur (C). Blue, DAPI (B,C,D). Scale bars = 100 μm.

in vitro endothelialization [22]. As a consequence, pulsatile bioreactors applying controlled physiological conditions have been introduced to improve the maintenance of EC after an orthotopic implantation of reseeded pulmonary heart valves in an ovine model [6]. Nevertheless, the bioreactor approach is time-consuming and cost-intensive, and harbors the additional risk of graft contamination and infection. Here, we follow an approach that omits labor- and time-consuming cell based pre-implantation modifications of the implant graft.

Implant areas close to the anastomoses were re-endothelialized earlier than regions remote to the anastomotic sites. This finding supports the hypothesis that luminal cellularization of cardiovascular implants may be mainly driven by cellular ingrowth from the anastomotic regions. Nevertheless, we also found islets of neointima distant from the anastomoses after 1 and 4 weeks. The latter observation suggests the additional influence of cellular repopulation via the blood stream. Another factor that may play a role in the regulation of repopulation speed is defined by locally different wall shear stress conditions. By means of computational fluid dynamics, the aortic arch anatomy has been shown to experience enhanced wall shear rates, which may negatively influence the attachment of autologous cells [23]. The latter issue may have contributed to the observed local delay in neointima formation.

Despite the beneficial effect of fibronectin on the luminal EC coverage, adverse effects that may be intrinsic to fibronectin coating have been elucidated in the present study. Our experiments revealed an aggravated intimal hyperplasia, with an early progress in the perianastomotic regions. It has been long known that hyperplastic intima formation is triggered by non-endothelialized graft surfaces exposed to the blood stream. Interestingly, certain approaches to accelerate the endothelialization process have been reported to support intimal hyperplasia as well.

Hyperplastic intima areas in the present study were primarily populated by aSMA positive myofibroblasts. However, after 8 weeks, additional chondroid cells occurred in areas of extensive hyperplasia. The collective findings of syndecan-3 expression and co-localized hydroxyapatite deposition suggest that these cells may undergo early chondro-osteogenic transformation. These signs of degenerative calcification were limited to advanced stages of hyperplasia, so that the prevention of hyperplastic neointima formation may inhibit the observed onset of calcifying degeneration of decellularized aortic conduits. Moreover, adverse matrix remodeling with increased activity of MMP was observed in these regions. These findings are in compliance with a previous report involving the long-term follow-up of polycaprolactone prostheses after abdominal implantation in rats, where a parallel development of intimal hyperplasia, chondroid interstitial metaplasia and final graft calcification was demonstrated after 18 months [24].

Interestingly, clinical PTFE grafts explanted due to failure are characterized by similar findings of neointimal hyperplasia, remarkable calcification, but also contain foreign body reaction as well as thrombosis. Here, we found no signs of inflammation or thrombosis in any of the explanted decellularized conduits at any time point, underlining the relevance of hyperplastic neointima formation as a major driving force for adverse graft remodeling. On the other hand, these findings of gross elimination of inflammatory response are consistent with previous small and large animal implantation reports on acellular heart valve grafts [25,26].

Altogether, our results indicate that in spite of accelerating the endothelialization of cardiovascular implants, fibronectin may not represent the optimal coating agent for the luminal surface of biologically derived cardiovascular implants, since it rather promotes an intimal hyperplasia. Therefore, future work on alternative biofunctional coating agents is necessary.

4.3. Fibronectin as adventitial coating agent

Fibronectin coating of the adventitial surface of decellularized aortic conduits induced a significantly increased autologous medial repopulation during the first 8 weeks *in vivo*, while uncoated grafts

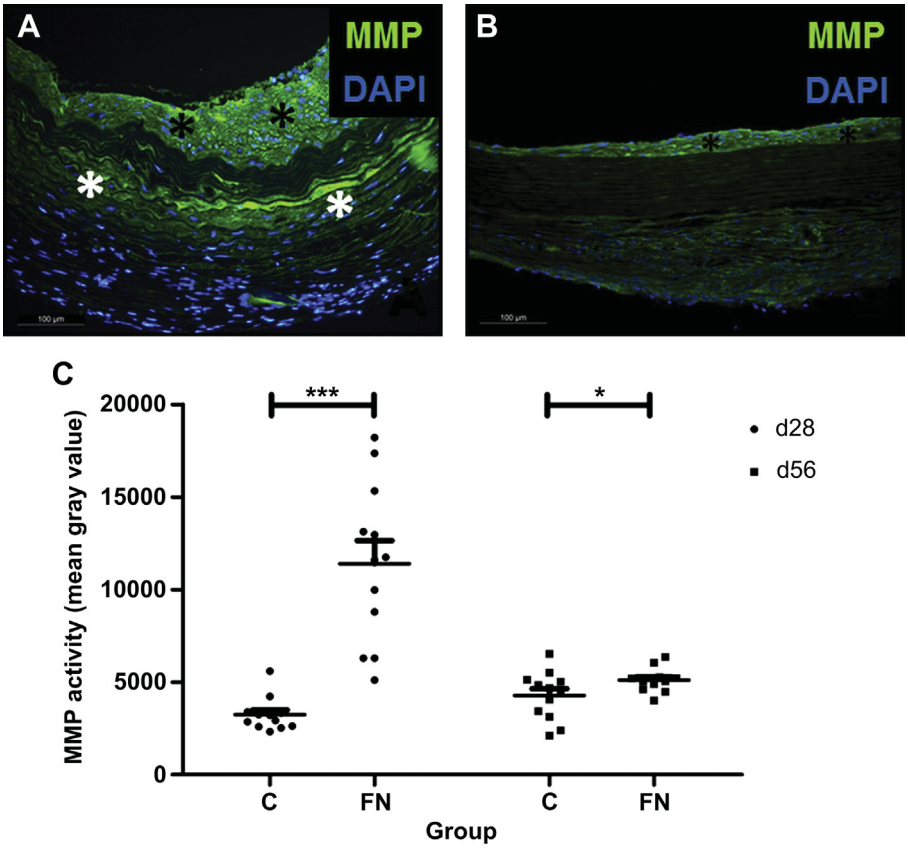

Fig. 13. Matrix metalloproteinase (MMP) gelatinase activity in aortic conduit explants. Representative cross-sections through the ascending aorta of conduit grafts (group FN: A; group C: B) after 8 weeks *in vivo* revealed enhanced MMP activity (green) around the media-repopulating cells (white asterisks in A) as well as in the neointima (black asterisks in A and B). After 4 and 8 weeks, the amount of MMP activity was significantly increased in group FN as compared to group C, whereas after 4 weeks, the activity in group FN was significantly higher than after 8 weeks ($p < 0.0001$). *In situ* zymography. $^{*}p = 0.029$. $^{***}p < 0.0001$. Blue, DAPI. Scale bars = 100 μm.

showed only sparse cell invasion. Repopulating cells predominantly originated from the adventitial side, underlining the importance of this region with respect to autologous medial repopulation. As already described in other studies, using decellularized cardiovascular grafts, cells originating from the blood stream failed to cross the luminal basal lamina of the prostheses.

The cell-attracting effects of fibronectin are predominantly mediated by direct binding to the cell adhesion receptor integrin-alpha-5-beta-1, thereby activating intracellular signal transduction cascades and further promoting the adhesion complex formation and cellular migration. After 8 weeks *in vivo*, quantitative real-time PCR analyses of the explants did not reveal an alteration of integrin-alpha-5-beta-1 expression by fibronectin-coating. However, these findings do not necessarily exclude the possibility of a crucial role for integrin-alpha-5-beta-1 signaling in the process of medial repopulation, since total RNA of the entire explants was analyzed and the relative amount of media-invading cells may have been outweighed by the large proportion of other recellularized areas.

We further characterized the entity of autologous cells repopulating the media region of the implants. In contrast to the myofibroblasts in the hyperplastic regions of the neointima, those cells repopulating the media region stained positive not only for aSMA but also for desmin, which is in line with previous reports on the neointima and media-localized cells of freshly injured arteries [27]. Despite the ongoing controversy on the cytoskeleton-based phenotype classification of activated interstitial cells and the respective functional role, we suggest the observed aSMA(+)/desmin(+) cells to be classified as smooth muscle cells, and aSMA(+)/desmin(−) cells to be accounted for myofibroblasts.

Finally, in the current study, the process of medial repopulation was closely co-localized with intensive MMP activity, indicating a concert of biological events involved in the activated graft remodeling leading to the autologous repopulation of the decellularized grafts. Furthermore, fibronectin was recently reported to stimulate the expression of integrin-alpha-5-beta-1 as well as MMP-2 in smooth muscle cells [28]. This mechanism may also have contributed to the observed enhancement of MMP activity around the media-repopulating smooth muscle cells. With regard to the whole graft wall, fibronectin-coated conduits showed increased MMP activity that was significantly enhanced after 4 weeks. The underlying cause for that observation may be an additional MMP stimulation by fibronectin, since recently, it was shown *in vitro* that the MMP-9 activity of fibroblasts increases in the presence of fibronectin [29].

According to immunofluorescence staining (CD3 and CD68) and PCR analyses (TGF-beta, VCAM-1 and ICAM-1), inflammation did not play a significant role in the observed matrix reorganization process, underlining the inflammation-independent action of fibronectin leading to an accelerated graft revitalization *in vivo*. The latter observation may reveal new perspectives for optimization strategies to improve the biocompatibility and durability of biological implants in the cardiovascular system.

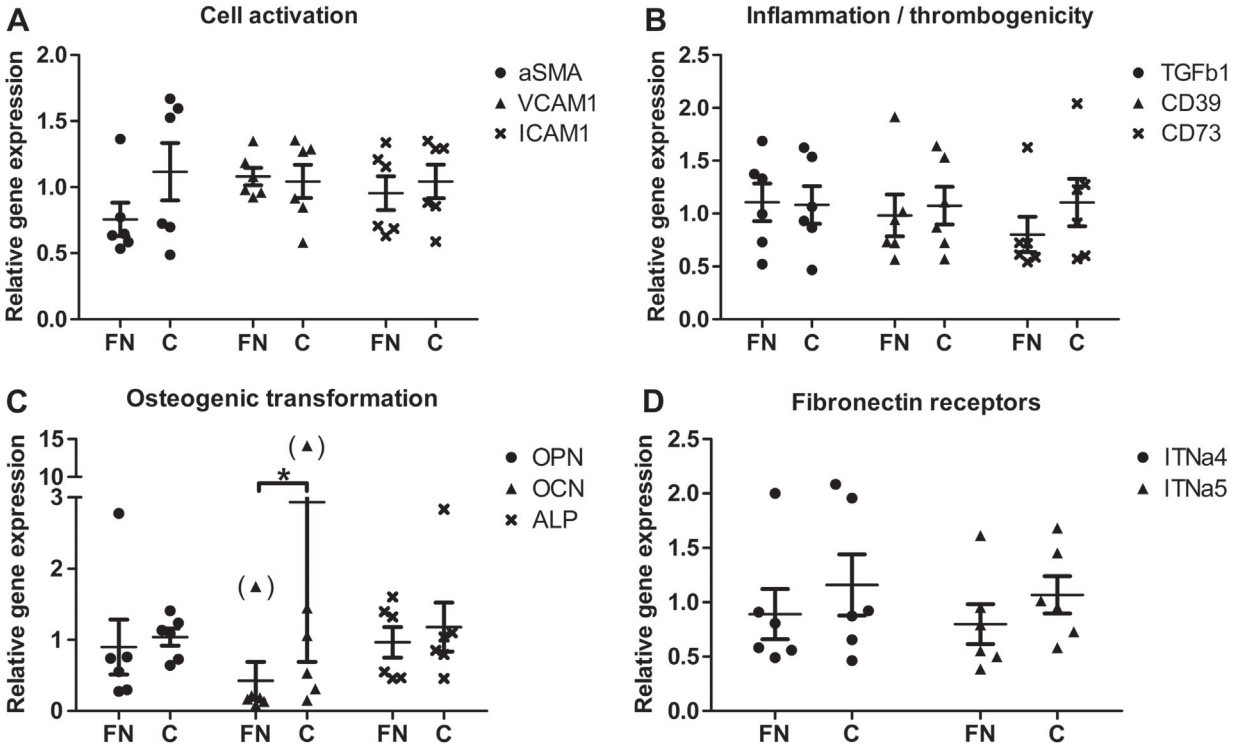

Fig. 14. Relative gene expression analysis in explanted aortic conduits (8 weeks *in vivo*) by means of quantitative real-time PCR (ddCt method). With regard to different markers of cell activation (aSMA, VCAM1, and ICAM1 (A)), inflammation and pro-thrombogenicity (TGFb1, CD39, and CD73 (B)), and the fibronectin key receptors ITNa4 and ITNa5 (D), no significant differences occurred between group FN and group C. Among the markers of chondro-osteogenic transformation (OPN, OCN, and ALP (C)), the relative gene expression of osteocalcin was significantly decreased in group FN (*$p = 0.045$; values in brackets, excluded from statistical group comparison). FN, group FN; C, group C; aSMA, alpha-smooth muscle actin; VCAM1, vascular cell adhesion molecule-1; ICAM1, intercellular adhesion molecule-1; TGFb1, transforming growth factor-beta-1; OPN, osteopontin; OCN, osteocalcin; ALP, alkaline phosphatase; ITNa4, integrin-alpha-4; ITNa5, integrin-alpha-5.

4.4. Study limitations

The presented work resembles a proof of concept study on the impact of fibronectin coating with a significant improvement of a number of outcome measures, most prominently the recellularization of the implanted aortic conduits. However, the employed rat model may not entirely mimic the specific events involved in the *in vivo* maturation of cardiovascular prostheses in humans. Differences may be inherently linked to the specific rodent species, but further limitations may arise from the lack of the complex constellation of co-morbidities that are present in most of the patients in the clinical scenario, e.g. age, metabolic disorders and medication etc. Therefore, further preclinical studies, ideally involving adequate large animal models are necessary to further evaluate the impact of fibronectin surface coating.

5. Conclusions

In the present study, we report on the *in vivo* results of targeted surface modification of decellularized aortic conduits with a biofunctional protein coating strategy. A fluorophore-based labeling approach enabled the *in vivo* tracking of fibronectin coating and proved its persistence for up to 8 weeks in the systemic circulation. Fibronectin improved the cell adhesion capacity and the biocompatibility of the decellularized grafts resulting in a significantly accelerated endothelialization at the cost of aggravated hyperplastic neointima formation. Interestingly, fibronectin coating induced medial graft repopulation in the absence of an inflammatory reaction or adverse gene expression, indicating the feasibility and potential of this strategy for the improvement of current clinically applied bioprostheses. Ongoing studies on alternative bioactive coating agents, applying a more sophisticated differential surface coating, are underway. The quest for the ideal cardiovascular graft has reached the next phase.

Acknowledgments

The authors gratefully acknowledge the work of Kai Zwirnmann regarding the establishment and performance of immunohistological methods and thank Gisela Müller for her work concerning the PCR analyses.

The authors confirm that there are no known conflicts of interest associated with this publication and there has been no significant financial support for this work that could have influenced its outcome.

References

[1] O'Brien MF, Stafford EG, Gardner MA, Pohlner PG, Tesar PJ, Cochrane AD, et al. Allograft aortic valve replacement (long-term follow-up). Ann Thorac Surg 1995;60:S65–70.
[2] Clarke DR, Campbell DN, Hayward AR, Bishop DA. Degeneration of aortic valve allografts in young recipients. J Thorac Cardiovasc Surg 1993;105:934–41.
[3] Green MK, Walsh MD, Dare A, Hogan PG, Zhao XM, Frazer IH, et al. Histologic and immunohistochemical responses after aortic valve allografts in the rat. Ann Thorac Surg 1998;66:S216–20.
[4] Shaddy RE, Hunter DD, Osborn KA, Lambert LM, Minich LL, Hawkins JA, et al. Prospective analysis of HLA immunogenicity of cryopreserved valved allografts used in pediatric heart surgery. Circulation 1996;94:1063–7.
[5] Grauss RW, Hazekamp MG, van Vliet S, Gittenberger-de Groot AC, DeRuiter MC. Decellularization of rat aortic valve allografts reduces leaflet destruction and extracellular matrix remodeling. J Thorac Cardiovasc Surg 2003;126:2003–10.

[6] Lichtenberg A, Tudorache I, Cebotari S, Suprunov M, Tudorache G, Goerler H, et al. Preclinical testing of tissue-engineered heart valves re-endothelialized under simulated physiological conditions. Circulation 2006;114:I559–65.
[7] Akhyari P, Kamiya H, Gwanmesia P, Aubin H, Tschierschke R, Hoffmann S, et al. In vivo functional performance and structural maturation of decellularised allogenic aortic valves in the subcoronary position. Eur J Cardiothorac Surg 2010;38:539–46.
[8] Cebotari S, Lichtenberg A, Tudorache I, Hilfiker A, Mertsching H, Leyh R, et al. Clinical application of tissue engineered human heart valves using autologous progenitor cells. Circulation 2006;114:I132–7.
[9] da Costa FD, Costa AC, Prestes R, Domanski AC, Balbi EM, Ferreira AD, et al. The early and midterm function of decellularized aortic valve allografts. Ann Thorac Surg 2010;90:1854–60.
[10] Kasimir MT, Rieder E, Seebacher G, Nigisch A, Dekan B, Wolner E, et al. Decellularization does not eliminate thrombogenicity and inflammatory stimulation in tissue-engineered porcine heart valves. J Heart Valve Dis 2006;15:278–86.
[11] Meyer SR, Chiu B, Churchill TA, Zhu L, Lakey JR, Ross DB. Comparison of aortic valve allograft decellularization techniques in the rat. J Biomed Mater Res A 2006;79:254–62.
[12] Zhou J, Fritze O, Schleicher M, Wendel HP, Schenke-Layland K, Harasztosi C, et al. Impact of heart valve decellularization on 3-D ultrastructure, immunogenicity and thrombogenicity. Biomaterials 2010;31:2549–54.
[13] Rieder E, Seebacher G, Kasimir MT, Eichmair E, Winter B, Dekan B, et al. Tissue engineering of heart valves: decellularized porcine and human valve scaffolds differ importantly in residual potential to attract monocytic cells. Circulation 2005;111:2792–7.
[14] Shimada T, Nishibe T, Miura H, Hazama K, Kato H, Kudo F, et al. Improved healing of small-caliber, long-fibril expanded polytetrafluoroethylene vascular grafts by covalent bonding of fibronectin. Surg Today 2004;34:1025–30.
[15] Zhou M, Liu Z, Wei Z, Liu C, Qiao T, Ran F, et al. Development and validation of small-diameter vascular tissue from a decellularized scaffold coated with heparin and vascular endothelial growth factor. Artif Organs 2009;33:230–9.
[16] Assmann A, Akhyari P, Delfs C, Flögel U, Jacoby C, Kamiya H, et al. Development of a growing rat model for the in vivo assessment of engineered aortic conduits. J Surg Res 2012;176:367–75.
[17] Joghetaei N, Akhyari P, Rauch BH, Cullen P, Lichtenberg A, Rudelius M, et al. Extracellular matrix metalloproteinase inducer (CD147) and membrane type 1-matrix metalloproteinase are expressed on tissue macrophages in calcific aortic stenosis and induce transmigration in an artificial valve model. J Thorac Cardiovasc Surg 2011;142:191–8.
[18] Ramalanjaona GR, Kempczinski RF, Ogle JD, Silberstein EB. Fibronectin coating of an experimental PTFE vascular prosthesis. J Surg Res 1986;41:479–83.
[19] Budd JS, Allen KE, Bell PR, James RF. The effect of varying fibronectin concentration on the attachment of endothelial cells to polytetrafluoroethylene vascular grafts. J Vasc Surg 1990;12:126–30.
[20] Baguneid M, Murray D, Salacinski HJ, Fuller B, Hamilton G, Walker M, et al. Shear-stress preconditioning and tissue-engineering-based paradigms for generating arterial substitutes. Biotechnol Appl Biochem 2004;39:151–7.
[21] Gwanmesia P, Ziegler H, Eurich R, Barth M, Kamiya H, Karck M, et al. Opposite effects of transforming growth factor-β1 and vascular endothelial growth factor on the degeneration of aortic valvular interstitial cell are modified by the extracellular matrix protein fibronectin: implications for heart valve engineering. Tissue Eng Part A 2010;16:3737–46.
[22] Griese DP, Ehsan A, Melo LG, Kong D, Zhang L, Mann MJ, et al. Isolation and transplantation of autologous circulating endothelial cells into denuded vessels and prosthetic grafts: implications for cell-based vascular therapy. Circulation 2003;108:2710–5.
[23] Assmann A, Benim AC, Gül F, Lux P, Akhyari P, Boeken U, et al. Pulsatile extracorporeal circulation during on-pump cardiac surgery enhances aortic wall shear stress. J Biomech 2012;45:156–63.
[24] de Valence S, Tille JC, Mugnai D, Mrowczynski W, Gurny R, Möller M, et al. Long term performance of polycaprolactone vascular grafts in a rat abdominal aorta replacement model. Biomaterials 2012;33:38–47.
[25] Meyer SR, Nagendran J, Desai LS, Rayat GR, Churchill TA, Anderson CC, et al. Decellularization reduces the immune response to aortic valve allografts in the rat. J Thorac Cardiovasc Surg 2005;130:469–76.
[26] Numata S, Fujisato T, Niwaya K, Ishibashi-Ueda H, Nakatani T, Kitamura S. Immunological and histological evaluation of decellularized allograft in a pig model: comparison with cryopreserved allograft. J Heart Valve Dis 2004;13:984–90.
[27] Shi Y, O'Brien JE, Fard A, Mannion JD, Wang D, Zalewski A. Adventitial myofibroblasts contribute to neointimal formation in injured porcine coronary arteries. Circulation 1996;94:1655–64.
[28] Yang G, Li H, Tang G, Wu L, Zhao K, Cao Q, et al. Increased neointimal formation in cystathionine gamma-lyase deficient mice: role of hydrogen sulfide in α5β1-integrin and matrix metalloproteinase-2 expression in smooth muscle cells. J Mol Cell Cardiol 2012;52:677–88.
[29] Cha MC, Purslow PP. The activities of MMP-9 and total gelatinase respond differently to substrate coating and cyclic mechanical stretching in fibroblasts and myoblasts. Cell Biol Int 2010;34:587–91.

3.4 Effects of systemic statin treatment on the *in vivo* degeneration of decellularized aortic conduit grafts

***Assmann A**, Horstkötter K, Munakata H, Schiffer F, Delfs C, Zwirnmann K, Barth M, Akhyari P, Lichtenberg A. Simvastatin does not diminish the in vivo degeneration of decellularized aortic conduits. **J Cardiovasc Pharmacol**. 2014; 64:332-342.*

Potential anti-degenerative effects of statins in the context of decellularized aortic conduit implantation were examined in our model of accelerated cardiovascular calcification for up to 12 weeks (n=16 statin-treated (group S) and n=17 control (group C) animals).

Statin treatment decreased the serum levels of cholesterol and calcium as compared to control rats, indicating the metabolic effect of the administered HMG-CoA reductase inhibitor. However, no significant anti-degenerative effect was observed. Neither the time course of recellularization nor the intima-to-media ratio differed between the groups. All explants were luminally covered with time-dependently progressing pannus formation by predominantly alpha-smooth muscle actin-positive cells and an endothelial barrier to the blood stream. The pannus areas consisted of spindle-shaped myofibroblastoid cells as well as chondroid cells at later time points in both groups. Immunostaining against CD3 and CD68 was throughout negative, which is consistent with data from the other projects on decellularized graft implantation.

Semi-quantification of the MMP gelatinase activity showed an increase over time and higher values in the statin group after 12 weeks. Hydroxyapatite deposition in the aortic conduits also had a time-dependent course, however, neither histologically nor by measuring the total calcium content in the implants statistically significant differences were found between the two groups. Inhibiting lipid-mediated inflammation is an anti-degenerative key mechanism of statins, and inflammation did not play a relevant role in decellularized implants of this study. This may at least partially explain why statins had no relevant effect on graft degeneration. Besides their pleiotropic anti-inflammatory and immunomodulatory properties, HMG-CoA reductase inhibitors have been reported to adversely stimulate the osteogenic differentiation of VICs and to increase the calcium content of atherosclerotic plaques [80,81], whereas the latter effect is regarded to be even beneficial in terms of plaque stabilization [82].

That there was also no pro-calcific action driven by statin treatment, might be due to the fact that the conduit media as main calcification site did not contain a lot of interstitial cells whose osteogenic differentiation could have been stimulated.

Among multiple markers of inflammation, thrombogenicity and osteogenic transformation, only the gene expression of interleukin-6 was downregulated by statin treatment. Although we did not detect major inflammation in the decellularized aortic conduits, the downregulation of interleukin-6 in the statin group may point at an implant-preserving effect, since elevated interleukin-6 levels are involved in the inflammatory response against artificial and biological grafts [83,84].

In summary, in the first *in vivo* examination of the effect of statin treatment on the calcifying degeneration of decellularized cardiovascular implants, simvastatin failed to inhibit graft calcification under conditions of accelerated cardiovascular sclerosis. Moreover, it did not significantly influence the speed of recellularization or the formation of pannus on the implants. These findings are in accordance with clinical data on statins failing to slow down the progression of CAVD and bioprosthesis degeneration. Furthermore, the lack of relevant inflammation in decellularized cardiovascular prostheses may abrogate a key mechanism of statins, and therefore, may explain the lack of beneficial effects on graft degeneration.

Simvastatin Does Not Diminish the In Vivo Degeneration of Decellularized Aortic Conduits

Alexander Assmann, MD,†‡ Kim Horstkötter,* Hiroshi Munakata, MD, PhD,* Franziska Schiffer,* Christofer Delfs,* Kai Zwirnmann,* Mareike Barth, PhD,* Payam Akhyari, MD, PhD,* and Artur Lichtenberg, MD, PhD**

Background: All present biological cardiovascular prostheses are prone to progressive in vivo degeneration, which can be partially impaired by decellularization. The administration of statins may provide an additional beneficial effect. We provide the first in vivo data on the effect of statins on decellularized cardiovascular implants.

Methods: Wistar rats with aortic valve insufficiency (day 14) were fed either with a pro-calcific diet (group C; n = 17), or the same diet additionally supplemented with simvastatin (group S; n = 16). Aortic conduits from Sprague-Dawley rats were detergent-decellularized, infrarenally implanted (day 0) in all recipients and explanted at day 28 or day 84.

Results: Sonographic competence of the conduit perfusion was 100%, and overall survival amounted to 97%. Simvastatin decreased the low-density lipoprotein cholesterol serum levels; however, it did not affect the calcification of the implants. Histology revealed alpha-smooth muscle actin-positive intima hyperplasia in both groups. Extensive matrix metalloproteinase activity was observed in calcified areas, especially in group S. Quantitative RNA analysis resulted in no differences with regard to several markers of calcifying degeneration (alkaline phosphatase, osteopontin, osteocalcin, osteoprotegerin, bone morphogenetic protein-2, runt-related transcription factor-2) and inflammation (tumor necrosis factor α, interleukin 1β, receptor for advanced glycation end products, CD39, CD73), but significantly lower levels of interleukin-6 in group S.

Conclusions: In a standardized small animal model of accelerated cardiovascular calcification, simvastatin failed to diminish the calcification of decellularized aortic conduit implants. This finding confirms the observations of recent clinical trials. However, further experiments are warranted to elucidate the value of partial benefits associated with lower circulating lipid and proinflammatory cytokine levels.

Received for publication January 7, 2014; accepted April 28, 2014.

From the *Department of Cardiovascular Surgery and Research Group for Experimental Surgery, Medical Faculty, Heinrich Heine University, Duesseldorf, Germany; †Department of Medicine, Center for Biomedical Engineering, Brigham and Women's Hospital, Harvard Medical School, Boston, MA; and ‡Harvard-MIT Division of Health Sciences and Technology, Massachusetts Institute of Technology, Cambridge, MA.

Supported by institutional funds of the Department of Cardiovascular Surgery, Medical Faculty, Heinrich Heine University, Duesseldorf.

The authors report no conflicts of interest.

Reprints: Payam Akhyari, MD, Department of Cardiovascular Surgery and Research Group for Experimental Surgery, Medical Faculty, Heinrich Heine University, Moorenstrasse 5, D-40225 Duesseldorf, Germany (e-mail: payam.akhyari@med.uni-duesseldorf.de).

Key Words: aortic valve prosthesis, calcification, graft degeneration, statin

(*J Cardiovasc Pharmacol*™ 2014;64:332–342)

INTRODUCTION

Decellularized cardiovascular implants are a raising alternative to overcome inherent problems of common bioprostheses, predominantly inflammatory and immune response of the recipient.[1,2] Acellular heart valve substitutes have been successfully implanted in the aortic and the pulmonary position with promising results in preclinical as well as in clinical studies.[3–6] Nevertheless, few reports on early pulmonary valve graft degeneration in pediatric patients have raised questions about the durability of decellularized valvular grafts.[7–9] Besides improvement of the manufacturing protocols for decellularized prostheses, anti–calcific treatment of the recipient may be supportive in slowing the graft deterioration.

Statins are known to beneficially affect atherosclerosis, and therefore, they have been implemented as the first-line therapy of coronary artery disease. However, their effect on the calcification of the native aortic valve is controversially discussed,[10,11] and there are even less data on the role of statins in preserving biological heart valve prostheses in vivo.[12] With regard to decellularized cardiovascular implants, both the lipid-lowering action and also the pleiotropic effect of statins theoretically may contribute to graft durability in the long term, especially by reducing intimal hyperplasia of the implants. However, this hypothesis has not been investigated yet, and experimental or clinical data on the effect of statins on decellularized cardiovascular implants are entirely missing.

The present study aimed at examining the potential of simvastatin to beneficially influence the calcifying degeneration of decellularized aortic conduits in a standardized rat implantation model of accelerated cardiovascular calcification.

METHODS

Animal Experiments

All animals were obtained from the local animal care facility of the University of Duesseldorf, Germany, and fed ad libitum. In all surgical procedures, anesthesia and analgesia were achieved by inhaled isoflurane (2.0%–2.5%) and intraperitoneally administered carprofen (5 $mg \cdot kg^{-1} \cdot d^{-1}$). All experiments were conducted according to the "Guide for

the Care and Use of Laboratory Animals," and approved by the state animal care committee (reference number 87-51.04.2010.A068).

Male Sprague-Dawley rats (n = 33, 200–250 g) served as aortic conduit graft donors, whereas the recipients were male Wistar rats (n = 33, 200–250 g). At day 14, aortic valve insufficiency (AI) was interventionally generated under echocardiographic guidance in all recipient rats as recently published.[13] Two weeks later, decellularized aortic conduits were infrarenally implanted into the systemic circulation as previously described (Fig. 1).[13,14] The purpose of the generation of an aortic insufficiency in the native aortic valve of the recipient is to improve the functionality of the implant valve.

Starting at day −14, all recipients were fed with a procalcific diet (300,000 U/kg vitamin D, 2% cholesterol, 1.5% calcium phosphate) until the final explantation of the prosthesis. In group S (n = 16), the 3-hydroxy-3-methylglutaryl-coenzyme A (HMG-CoA) reductase inhibitor simvastatin (10 mg/kg chow; equivalent dose to 40 mg/d in patients weighing 70 kg) was additionally supplemented during the whole experiment. Animals in group C without simvastatin supplementation served as controls (n = 17).

Four or 12 weeks after implantation, the grafts were again controlled for sonographic competence, rinsed with heparinized phosphate-buffered saline (PBS), thoroughly excised and further processed for histology, immunohistology, in situ zymography (each with n = 3 per group at day 28 and n = 5 per group at day 84), calcium content measurement (n = 3 per group at day 84) and quantitative real-time polymerase chain reaction (RT-PCR) (n = 5 per group at day 84).

Aortic Valve Insufficiency Operation

At day −14, Wistar rats were anesthetized with isoflurane (2.0%–2.5%), and carprofen (5 $mg \cdot kg^{-1} \cdot d^{-1}$) was intraperitoneally administered. The right common carotid artery was exposed, and a cannula was inserted through which a guide wire was advanced toward the aortic valve. Under echocardiographic control with a Philips HDX11 ultrasonography system equipped with a 15 MHz probe (Philips, Amsterdam, the Netherlands), the aortic valve leaflets were perforated to induce an AI grade II–III. After wound closure, the anesthesia was terminated. Animals with AI grade I or grade IV were excluded from the study. Echocardiographic data of several animals of the control group were partially published in an article describing the development of the animal model.[13]

Graft Engineering

U-shaped aortic conduits were harvested from donor rats and prepared as recently described.[14] Briefly, after ligature of the coronary and supraaortic arteries, the grafts were decellularized by means of a detergent-based protocol consisting of 4 cycles (12 hours) with 0.5% sodium dodecyl sulfate + 0.5% deoxycholate, followed by 24 hours rinsing with distilled water and 3 further rinsing cycles (24 hours each) with PBS supplemented with 1% penicillin/streptomycin and 0.05% sodium azide.

Heterotopic Graft Implantation and Explantation Procedures

Recipient rats were anesthetized as described above, and a central venous jugular vein catheter was inserted. After median laparotomy and systemic administration of heparin (300 IU/kg), the abdominal aorta was clamped, and a decellularized aortic conduit graft was sutured to the infrarenal aorta in an end-to-side manner. Afterward, the native aorta between the 2 anastomoses was ligated to improve the perfusion of the implant, the abdomen was closed, and after sonographic confirmation of unimpaired conduit perfusion, the recipients recovered from anesthesia.

Four or 12 weeks after implantation, the recipient rats were anesthetized, and Doppler sonography was conducted to control the perfusion of the prostheses. After laparotomy, the implanted conduits were rinsed with heparinized PBS by abdominal cannulation, thoroughly excised and further processed for histology, immunofluorescence, in situ zymography

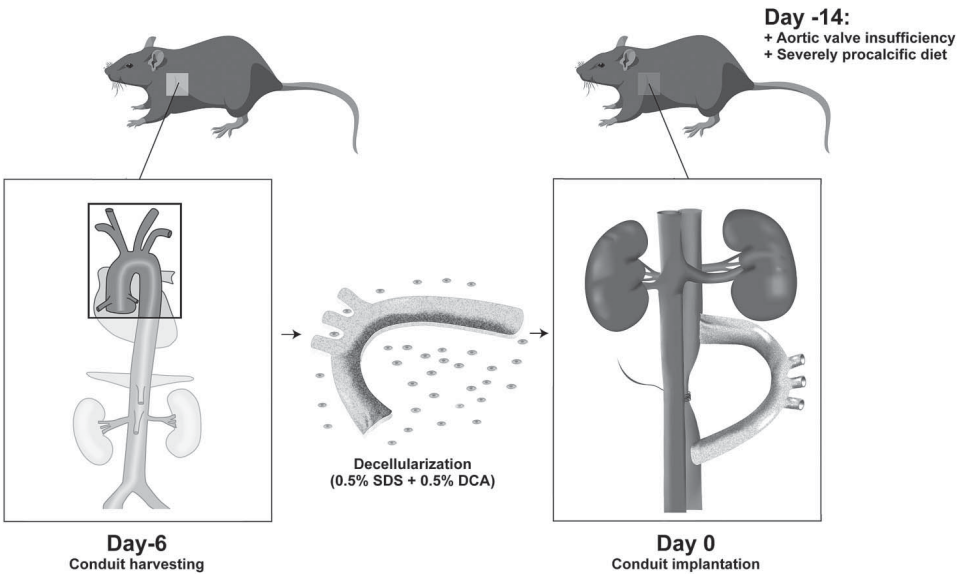

FIGURE 1. Experimental design of infrarenally implanting decellularized aortic conduits in rats receiving a pro-calcifying diet and suffering from AI. SDS, sodium dodecyl sulfate; DCA, deoxycholic acid.

(each with n = 3 per group at day 28 and n = 5 per group at day 84), calcium content measurement (n = 3 per group at day 84) and quantitative RT-PCR (n = 5 per group at day 84).

Blood Serum Analyses

At days −14, 0, and 84, blood was taken, and the serum levels of calcium, phosphate, urea, cholesterol, triglycerides and glucose were analyzed in the Institute of Clinical Chemistry and Laboratory Diagnostics, Medical Faculty, Heinrich Heine University, Duesseldorf, Germany, applying commercially available standard assays designed for the automated clinical chemistry analyzer series Cobas (Roche, Basel, Switzerland).

Explant Histology

Histology was performed on cryosections [hematoxylin–eosin staining, Movat's pentachrome staining, and von Kossa staining]. Morphometric analyses for the detection of intergroup differences were performed using Image J v1.46 (Wayne Rasband, National Institutes of Health).

For comparative quantification of luminal neointima formation, a standardized scoring system was used as recently established.[15] In brief, each conduit was divided into 4 regions: aortic valve (region A1), ascending aorta (region A2), descending aorta (region B1), and distal anastomosis with the native recipient aorta (region B2). In each region, 3 cross sections in a distance of 200 μm to each other were histomorphologically analyzed. In the regions A2, B1, and B2, each cross section was divided into 8 radially orientated segments, in which the percentage of recellularized surface was determined. In region A1, the cross section of the aortic valve was divided into 9 segments reflecting the aortic sinuses, commissures, and leaflets. For each of the 4 regions of a conduit (A1-B2), the percentage of recellularized surface was segmentally calculated.

Regarding quantification of the intimal hyperplasia, the explants were systematically analyzed as described above. In each segment, the media thickness and the thickness of the neointima were measured to determine the median intima-to-media ratio in each of the 4 regions.

To quantify the calcification of the aortic conduit grafts, separate scoring systems for the neointima and the media of the explant ascending aorta were developed: In each of the 4 conduit regions defined above, cross sections were divided into 8 radially orientated segments, in which the scoring was conducted. For the neointima, the scoring range was 0–3 (0 = no calcification; 1 = microcalcification; 2 = macrocalcification <50% of the neointima area; 3 = macrocalcification >50% of the neointima area), and 0–5 for the media (0 = no calcification; 1 = microcalcification; 2 = macrocalcification <25% of the neointima area; 3 = macrocalcification 25%–50% of the neointima area; 4 = macrocalcification 50%–75% of the neointima area; 5 = macrocalcification >75% of the neointima area), resulting in maximum values of 24 and 40, respectively.

Explant Immunofluorescence

Fixed cryosections (4 μm) were incubated at room temperature for 10 minutes with 0.25% Triton X-100 and for 1 hour with 5% bovine serum albumin + 0.1% Tween-20. Incubation with primary antibodies [anti-vonWillebrand factor (DAKO, Hamburg, Germany); anti–alpha-smooth muscle actin (aSMA) (Sigma-Aldrich, Taufkirchen, Germany); anti-syndecan-3 (Abcam, Cambridge, United Kingdom); anti-CD3 (Sigma–Aldrich); anti-CD68 (Abcam)] + 1% bovine serum albumin + 0.1% Tween-20 lasted 1 hour at 37°C. Secondary antibodies conjugated to the fluorophores Alexa488 and Alexa546 (Invitrogen, Carlsbad, CA) were applied (in PBS containing 1% bovine serum albumin and 0.1% Tween-20) for 45 minutes in a dark and humid chamber at 37°C. Sections were covered with Vectashield mounting medium containing 4′,6-diamidino-2-phenylindole (Vector Labs, Peterborough, United Kingdom), and image acquisition was conducted with a microscope system DM2000, equipped with a digital camera DFC 425C (Leica, Wetzlar, Germany) and the Leica Application Suite V3.7 software.

In Situ Zymography

In situ zymography to determine the matrix metalloproteinase (MMP) activity in the explants was performed as recently published.[16] In brief, cryosections (6 μm) were incubated with 40 μg/mL fluorescein-labeled gelatin (Invitrogen) in 50 mM Tris-HCl + 10 mM $CaCl_2$ + 150 mM NaCl + 5% Triton X-100 for 24 hours at 37°C. Finally, sections were mounted with Vectashield medium containing DAPI, and the MMP gelatinase activity was visualized by fluorescence microscopy. Specificity of gelatinase activity was confirmed by incubation with gelatin in the presence of 20 mM ethylenediaminetetraacetic acid. Quantitative analysis of the MMP activity was performed with Image J measuring the fluorescence intensity in the aortic conduit wall as mean gray value in arbitrary units.

Calcium Tissue Content Measurement

To quantify the extent of calcium deposition in the aortic conduit explants, an o-cresolphthalein-calcium reaction assay was used according to the manufacturer's protocol (Calcium Assay Kit, item no. 700550; Cayman Chemical Company, Ann Arbor, MI).

Semiquantitative RNA Analysis

Gene expression analysis of whole aortic conduit explants was performed by semiquantitative RT-PCR as recently described.[15]

Semiquantitative RT-PCR was conducted to determine the gene expression in aortic conduit explants. Total RNA was isolated using the RNeasy Mini Kit (Qiagen, Hilden, Germany). In brief, tissue was homogenized in TRIzol (Invitrogen), and RNA was precipitated by isopropanol. After passaging through a DNA-removing column (Qiagen), the RNA sample was collected and the following quality analyses were performed. Purity and quantity of isolated RNA were determined spectrophotometrically (BioPhotometer plus; Eppendorf, Hamburg, Germany), and optical density values at 230, 260, and 280 nm were recorded. Additionally, the Agilent RNA 6000 Nano Kit (Agilent Technologies, Santa Clara, CA) was used to examine the level of RNA degradation. cDNA was generated with the QuantiTect Reverse Transcription Kit (Qiagen) according to the manufacturer's protocol. Semiquantitative RT-PCR was conducted on a StepOnePlus

cycler (Applied Biosystems, Foster City, CA) using the Platinum SYBR Green PCR Master Mix (Invitrogen) and the following protocol with a reaction volume of 20 μL: 50°C for 2 minutes, 95°C for 2 minutes, 95°C for 15 seconds + 60°C for 30 seconds (40 cycles), 95°C for 15 seconds, 60°C for 1 minute, 95°C for 15 seconds and 60°C for 15 seconds.

After normalization to β-actin expression (dCt method), and subsequently to the mean dCt value of the gene in the control group (ddCt method), the resulting relative gene expression values of the samples of both groups were statistically compared with each other.

Primers for the following genes were obtained from Invitrogen: αSMA, genes associated with inflammation [tumor necrosis factor α; interleukin 1β (IL-1β); IL-6; receptor for advanced glycation end products (RAGE)], CD39, CD73, genes associated with vascular degeneration and chondro-osteogenic transformation (osteopontin, OPN; osteoprotegerin, OPG; osteocalcin, OCN; alkaline phosphatase, ALP), and transcription factors associated with osteogenic differentiation (bone morphogenetic protein-2 [BMP2]; runt-related T1 transcription factor-2 [RUNX2]). Primer sequences are given in Table 1.

Statistics

Continuous variables are presented as mean ± SEMs. Direct group comparisons at one time point were conducted by unpaired Student's *t* tests with or without Welch's correction or Mann–Whitney *U* tests, as indicated. For group comparisons at multiple time points, 2-way-analysis of variance with Bonferroni post hoc tests were applied. $P < 0.05$ were assumed to indicate significance. Data analysis was conducted with GraphPad Prism v5.04 (GraphPad Software, San Diego, CA).

RESULTS

Metabolic Effect of Simvastatin Under Pro-calcific Diet

To determine the metabolic effect of the HMG-CoA reductase inhibitor simvastatin in the presence of pro-calcific diet, the blood serum levels of cholesterol were measured. During the observation period, the cholesterol levels of group C increased to a larger extent as compared with group S, resulting in a significantly higher value after 84 days ($P < 0.05$) (Fig. 2). Moreover, simvastatin treatment reduced the calcium serum levels, which had been increased by the pro-calcific diet ($P < 0.05$). Simvastatin did not significantly affect the serum levels of urea, phosphate, glucose, or triglycerides at any time point.

Surgical Outcome and Hemodynamics

Overall survival after implantation of the aortic conduit grafts amounted to 97.0% (96.3% among the 12 weeks rats). One rat in group C had to be killed because of physical impairment as a consequence of severe generalized calcification 11 weeks after implantation. At the beginning of the study, body weight and food intake increased, with a slight break after the implantation procedure while slowly but steadily declining during the further follow-up (Fig. 3A). Following the generation of AI and the onset of the pro-calcific feeding, in both groups, the left ventricular end-diastolic diameter significantly increased (Fig. 3B), whereas the left ventricular ejection fraction decreased (Fig. 3C). Doppler sonography of the aortic conduits at day 0 and at explantation confirmed all grafts to be adequately perfused.

Quantity and Quality of Neointima Formation

Independently on the experimental group or the time point, histology of the explants revealed neointima areas with single-layer endothelium (Fig. 4A) and hyperplastic intima (Fig. 4B). At 12 weeks, areas of hyperplastic neointima were predominant in all explants. The percentage of recellularized luminal graft area increased significantly during the study ($P < 0.0001$) and amounted for nearly 100% in the simvastatin group after 12 weeks; however, the intergroup differences did not reach statistical significance (Fig. 4C). For a comparative quantification of the neointima formation, the intima-to-media ratio was calculated. There were no differences between group C and group S over the entire study duration (Fig. 4D).

TABLE 1. Primer Sequences for Semiquantitative RT-PCR

Primer	Forward Sequence	Reverse Sequence
β-actin	5′-CCGCGAGTACAACCTTCTTG-3′	5′-GCAGCGATATCGTCATCCA-3′
αSMA	5′-GCTCTGGTGTGTGACAATGG-3′	5′-CCCCACATAGCTGTCCTTTT-3′
Tumor necrosis factor α	5′-GCTCCCTCTCATCAGTTCCA-3′	5′-GCTTGGTGGTTTGCTACGAC-3′
IL-1β	5′-AGGACCCAAGCACCTTCTTT-3′	5′-CATCATCCCACGAGTCACAG-3′
IL-6	5′-ACCACCCACAACAGACCAGT-3′	5′-AGTGCATCATCGCTGTTCAT-3′
CD39	5′-GGGCCTATGGGTGGATTACT-3′	5′-CAAAGGTTGCCTGTTTCTGG-3′
CD73	5′-ACGTGTCCATGTGCATTGTAA-3′	5′-GGTTCTCCCAGGTGATGGTA-3′
RAGE	5′-TGAACTCACAGCCAATGTCC-3′	5′-TCAGAGGTTTCCCATCCAAG-3′
Osteopontin	5′-AAGCCTGACCCATCTCAGAA-3′	5′-ATGGCTTTCATTGGAGTTGC-3′
Osteoprotegerin	5′-GAGTGTGCGAATGTGAGGAA-3′	5′-CACCTGAGAAGAACCCATCC-3′
Osteocalcin	5′-AAGCAGGAGGGCAGTAAGGT-3′	5′-GTCCGCTAGCTCGTCACAAT-3′
Alkaline phosphatase	5′-GCACTCCCACTATGTCTGGAA-3′	5′-AGGGAAGGGTCAGTCAGGTT-3′
Bone morphogenetic protein-2	5′-GCTCAGCTTCCATCACGAA-3′	5′-AAGAAGCGTCGGGAAGTTTT-3′
Runt-related transcription factor-2	5′-GATGACACTGCCACCTCTGA-3′	5′-GATGAAATGCCTGGGAACTG-3′

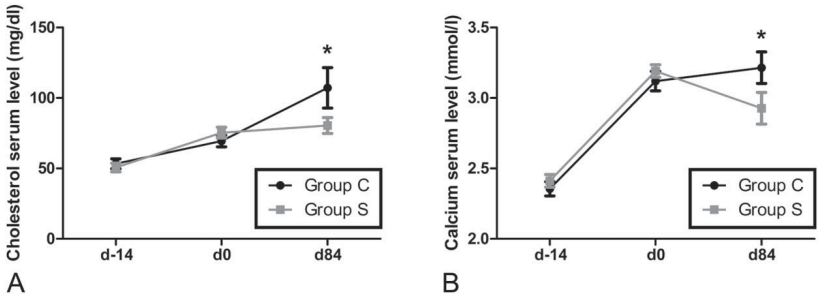

FIGURE 2. Cholesterol (A) and calcium (B) blood serum levels of recipient animals with (group S) and without (group C) simvastatin therapy. Simvastatin lowered the cholesterol and the calcium levels after 14 weeks of treatment. $*P < 0.05$.

Qualitative examination of the cells forming the neointima revealed positive staining for aSMA in the hyperplastic regions and a luminal endothelial cell layer staining positive for vonWillebrand factor in both groups (Figs. 5A, B). The hyperplastic neointima consisted of areas with spindle-shaped cells (Figs. 5C, D) and areas with chondroid cells (Figs. 5E, F), whereas the latter did not appear before week 12. Staining against the early chondrocyte differentiation marker syndecan-3 was negative in both groups at all time points. After 4 and 12 weeks, the inflammatory cell markers CD3 (for T cells) and CD68 (for macrophages) proved negative in all explants, regardless of the experimental group.

Cell invasion into the media of the implants was a quite rare event, which was exclusively observed close to the adventitial conduit surface after 12 weeks.

Calcifying Graft Degeneration

Calcification in the explant grafts was visualized by von Kossa hydroxyapatite staining. In both groups, the severely pro-calcific diet resulted in progressive calcification of the aortic conduits focused primarily at the level of the media, whereas a relevant affection of the neointima was observed not before 12 weeks after implantation (Figs. 6A–D).

A semiquantitative determination of the calcium burden was performed by applying a scoring system based on von Kossa staining. In the graft intima and graft media of both groups, the hydroxyapatite deposition increased during the study ($P < 0.0001$), whereas the intima was remarkably affected only at 12 weeks after implantation. However, neither in the intima nor in the media, the tissue calcification in the simvastatin group was significantly different from the control group (Figs. 6E, F). As calcium deposition represents a major focus of this study, a second method was chosen to compare the 2 experimental groups, and a quantitative analysis of the calcium tissue content in whole aortic conduit explants was conducted with an o-cresolphthalein-calcium reaction assay. The calcium content of the grafts was significantly higher than in native aortic tissue. However, when graft calcification was compared between the 2 groups, the measurements 12 weeks after implantation confirmed the semiquantitative von Kossa scoring results, demonstrating that simvastatin treatment did not influence the calcium tissue content (Fig. 6G).

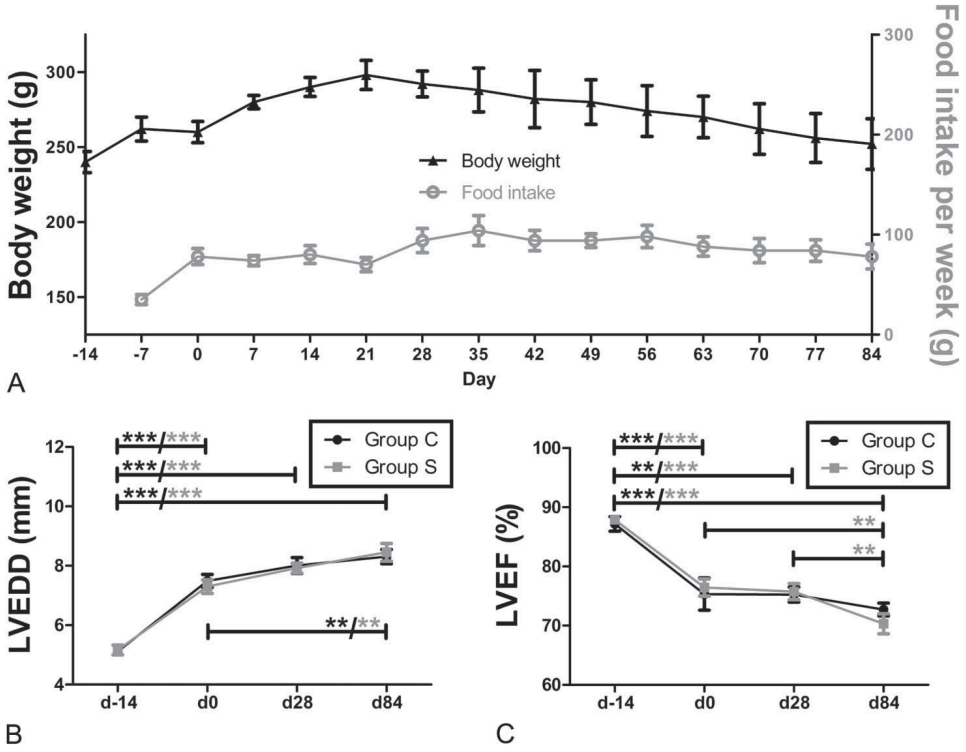

FIGURE 3. Food intake and hemodynamics. Food intake and body weight increased at the beginning and declined at the end of the study (A). In both groups, the LVEDD increased (B), and the LVEF decreased significantly (C) after the generation of AI. There were no intergroup differences. $**P < 0.01$; $***P < 0.001$. LVEDD, left ventricular end diastolic diameter; LVEF, left ventricular ejection fraction.

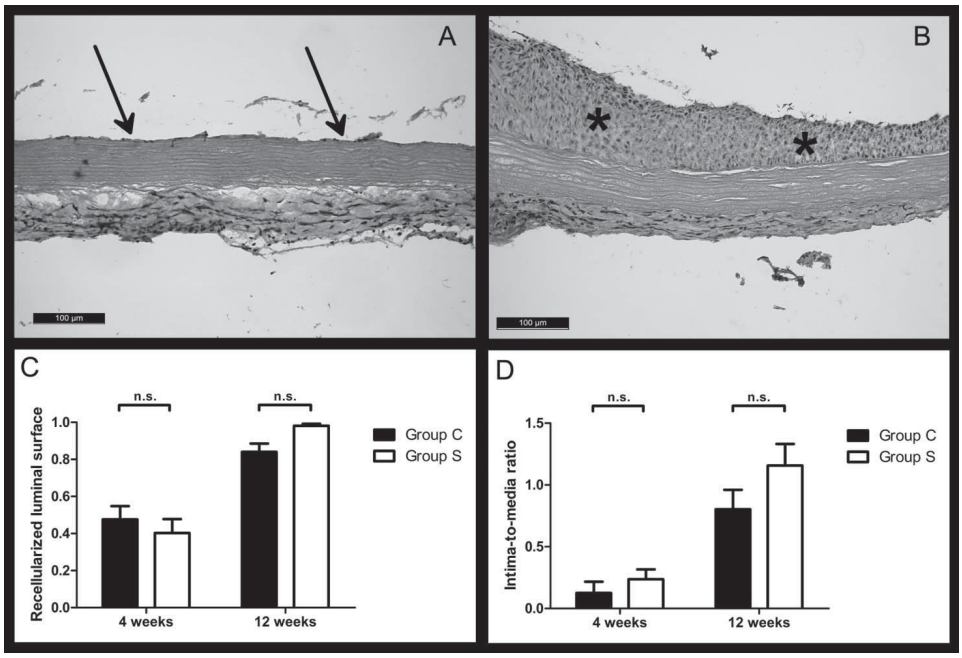

FIGURE 4. Neointima formation in the aortic conduit grafts. Representative cross sections through the ascending aorta of conduit grafts showing (A) areas with single-layer endothelium (arrows; 4 weeks) and (B) areas with multilayer intima hyperplasia (asterisks; 12 weeks) in both groups. hematoxylin–eosin staining; scale bars = 100 μm. At both explantation time points, simvastatin treatment (group S) did not significantly influence the percentage of recellularized luminal surface (C) or the intima-to-media ratio (D) of the grafts (n.s.). n.s., statistically not significantly different.

We chose to perform relative gene expression analysis to elucidate intergroup differences regarding inflammatory, prothrombogenic, and chondro-osteogenic events. Therefore, we examined tumor necrosis factor α, IL-1β, IL6, CD39, CD73, and RAGE for the evaluation of inflammatory and prothrombogenic events in the grafts (Fig. 7A), OPN, OPG, OCN, ALP, BMP2, and RUNX2 as markers of chondro-osteogenic transformation of interstitial cells (Fig. 7B), and aSMA with regard to interstitial cell activation. Only IL-6 showed a significantly different relative expression in group C versus group S ($P < 0.05$).

By means of in situ zymography, the MMP gelatinase activity in the aortic conduit grafts was determined. After 12 weeks, the MMP activity of both groups was enhanced as compared with the grafts explanted after 4 weeks (Figs. 8A–D). Quantification of the MMP activity revealed a significant increase over time ($P < 0.0001$) with enhanced values in the simvastatin group ($P < 0.01$) (Fig. 8E).

DISCUSSION

In the present study, the impact of statin therapy on the calcifying degeneration of decellularized aortic conduits was examined in a recently published standardized small animal model supplemented with pro-calcific diet.[13,14]

The diet consisted of high-dose supplementation with vitamin D, cholesterol, and calcium phosphate to generate a pro-degenerative in vivo environment.[17–19] These conditions have led to the development of a clearly distinguishable calcification pattern in the native cardiovascular system and in the bioimplants. Furthermore, the diet increased the blood serum levels of cholesterol and calcium, both of which were decreased by simvastatin application, proving a metabolic effect of the HMG-CoA reductase inhibitor in the utilized model of accelerated cardiovascular calcification.

Graft Recellularization

A rapid autologous neointima formation may be regarded as supportive to enhance the biocompatibility of cardiovascular implants by restoring a protective endothelial lining on the luminal surface of implants. After 4 weeks, half of the luminal surface of all implanted decellularized aortic conduits was covered with neointima, whereas after 12 weeks, the inner surface was nearly completely recellularized. These results confirm the findings of a previous study showing that detergent-decellularized cardiovascular implants are repopulated in vivo at the luminal side within short time periods.[14,15] However, progressive neointima hyperplasia by aSMA-positive cells with a myofibroblastic phenotype was observed in both groups. After 12 weeks, another cell population with a chondroid phenotype was observed in areas of severe calcification. In contrast to a previous study without pro-calcific diet and a follow-up period of 8 weeks, these chondroid cells did not stain positive for the early chondrocyte differentiation marker syndecan-3, suggesting a more advanced stage of chondro-osteogenic differentiation.[15]

Statin treatment neither significantly influenced the time course of implant recellularization, nor did it affect the extent of hyperplastic intima formation. These data are in contrast to previous experimental and clinical studies in which statins were reported to decrease the intima hyperplasia in vein grafts or the injured native aorta.[20–22] The effect of simvastatin on intima hyperplasia in decellularized cardiovascular prostheses has not been described before. The present data suggest statins not to influence the autologous cellular repopulation of decellularized cardiovascular grafts in the systemic circulation of rats.

Calcifying Graft Degeneration

In the present small animal model of accelerated cardiovascular calcification, we observed progressive

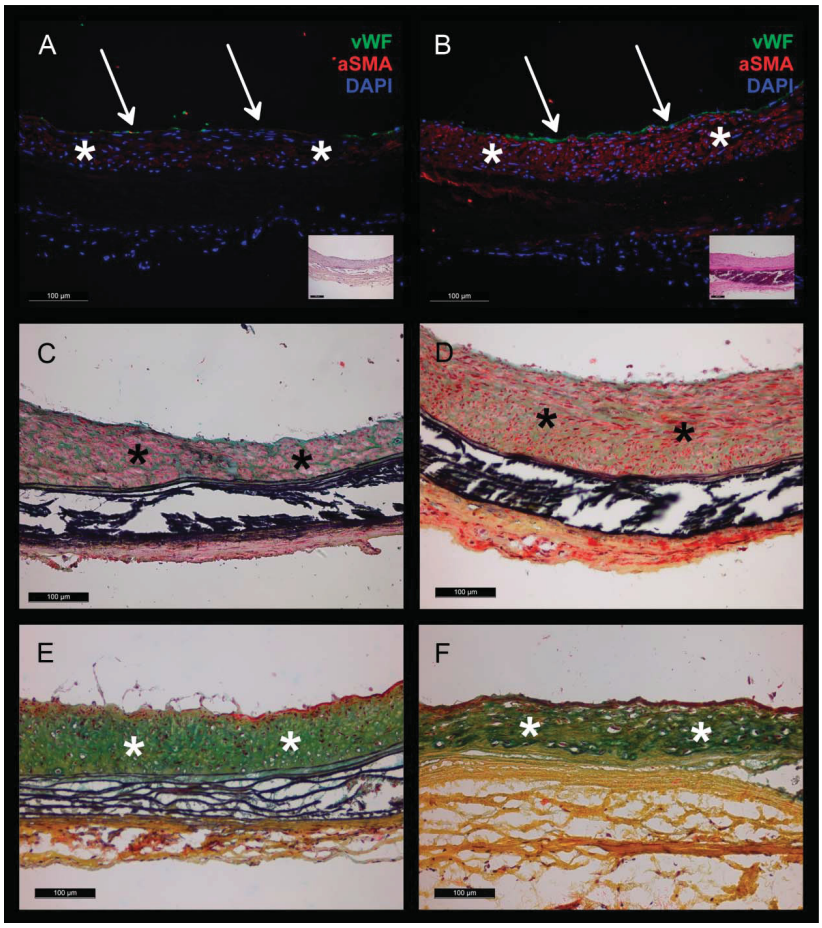

FIGURE 5. Cell characterization in the neointima of the aortic conduit grafts. Representative cross sections through the ascending aorta of conduit grafts after 12 weeks (A: group C; B: group S) showed aSMA(+) cells (red; white asterisks) in the hyperplastic areas and vonWillebrand factor(+) cells (green; white arrows) at the luminal border. Blue, DAPI; small pictures inside (A) and (B), corresponding hematoxylin–eosin-stained cross sections. Movat's pentachrome staining after 12 weeks revealed hyperplastic neointima with spindle-shaped cells (black asterisks in C and D) and areas with chondroid cells (white asterisks in E and F) in both groups (C and E: group C; D and F: group S). Scale bars = 100 μm.

hydroxyapatite deposition focused on the media of the implants. Without pro-calcific feeding, decellularized aortic conduit grafts exhibited only microcalcification or sparse hydroxyapatite islets in the media after 8 weeks in the same heterotopic graft implantation model.[14,15] These observations are generally in line with previous studies on glutaraldehyde cross-linked bovine pericardial and porcine aortic tissues subcutaneously implanted in rats, where collagen and elastin fibers act as early nucleation sites for calcium phosphate deposition,[23,24] whereas cellular remnants in the devitalized grafts were observed to play a major role in initiating the calcium deposition.[25]

However, under the experimentally induced severely pro-calcific metabolic conditions, statin treatment could not decrease the calcium deposition or the gene expression of several markers of chondro-osteogenic transformation in the implants along this study. Recently, a "statin paradox" regarding the effect on aortic valve calcification has been proposed, according to which the effect of statins on interstitial cells largely depends on the particular subtype and predetermination of these cells, and can even result in increased calcification.[26,27] Moreover, enhanced calcium deposition was reported to stabilize atherosclerotic plaques and to lower the rate of major adverse cardiovascular events.[28,29] In this context, the observation that statin treatment did not influence the calcification of decellularized cardiovascular implants may be partially attributed to the characteristics of the model: The main calcium burden was located in the acellular graft media, which was not repopulated during the entire study period. It may be that the lack of interstitial cells in the media prevented statin treatment to exert adverse pro-calcific effects. The pro-calcifying modulation of interstitial cells may be beneficial in human atherosclerotic plaques; however, in decellularized grafts with progressive media calcification, it would have been deleterious.

Advanced glycation end products (AGE) are supposed to enhance vascular calcification in rats through a receptor for AGE (RAGE)/oxidative stress pathway.[30] In the present study, simvastatin did not influence the RAGE levels in the calcified aortic conduit grafts. Interestingly, atorvastatin was recently shown to reduce the gene expression and the protein content of RAGE in the kidneys of rats with diabetic nephropathy, whereas it did not affect the RAGE tissue content in the control group without diabetes.[31] Wei et al[30] reported that the aortic levels of AGE were increased in diabetic rats, but not in animals with 8 weeks of high-dose vitamin D supplementation. This may explain the observation of the present study that statin therapy did not decrease the RAGE levels in the conduit explants in an animal model of chow-induced accelerated cardiovascular calcification without diabetic component. Therefore, the evaluation of statin treatment in recipients of decellularized

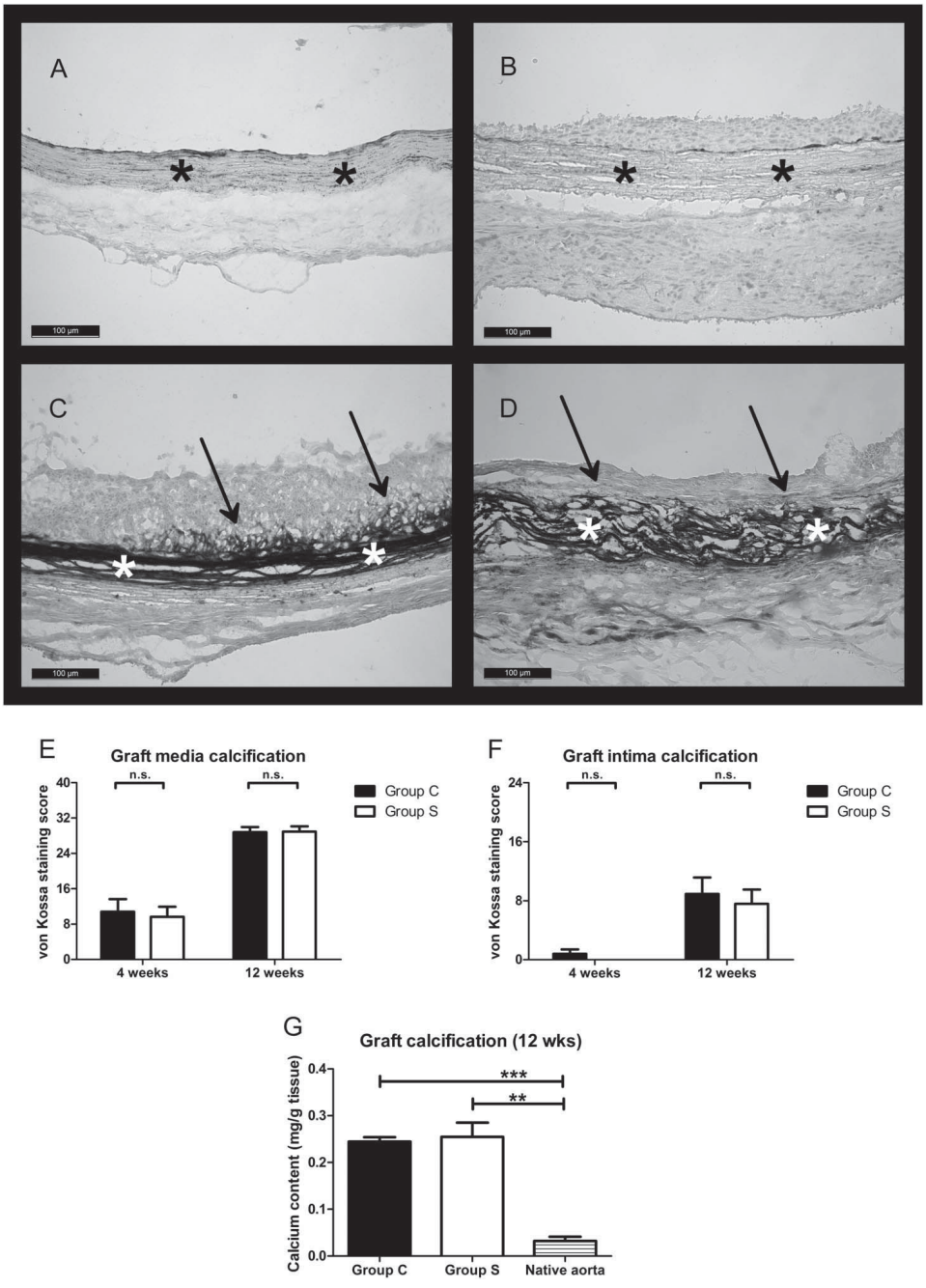

FIGURE 6. Graft calcification. Representative cross sections through the ascending aorta of conduit grafts after 4 weeks (A and B) and 12 weeks (C and D) showed a progressive hydroxyapatite burden (brown; black asterisks in A and B; white asterisks in C and D) predominantly in the media of the explants of group C (A and C) and group S (B and D). After 12 weeks, calcification of the neointima occurred (black arrows in C and D). von Kossa staining; scale bars = 100 μm. A semiquantitative von Kossa staining scoring system showed a progressive hydroxyapatite deposition predominantly in the media (E) and at later time points also in the neointima (F) of the explants (for both regions with $P < 0.0001$ between week 4 and week 12). At no explantation time point, the intergroup differences were statistically significant (n.s.). Calcium content measurements in aortic conduit explants 12 weeks after implantation revealed significantly increased values in both groups versus native aortic tissue (G). Again, there was no difference between group C and group S. $^{**}P < 0.01$; $^{***}P < 0.001$.

cardiovascular implants suffering from diabetic metabolism may be an interesting target for consecutive studies following this work.

In the current study, the MMP gelatinase activity, which is predominantly attributed to MMP-2 and MMP-9, increased over the observation time, and statin therapy resulted in enhanced activity values indicating intensified graft remodeling. Based on previous reports, MMP-2 expression and activity are known to be enhanced in human atherosclerotic lesions, and increased MMP-9 activity has been shown in unstable carotid plaques.[32,33] Moreover, increased levels of MMP-2 and MMP-9 have been found in ruptured noncalcified explanted pericardial bioprostheses.[34] Whether enhanced MMP activity aggravates graft tissue degeneration or rather mirrors a crucial aspect of a regenerative remodeling process is not clear and may depend on type and tissue properties of the examined cardiovascular implant and on the observed subtype of MMP.

Decellularization has been reported to diminish the inflammatory response of the recipient against cardiovascular prostheses in small and large animal models.[1,2] In accordance, we did not detect inflammatory cells in the explants after 4 and 12 weeks in vivo. However, we found gene expression of IL-6, which was decreased by statin treatment. IL-6 is

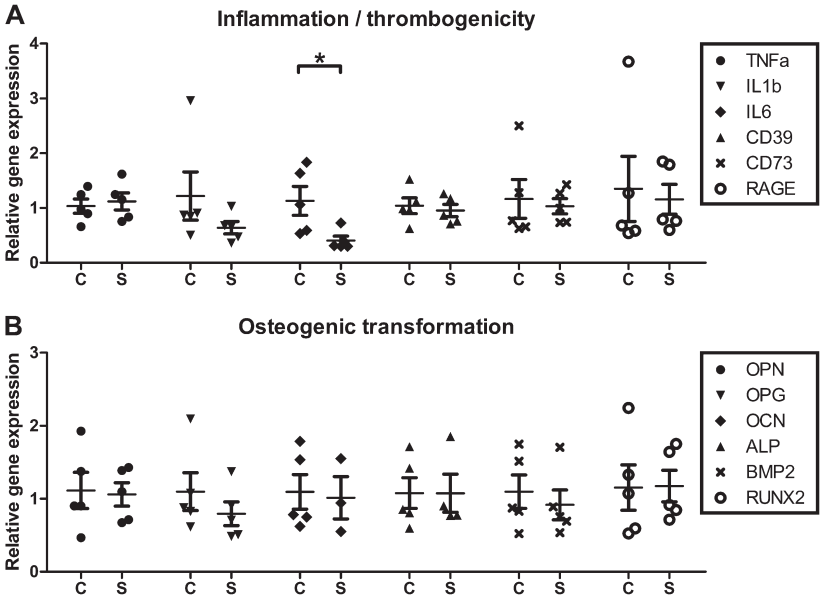

FIGURE 7. Relative gene expression analysis in explanted aortic conduits (12 weeks in vivo) by means of semiquantitative RT-PCR (ddCt method). With regard to different markers of chondro-osteogenic transformation [OPN, OPG, OCN, ALP, BMP2, and RUNX2 (B)], no significant differences occurred between group S and group C. Among the markers of inflammation and thrombogenicity [TNF-α, IL-1β, IL-6, CD39, CD73, and RAGE (A)], the relative gene expression of IL-6 was significantly decreased in group S (*P = 0.029). C, group C; S, group S; TNF-α, tumor necrosis factor α; OPN, osteopontin; OPG, osteoprotegerin; OCN, osteocalcin; ALP, alkaline phosphatase; BMP2, bone morphogenetic protein-2; RUNX2, runt-related transcription factor-2.

involved in the inflammatory response against cardiovascular implants.[35] In a rat allograft transplantation model, high IL-6 levels were associated with graft inflammation and degeneration.[36] Furthermore, IL-6 is known to induce the development and destabilization of atherosclerotic plaques.[37] Especially in the presence of enhanced graft tissue remodeling activity, which is further increased by statin therapy, the suppression of IL-6 by administration of a HMG-CoA reductase inhibitor may beneficially influence the outcome of biological cardiovascular implants.

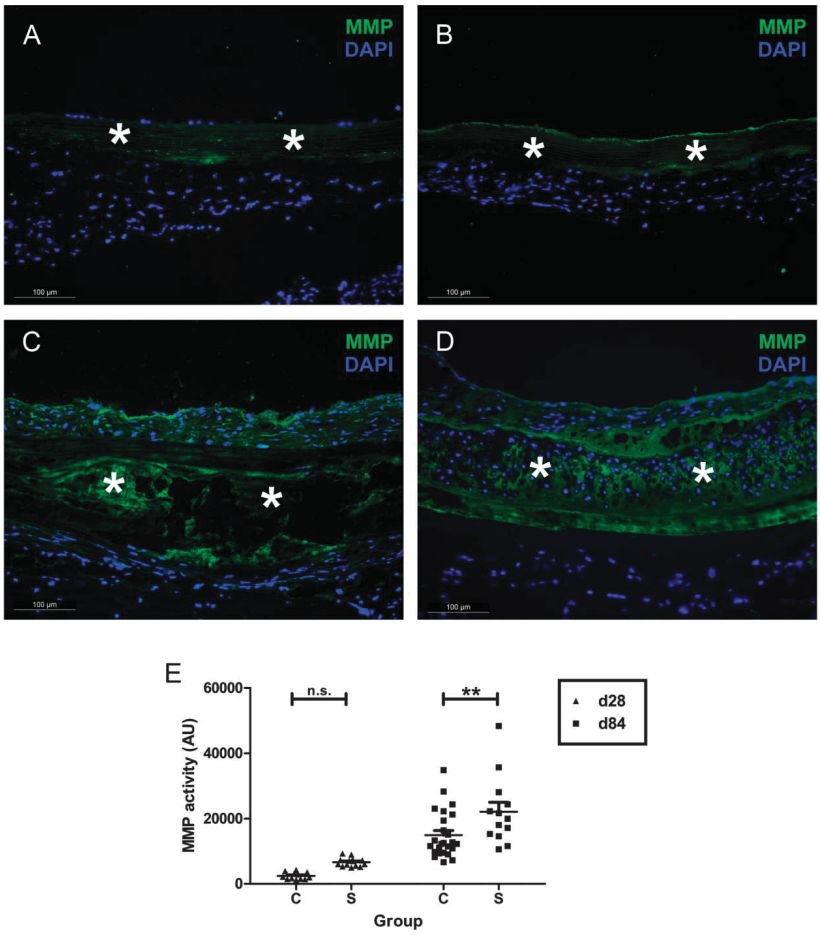

FIGURE 8. MMP activity in the aortic conduit grafts. Representative cross sections through the ascending aorta of conduit grafts (A and C: group C; B and D: group S) showed enhanced MMP gelatinase activity (green; white asterisks) after 12 weeks in vivo (C and D) as compared with the explants after 4 weeks (A and B). In situ zymography; blue, DAPI; scale bars = 100 μm. Quantitative analysis revealed that the MMP activity increased from week 4 to week 12 ($P < 0.0001$), whereas the values in group S were significantly higher than in group C (E). **$P < 0.01$; AU, arbitrary unit (mean gray value); n.s., statistically not significantly different.

Correlation With Clinical Studies

Statin treatment is known to decelerate the process of atherosclerosis progression in humans, which may be attributed to lowering the cholesterol levels and the following non–lipid-mediated pleiotropic effects of statins: improvement of preexisting endothelial dysfunction, increase in nitric oxide bioavailability, antioxidant effects, anti-inflammatory and immunomodulatory properties, and stabilization of atherosclerotic plaques.[10] Recently, the YELLOW trial showed intensified statin treatment for 7 weeks to lower the lipid content of coronary artery plaques in patients with multivessel disease undergoing percutaneous intervention.[38] Reducing the lipid core of atherosclerotic plaques is supposed to contribute to plaque stabilization.[39]

With regard to calcific aortic valve disease (CAVD), the beneficial potential of statins is controversially discussed. In the randomized prospective SALTIRE trial in 155 CAVD patients, atorvastatin failed to decelerate the progression of CAVD within a follow-up period of 25 months.[40] The randomized SEAS trial in more than 1800 CAVD patients revealed simvastatin + ezetimibe to reduce ischemic events, predominantly the need for coronary artery bypass grafting. However, after a median follow-up of 52 months, there was no decrease in the rate of aortic valve replacement surgery, congestive heart failure as a result of progression of aortic stenosis, or death from cardiovascular causes.[41] In contrast, the prospective, nonrandomized RAAVE study in 121 patients with CAVD slowed the hemodynamic progression of aortic stenosis measured by echocardiography during the first 18 months after onset of rosuvastatin therapy versus placebo.[42] An important difference in the inclusion criteria of the 3 studies may explain the controversial results. Because of ethical reasons, the randomized SALTIRE and SEAS trials were conducted in patients without a need for statin therapy, that is, without relevant hypercholesterolemia. In the RAAVE study, patients with high cholesterol levels were assigned to the statin treatment group, whereas patients with normal values received placebo. Therefore, the beneficial potential of statins in CAVD, as demonstrated in RAAVE, may be predominantly present in patients with hypercholesterolemia. In a retrospective study on patients after valve bioprosthesis implantation, increased serum cholesterol levels were reported to be also a risk factor for graft degeneration,[43] whereas a multivariate analysis in another aortic valve bioprosthesis study could not confirm that preoperative cholesterol levels are a risk factor for structural implant degeneration.[44]

Finally, lipid-mediated inflammation has been reported to contribute to the degeneration of biological heart valves.[45] The absence of inflammation in the decellularized implants may have contributed to the finding that simvastatin could not reduce the graft degeneration in the current model.

The results of this study collectively confirm the beneficial effects of statins on the metabolic conditions (as shown by decreased calcium and cholesterol serum levels) and on general inflammation in biological aortic conduit implants. However, a benefit for structural and functional maintenance of decellularized grafts is questioned by the presented data.

Study Limitations

The applied rat implantation model of accelerated cardiovascular calcification may not exactly mimic the in vivo fate of cardiovascular grafts in humans because different metabolic characteristics and complex comorbidities in cardiovascular patients with atherosclerosis or aortic valve sclerosis may influence the maturation of the implanted prostheses. As a consequence, animal models with different metabolic conditions, for example, diabetic, hypertensive or renally insufficient recipients, may be considered for further studies evaluating the effect of statins on the calcifying degeneration of decellularized cardiovascular grafts.

CONCLUSIONS

The present study is the first in vivo examination of the effect of statin treatment on the calcifying degeneration of decellularized cardiovascular implants. Simvastatin failed to inhibit the graft calcification in a standardized rat implantation model of accelerated cardiovascular sclerosis. Moreover, it did not significantly influence the speed of recellularization or the formation of hyperplastic neointima in the implants. These findings are in accordance with clinical data on statins failing to slow the progression of CAVD. Furthermore, the lack of relevant inflammation in decellularized cardiovascular prostheses may abrogate a key mechanism of statins, and therefore, may explain the lack of beneficial effects on graft degeneration.

ACKNOWLEDGMENTS

The authors gratefully acknowledge the blood serum analyses conducted by the Institute of Clinical Chemistry and Laboratory Diagnostics, Medical Faculty, Heinrich Heine University, Duesseldorf, Germany.

REFERENCES

1. Meyer SR, Nagendran J, Desai LS, et al. Decellularization reduces the immune response to aortic valve allografts in the rat. *J Thorac Cardiovasc Surg.* 2005;130:469–476.
2. Numata S, Fujisato T, Niwaya K, et al. Immunological and histological evaluation of decellularized allograft in a pig model: comparison with cryopreserved allograft. *J Heart Valve Dis.* 2004;13:984–990.
3. Akhyari P, Kamiya H, Gwanmesia P, et al. In vivo functional performance and structural maturation of decellularised allogenic aortic valves in the subcoronary position. *Eur J Cardiothorac Surg.* 2010;38:539–546.
4. Cebotari S, Lichtenberg A, Tudorache I, et al. Clinical application of tissue engineered human heart valves using autologous progenitor cells. *Circulation*. 2006;114:I132–I137.
5. da Costa FD, Costa AC, Prestes R, et al. The early and midterm function of decellularized aortic valve allografts. *Ann Thorac Surg.* 2010;90:1854–1860.
6. Lichtenberg A, Tudorache I, Cebotari S, et al. Preclinical testing of tissue-engineered heart valves re-endothelialized under simulated physiological conditions. *Circulation*. 2006;114:I559–I565.
7. Cicha I, Rüffer A, Cesnjevar R, et al. Early obstruction of decellularized xenogenic valves in pediatric patients: involvement of inflammatory and fibroproliferative processes. *Cardiovasc Pathol.* 2011;20:222–231.
8. Rüffer A, Purbojo A, Cicha I, et al. Early failure of xenogenous decellularised pulmonary valve conduits: a word of caution! *Eur J Cardiothorac Surg.* 2010;38:78–85.

9. Simon P, Kasimir MT, Seebacher G, et al. Early failure of the tissue engineered porcine heart valve SYNERGRAFT in pediatric patients. *Eur J Cardiothorac Surg.* 2003;23:1002–1006.
10. Jasińska M, Owczarek J, Orszulak-Michalak D. Statins: a new insight into their mechanisms of action and consequent pleiotropic effects. *Pharmacol Rep.* 2007;59:483–499.
11. Parolari A, Tremoli E, Cavallotti L, et al. Do statins improve outcomes and delay the progression of non-rheumatic calcific aortic stenosis? *Heart*. 2011;97:523–529.
12. Gilmanov D, Bevilacqua S, Mazzone A, et al. Do statins slow the process of calcification of aortic tissue valves? *Interact Cardiovasc Thorac Surg.* 2010;11:297–301.
13. Munakata H, Assmann A, Poudel-Bochmann B, et al. Aortic conduit valve model with controlled moderate aortic regurgitation in rats: a technical modification to improve short- and long-term outcome and to increase the functional results. *Circ J.* 2013;77:2295–2302.
14. Assmann A, Akhyari P, Delfs C, et al. Development of a growing rat model for the in vivo assessment of engineered aortic conduits. *J Surg Res.* 2012;176:367–375.
15. Assmann A, Delfs C, Munakata H, et al. Acceleration of autologous in vivo recellularization of decellularized aortic conduits by fibronectin surface coating. *Biomaterials*. 2013;34:6015–6026.
16. Joghetaei N, Akhyari P, Rauch BH, et al. Extracellular matrix metalloproteinase inducer (CD147) and membrane type 1-matrix metalloproteinase are expressed on tissue macrophages in calcific aortic stenosis and induce transmigration in an artificial valve model. *J Thorac Cardiovasc Surg.* 2011;142:191–198.
17. Bajwa GS, Morrison LM, Ershoff BH. Induction of aortic and coronary athero-arteriosclerosis in rats fed a hypervitaminosis D, cholesterol-containing diet. *Proc Soc Exp Biol Med.* 1971;138:975–982.
18. Eisenstein R, Zeruolis L. Vitamin D-induced aortic calcification. *Arch Pathol.* 1964;77:27–35.
19. Kitagawa S, Yamaguchi Y, Kunitomo M, et al. Impairment of endothelium-dependent relaxation in aorta from rats with arteriosclerosis induced by excess vitamin D and a high-cholesterol diet. *Jpn J Pharmacol.* 1992;59:339–347.
20. Aydin U, Ugurlucan M, Gungor F, et al. Effects of atorvastatin on vascular intimal hyperplasia: an experimental rodent model. *Angiology*. 2009;60:370–377.
21. Zhang L, Jin H, Huang J, et al. Local delivery of pravastatin inhibits intimal formation in a mouse vein graft model. *Can J Cardiol.* 2012;28:750–757.
22. Kulik A, Voisine P, Mathieu P, et al. Statin therapy and saphenous vein graft disease after coronary bypass surgery: analysis from the CASCADE randomized trial. *Ann Thorac Surg.* 2011;92:1284–1290.
23. Bailey MT, Pillarisetti S, Xiao H, et al. Role of elastin in pathologic calcification of xenograft heart valves. *J Biomed Mater Res A.* 2003;66:93–102.
24. Schoen FJ, Tsao JW, Levy RJ. Calcification of bovine pericardium used in cardiac valve bioprostheses. Implications for the mechanisms of bioprosthetic tissue mineralization. *Am J Pathol.* 1986;123:134–145.
25. Valente M, Bortolotti U, Thiene G. Ultrastructural substrates of dystrophic calcification in porcine bioprosthetic valve failure. *Am J Pathol.* 1985;119:12–21.
26. Monzack EL, Masters KS. A time course investigation of the statin paradox among valvular interstitial cell phenotypes. *Am J Physiol Heart Circ Physiol.* 2012;303:H903–H909.
27. Zhao XQ, Yuan C, Hatsukami TS, et al. Effects of prolonged intensive lipid-lowering therapy on the characteristics of carotid atherosclerotic plaques in vivo by MRI: a case-control study. *Arterioscler Thromb Vasc Biol.* 2001;21:1623–1629.
28. Brown BG, Zhao XQ, Sacco DE, et al. Lipid lowering and plaque regression. New insights into prevention of plaque disruption and clinical events in coronary disease. *Circulation*. 1993;87:1781–1791.
29. Vaughan CJ, Gotto AM Jr, Basson CT. The evolving role of statins in the management of atherosclerosis. *J Am Coll Cardiol.* 2000;35:1–10.
30. Wei Q, Ren X, Jiang Y, et al. Advanced glycation end products accelerate rat vascular calcification through RAGE/oxidative stress. *BMC Cardiovasc Disord.* 2013;13:13.
31. Lu L, Peng WH, Wang W, et al. Effects of atorvastatin on progression of diabetic nephropathy and local RAGE and soluble RAGE expressions in rats. *J Zhejiang Univ Sci B.* 2011;12:652–659.
32. Li Z, Li L, Zielke R, et al. Increased expression of 72-kD type IV collagenase (MMP2) in human aortic atherosclerotic lesions. *Am J Pathol.* 1996;148:121–128.
33. Loftus IM, Naylor AR, Goodall S, et al. Increased matrix metalloproteinase-9 activity in unstable carotid plaques. A potential role in acute plaque disruption. *Stroke*. 2000;31:40–47.
34. Simionescu A, Simionescu D, Deac R. Biochemical pathways of tissue degeneration in bioprosthetic cardiac valves. The role of matrix metalloproteinases. *ASAIO J.* 1996;42:M561–M567.
35. Swartbol P, Truedsson L, Pärsson H, et al. Tumor necrosis factor-alpha and interleukin-6 release from white blood cells induced by different graft materials in vitro are affected by pentoxifylline and iloprost. *J Biomed Mater Res.* 1997;36:400–406.
36. Sun H, Lu X, Wu S, et al. The effects of C-reactive protein, interleukin-6, and tumor necrosis factor-alpha in rat allograft adventitial inflammation and allograft arteriosclerosis. *Transplant Proc.* 2009;41:3909–3912.
37. Schuett H, Luchtefeld M, Grothusen C, et al. How much is too much? Interleukin-6 and its signalling in atherosclerosis. *Thromb Haemost.* 2009;102:215–222.
38. Kini AS, Baber U, Kovacic JC, et al. Changes in plaque lipid content after short-term, intensive versus standard statin therapy: the YELLOW trial. *J Am Coll Cardiol.* 2013;62:21–29.
39. Fernández-Ortiz A, Badimon JJ, Falk E, et al. Characterization of the relative thrombogenicity of atherosclerotic plaque components: implications for consequences of plaque rupture. *J Am Coll Cardiol.* 1994;23:1562–1569.
40. Cowell SJ, Newby DE, Prescott RJ, et al; Scottish Aortic Stenosis and Lipid Lowering Trial; Impact on Regression (SALTIRE) Investigators. A randomized trial of intensive lipidlowering therapy in calcific aortic stenosis. *N Engl J Med.* 2005;352:2389–2397.
41. Rossebø AB, Pedersen TR, Boman K, et al; SEAS Investigators. Intensive lipid lowering with simvastatin and ezetimibe in aortic stenosis. *N Engl J Med.* 2008;359:1343–1356.
42. Moura LM, Ramos SF, Zamorano JL, et al. Rosuvastatin affecting aortic valve endothelium to slow the progression of aortic stenosis. *J Am Coll Cardiol.* 2007;49:554–561.
43. Farivar RS, Cohn LH. Hypercholesterolemia is a risk factor for bioprosthetic valve calcification and explantation. *J Thorac Cardiovasc Surg.* 2003;126:969–975.
44. Gring CN, Houghtaling P, Novaro GM, et al. Preoperative cholesterol levels do not predict explant for structural valve deterioration in patients undergoing bioprosthetic aortic valve replacement. *J Heart Valve Dis.* 2006;15:261–268.
45. Shetty R, Pibarot P, Audet A, et al. Lipid-mediated inflammation and degeneration of bioprosthetic heart valves. *Eur J Clin Invest.* 2009;39:471–480.

3.5 **Limitations**

The developed and standardized rat implantation model of accelerated cardiovascular calcification may not exactly mimic the *in vivo* fate of cardiovascular grafts in humans, since different metabolic characteristics and complex co-morbidities in cardiovascular patients with atherosclerosis or aortic valve sclerosis may influence the maturation of the implanted prostheses. As a consequence, animal models with different mechanisms of accelerated degeneration, e.g. apolipoprotein E knockout animals, or metabolic conditions, e.g. diabetic, hypertensive or renally insufficient recipients, may be considered for further studies evaluating the *in vivo* fate of decellularized cardiovascular grafts.

3.6 **Conclusions**

With regard to the specific aims defined for this study, the following results were achieved:

I-a) A standardized *in vivo* model of aortic conduit implantation into the systemic circulation of rats was developed and functionally improved.

I-b) A standardized model of diet-induced accelerated cardiovascular calcification in rats was developed and elaborately characterized.

Utilizing these models or combined approaches, the following data were obtained:

II) Decellularization was shown to diminish the *in vivo* degeneration of aortic conduit grafts in terms of inflammation, pannus formation and calcification.

III) FN surface coating of aortic conduit implants persisted for at least 8 weeks *in vivo* and improved the biocompatibility of the grafts. Especially, it accelerated luminal and medial repopulation of the prostheses.

IV) Systemic statin treatment did not influence the *in vivo* deterioration of decellularized aortic conduits under severely pro-calcific conditions.

3.7 **Perspectives**

Decellularized cardiovascular grafts have become serious alternatives to clinical bioprosthesis standards, promising to overcome in particular the issues of inflammatory degeneration and lack of growth, which are inherent to common bioimplants. However, decellularization protocols have to be further optimized to thoroughly balance cellular protein removal and extracellular protein preservation at the same time. Moreover, FN has been shown to improve the biocompatibility of acellular cardiovascular grafts, suggesting other bioactive proteins to be promising candidates as well. Especially fast autologous *in vivo* re-endothelialization has to be induced, since this counteracts neointima hyperplasia and thrombus formation.

The developed and functionally optimized model of aortic conduit implantation with optionally accelerated cardiovascular degeneration is a unique platform to comparatively study aspects of biocompatibility and degeneration of cardiovascular implants *in vivo*. The species rat does not only allow for large animal numbers to examine multiple degenerative mechanisms and anti-degenerative interventional strategies in short time periods, but also provides a multitude of available readout methods. Furthermore, existing disease models of e.g. hypertension, obesity or diabetes may be combined with the present model to simulate the *in vivo* fate of biological prostheses in scenarios of multimorbidity.

Considering all these aspects, the standardized rat model of aortic conduit implantation is a worthwhile tool for the quest of optimizing the biocompatibility and durability of cardiovascular implants.

4 Summary

4.1 Summary (English)

In order to overcome inherent limitations of currently available heart valve prostheses, diverse tissue engineering approaches have been developed. Since comparative evaluation of different scaffolds and modifying substances in terms of biocompatibility and degeneration requires adequate *in vivo* studies, the present series of projects aimed at developing a rat model of aortic conduit implantation into the systemic circulation, furthermore featuring accelerated cardiovascular calcification. Applying this model, the effects of decellularization, fibronectin surface coating and statin treatment on the biocompatibility and calcifying degeneration of the grafts should be examined *in vivo*.

The models of functional aortic conduit implantation as well as diet-induced accelerated cardiovascular calcification were developed, optimized and standardized. The effects of different diet regimens on valvular as well as vascular remodeling in terms of chondro-osteogenic degeneration, inflammation and lipid metabolism were elucidated in detail.

The implantation studies revealed the following results:

a) Decellularization of aortic conduit grafts decreased pannus formation, inflammation and calcifying degeneration.

b) Surface coating with fibronectin significantly accelerated the autologous *in vivo* recellularization of decellularized implants.

c) Systemic statin treatment did not influence the degeneration of decellularized implants under severely pro-calcific conditions.

Decellularized cardiovascular grafts have become serious alternatives to clinical bioprosthesis standards, and surface coating with bioactive proteins seems to be suitable to improve the biocompatibility of the implants. Further studies focusing on biocompatibility and *in vivo* degeneration of tissue-engineered prostheses will be conducted in our unique standardized small animal model.

4.2 **Summary (German)**

Herzklappen-*Tissue Engineering* zielt auf die Behebung inhärenter Limitationen klinischer Standard-Prothesen. Um eine komparative Evaluation verschiedener Ansätze im Hinblick auf Biokompatibilität und Degeneration der Implantate zu ermöglichen, diente die vorliegende Studie der Entwicklung eines Ratten-Modells der system-arteriellen Implantation von Aortenkonduits, welches optional akzelerierte kardiovaskuläre Kalzifizierung bieten sollte. In diesem Modell sollten die Effekte von Dezellularisierung und Oberflächen-Beschichtung mit Fibronektin sowie von systemischer Statin-Therapie auf die Biokompatibilität und *in vivo*-Degeneration der Prothesen untersucht werden.

Die Modelle der funktionellen Aortenkonduit-Implantation sowie der Diät-induzierten akzelerierten kardiovaskulären Kalzifizierung wurden entwickelt, optimiert und standardisiert. Die Auswirkungen verschiedener Diät-Regime sowohl auf den valvulären als auch auf den vaskulären Gewebeumbau wurden unter Berücksichtigung chondro-osteogen degenerativer, inflammatorischer und Lipid-metabolischer Vorgänge detailliert dargelegt.

Die Implantations-Studien zeigten folgende Resultate:

a) Dezellularisierung der Aortenkonduits verringerte Pannus-Bildung, Inflammation und kalzifizierende Degeneration signifikant.

b) Bilaterale Oberflächen-Beschichtung mit Fibronektin beschleunigte die autolog zelluläre *in vivo*-Repopulation dezellularisierter Implantate signifikant.

c) Systemische Statin-Therapie ergab keine relevante Beeinflussung der Degeneration dezellularisierter Prothesen unter extrem pro-kalzifizierenden Konditionen.

Dezellularisierte kardiovaskuläre Prothesen sind mittlerweile ernstzunehmende Alternativen zu klinischen Standard-Implantaten geworden, und eine Oberflächen-Beschichtung mit bioaktiven Proteinen scheint geeignet zu sein die Biokompatibilität der Prothesen zu steigern. Weiterführende Studien zur Optimierung der Biokompatibilität sowie zur Reduktion der *in vivo*-Degeneration werden in unserem einzigartigen, standardisierten Kleintiermodell durchgeführt werden.

5 Acknowledgments

I gratefully acknowledge the unconfined support of Professor Dr. med. Artur Lichtenberg, head of the Department of Cardiovascular Surgery, Heinrich-Heine University Duesseldorf, Germany, in terms of my clinical as well as scientific progress, and particularly the opportunity to integrate substantial experimental research in my cardiosurgical residency.

I cordially appreciate my friend and scientific mentor PD Dr. med. Payam Akhyari, head of the Research Group for Experimental Surgery, Department of Cardiovascular Surgery, Heinrich-Heine University Duesseldorf, Germany, for his indefatigable conceptual and technical advice as well as constructive criticism in all research affairs.

My sincere thanks are given to Professor Dr. med. Jürgen Schrader, head of the Institute of Molecular Cardiology, Heinrich-Heine University Duesseldorf, Germany, and Professor Ali Khademhosseini, PhD, Biomaterials Innovation Research Center, Division of Biomedical Engineering, Harvard Medical School, Cambridge, MA, USA, who shaped, inspired and wholeheartedly supported my scientific work and interest in particular with regard to my doctoral thesis at the Heinrich-Heine University and my postdoctoral research fellowship at the Harvard Medical School.

I emphatically emphasize my appreciative thanks to PD Dr. med. Alexander Albert, vice chief of the Department of Cardiovascular Surgery, Heinrich-Heine University Duesseldorf, Germany, for guiding my clinical and surgical education, while insightfully supporting my scientific activities as well.

Special thanks go to Christofer Delfs, Kim Horstkötter, Kai Zwirnmann, Friederike Heidelberg, Franziska Schiffer und Marc Struß, whose experimental work as medical doctoral candidates has significantly contributed to all projects summarized in this thesis.

My family deserves more gratefulness than words can say

6 References

[1] d'Arcy JL, Prendergast BD, Chambers JB, Ray SG, Bridgewater B. Valvular heart disease: the next cardiac epidemic. Heart. 2011; 97:91-93.

[2] Nkomo VT, Gardin JM, Skelton TN, Gottdiener JS, Scott CG, Enriquez-Sarano M. Burden of valvular heart diseases: a population-based study. Lancet. 2006; 368:1005-1011.

[3] Coffey S, Cox B, Williams MJ. Lack of progress in valvular heart disease in the pre-transcatheter aortic valve replacement era: increasing deaths and minimal change in mortality rate over the past three decades. Am Heart J. 2014; 167:562-567.

[4] Carapetis JR, Steer AC, Mulholland EK, Weber M. The global burden of group A streptococcal diseases. Lancet Infect Dis. 2005; 5:685-694.

[5] Beckmann A, Funkat AK, Lewandowski J, Frie M, Schiller W, Hekmat K, Gummert JF, Mohr FW. Cardiac surgery in Germany during 2012: a report on behalf of the German Society for Thoracic and Cardiovascular Surgery. Thorac Cardiovasc Surg. 2014; 62:5-17.

[6] Takkenberg JJ, Rajamannan NM, Rosenhek R, Kumar AS, Carapetis JR, Yacoub MH; Society for Heart Valve Disease. The need for a global perspective on heart valve disease epidemiology. The SHVD working group on epidemiology of heart valve disease founding statement. J Heart Valve Dis. 2008; 17:135-139.

[7] Iung B, Baron G, Butchart EG, Delahaye F, Gohlke-Bärwolf C, Levang OW, Tornos P, Vanoverschelde JL, Vermeer F, Boersma E, Ravaud P, Vahanian A. A prospective survey of patients with valvular heart disease in Europe: The Euro Heart Survey on Valvular Heart Disease. Eur Heart J. 2003; 24:1231-1243.

[8] Kamath AR, Pai RG. Risk factors for progression of calcific aortic stenosis and potential therapeutic targets. Int J Angiol. 2008; 17:63-70.

[9] Prasad Y, Bhalodkar NC. Aortic sclerosis--a marker of coronary atherosclerosis. Clin Cardiol. 2004; 27:671-673.

[10] Pomerance A. Pathogenesis of aortic stenosis and its relation to age. Br Heart J. 1972; 34:569-574.

[11] Liebe V, Brueckmann M, Borggrefe M, Kaden JJ. Statin therapy of calcific aortic stenosis: hype or hope Eur Heart J. 2006; 27:773-778.

[12] Sacks MS, Yoganathan AP. Heart valve function: a biomechanical perspective. Philos Trans R Soc Lond B Biol Sci. 2007; 362:1369-1391.

[13] Sorescu GP, Song H, Tressel SL, Hwang J, Dikalov S, Smith DA, Boyd NL, Platt MO, Lassègue B, Griendling KK, Jo H. Bone morphogenic protein 4 produced in endothelial cells by oscillatory shear stress induces monocyte adhesion by stimulating reactive oxygen species production from a nox1-based NADPH oxidase. Circ Res. 2004; 95: 773-779.

[14] Kaden JJ, Dempfle CE, Grobholz R, Fischer CS, Vocke DC, Kiliç R, Sarikoç A, Piñol R, Hagl S, Lang S, Brueckmann M, Borggrefe M. Inflammatory regulation of extracellular matrix remodeling in calcific aortic valve stenosis. Cardiovasc Pathol. 2005; 14:80-87.

[15] Rabkin E, Aikawa M, Stone JR, Fukumoto Y, Libby P, Schoen FJ. Activated interstitial myofibroblasts express catabolic enzymes and mediate matrix remodeling in myxomatous heart valves. Circulation. 2001; 104:2525-2532.

[16] Olsson M, Thyberg J, Nilsson J. Presence of oxidized low density lipoprotein in nonrheumatic stenotic aortic valves. Arterioscler Thromb Vasc Biol. 1999; 19:1218-1222.

[17] Côté C, Pibarot P, Després JP, Mohty D, Cartier A, Arsenault BJ, Couture C, Mathieu P. Association between circulating oxidised low-density lipoprotein and fibrocalcific remodelling of the aortic valve in aortic stenosis. Heart. 2008; 94:1175-1180.

[18] Osman L, Yacoub MH, Latif N, Amrani M, Chester AH. Role of human valve interstitial cells in valve calcification and their response to atorvastatin. Circulation. 2006; 114:I547-I552.

[19] O'Brien KD, Kuusisto J, Reichenbach DD, Ferguson M, Giachelli C, Alpers CE, Otto CM. Osteopontin is expressed in human aortic valvular lesions. Circulation. 1995; 92:2163-2168.

[20] Yang X, Meng X, Su X, Mauchley DC, Ao L, Cleveland JC Jr, Fullerton DA. Bone morphogenic protein 2 induces Runx2 and osteopontin expression in human aortic valve interstitial cells: role of Smad1 and extracellular signal-regulated kinase 1/2. J Thorac Cardiovasc Surg. 2009; 138:1008-1015.

[21] Ortlepp JR, Hoffmann R, Ohme F, Lauscher J, Bleckmann F, Hanrath P. The vitamin D receptor genotype predisposes to the development of calcific aortic valve stenosis. Heart. 2001; 85:635-638.

[22] Linefsky JP, O'Brien KD, Sachs M, Katz R, Eng J, Michos ED, Budoff MJ, de Boer I, Kestenbaum B. Serum phosphate is associated with aortic valve calcification in the Multi-ethnic Study of Atherosclerosis (MESA). Atherosclerosis. 2014; 233:331-337.

[23] Hjortnaes J, Butcher J, Figueiredo JL, Riccio M, Kohler RH, Kozloff KM, Weissleder R, Aikawa E. Arterial and aortic valve calcification inversely correlates with osteoporotic bone remodelling: a role for inflammation. Eur Heart J. 2010; 31:1975-1984.

[24] Yip CY, Chen JH, Zhao R, Simmons CA. Calcification by valve interstitial cells is regulated by the stiffness of the extracellular matrix. Arterioscler Thromb Vasc Biol. 2009; 29:936-942.

[25] Hoffman JI, Kaplan S. The incidence of congenital heart disease. J Am Coll Cardiol. 2002; 39:1890-1900.

[26] Dilley RJ, McGeachie JK, Prendergast FJ. A review of the proliferative behaviour, morphology and phenotypes of vascular smooth muscle. Atherosclerosis. 1987; 63:99-107.

[27] Rabkin-Aikawa E, Farber M, Aikawa M, Schoen FJ. Dynamic and reversible changes of interstitial cell phenotype during remodeling of cardiac valves. J Heart Valve Dis. 2004; 13:841-847.

[28] Bonow RO, Carabello BA, Kanu C, de Leon AC Jr, Faxon DP, Freed MD, Gaasch WH, Lytle BW, Nishimura RA, O'Gara PT, O'Rourke RA, Otto CM, Shah PM, Shanewise JS, Smith SC Jr, Jacobs AK, Adams CD, Anderson JL, Antman EM, Faxon DP, Fuster V, Halperin JL, Hiratzka LF, Hunt SA, Lytle BW, Nishimura R, Page RL, Riegel B. ACC/AHA 2006 guidelines for the management of patients with valvular heart disease: a report of the American College of Cardiology/American Heart Association Task Force on Practice Guidelines (writing committee to revise the 1998 Guidelines for the Management of Patients With Valvular Heart Disease): developed in collaboration with the Society of Cardiovascular Anesthesiologists: endorsed by the Society for Cardiovascular Angiography and Interventions and the Society of Thoracic Surgeons. Circulation. 2006; 114:e84-e231.

[29] Cowell SJ, Newby DE, Prescott RJ, Bloomfield P, Reid J, Northridge DB, Boon NA; Scottish Aortic Stenosis and Lipid Lowering Trial, Impact on Regression (SALTIRE) Investigators. A randomized trial of intensive lipidlowering therapy in calcific aortic stenosis. N Engl J Med. 2005; 352:2389-2397.

[30] Rossebø AB, Pedersen TR, Boman K, Brudi P, Chambers JB, Egstrup K, Gerdts E, Gohlke-Bärwolf C, Holme I, Kesäniemi YA, Malbecq W, Nienaber CA, Ray S, Skjaerpe T, Wachtell K, Willenheimer R; SEAS Investigators. Intensive lipid lowering with simvastatin and ezetimibe in aortic stenosis. N Engl J Med. 2008; 359:1343-1356.

[31] Moura LM, Ramos SF, Zamorano JL, Barros IM, Azevedo LF, Rocha-Gonçalves F, Rajamannan NM. Rosuvastatin affecting aortic valve endothelium to slow the progression of aortic stenosis. J Am Coll Cardiol. 2007; 49:554-561.

[32] Roberts WC. Choosing a substitute cardiac valve: type, size, surgeon. Am J Cardiol. 1976; 38:633-644.

[33] Moroni F, Mirabella T. Decellularized matrices for cardiovascular tissue engineering. Am J Stem Cells. 2014; 3:1-20.

[34] Lichtenberg A, Tudorache I, Cebotari S, Suprunov M, Tudorache G, Goerler H, Park JK, Hilfiker-Kleiner D, Ringes-Lichtenberg S, Karck M, Brandes G, Hilfiker A, Haverich A. Preclinical testing of tissue-engineered heart valves re-endothelialized under simulated physiological conditions. Circulation. 2006; 114:I559-I565.

[35] Green MK, Walsh MD, Dare A, Hogan PG, Zhao XM, Frazer IH, Bansal AS, O'Brien MF. Histologic and immunohistochemical responses after aortic valve allografts in the rat. Ann Thorac Surg. 1998; 66:S216-S220.

[36] Shaddy RE, Hunter DD, Osborn KA, Lambert LM, Minich LL, Hawkins JA, McGough EC, Fuller TC. Prospective analysis of HLA immunogenicity of cryopreserved valved allografts used in pediatric heart surgery. Circulation. 1996; 94:1063-1067.

[37] Grauss RW, Hazekamp MG, van Vliet S, Gittenberger-de Groot AC, DeRuiter MC. Decellularization of rat aortic valve allografts reduces leaflet destruction and extracellular matrix remodeling. J Thorac Cardiovasc Surg. 2003; 126:2003-2010.

[38] Akhyari P, Kamiya H, Gwanmesia P, Aubin H, Tschierschke R, Hoffmann S, Karck M, Lichtenberg A. In vivo functional performance and structural maturation of decellularised allogenic aortic valves in the subcoronary position. Eur J Cardiothorac Surg. 2010; 38:539-546.

[39] Cebotari S, Lichtenberg A, Tudorache I, Hilfiker A, Mertsching H, Leyh R, Breymann T, Kallenbach K, Maniuc L, Batrinac A, Repin O, Maliga O, Ciubotaru A, Haverich A. Clinical application of tissue engineered human heart valves using autologous progenitor cells. Circulation. 2006; 114:I132-I137.

[40] da Costa FD, Costa AC, Prestes R, Domanski AC, Balbi EM, Ferreira AD, Lopes SV. The early and midterm function of decellularized aortic valve allografts. Ann Thorac Surg. 2010; 90:1854-1860.

[41] O'Brien MF, Stafford EG, Gardner MA, Pohlner PG, Tesar PJ, Cochrane AD, Mau TK, Gall KL, Smith SE. Allograft aortic valve replacement (long-term follow-up). Ann Thorac Surg. 1995; 60:S65-S70.

[42] Clarke DR, Campbell DN, Hayward AR, Bishop DA. Degeneration of aortic valve allografts in young recipients. J Thorac Cardiovasc Surg. 1993; 105:934-941.

[43] Lehr EJ, Rayat GR, Chiu B, Churchill T, McGann LE, Coe JY, Ross DB. Decellularization reduces immunogenicity of sheep pulmonary artery vascular patches. J Thorac Cardiovasc Surg. 2011; 141:1056-1062.

[44] Meyer SR, Nagendran J, Desai LS, Rayat GR, Churchill TA, Anderson CC, Rajotte RV, Lakey JR, Ross DB. Decellularization reduces the immune response to aortic valve allografts in the rat. J Thorac Cardiovasc Surg. 2005; 130:469-476.

[45] Cicha I, Rüffer A, Cesnjevar R, Glöckler M, Agaimy A, Daniel WG, Garlichs CD, Dittrich S. Early obstruction of decellularized xenogenic valves in pediatric patients: involvement of inflammatory and fibroproliferative processes. Cardiovasc Pathol. 2011; 20:222-231.

[46] Kasimir MT, Rieder E, Seebacher G, Nigisch A, Dekan B, Wolner E, Weigel G, Simon P. Decellularization does not eliminate thrombogenicity and inflammatory stimulation in tissue-engineered porcine heart valves. J Heart Valve Dis. 2006; 15:278-286.

[47] Meyer SR, Chiu B, Churchill TA, Zhu L, Lakey JR, Ross DB. Comparison of aortic valve allograft decellularization techniques in the rat. J Biomed Mater Res A. 2006; 79:254-262.

[48] Zhou J, Fritze O, Schleicher M, Wendel HP, Schenke-Layland K, Harasztosi C, Hu S, Stock UA. Impact of heart valve decellularization on 3-D ultrastructure, immunogenicity and thrombogenicity. Biomaterials. 2010; 31:2549-2554.

[49] Rieder E, Seebacher G, Kasimir MT, Eichmair E, Winter B, Dekan B, Wolner E, Simon P, Weigel G. Tissue engineering of heart valves: decellularized porcine and human valve scaffolds differ importantly in residual potential to attract monocytic cells. Circulation. 2005; 111:2792-2797.

[50] Lichtenberg A, Tudorache I, Cebotari S, Ringes-Lichtenberg S, Sturz G, Hoeffler K, Hurscheler C, Brandes G, Hilfiker A, Haverich A. In vitro re-endothelialization of

detergent decellularized heart valves under simulated physiological dynamic conditions. Biomaterials. 2006; 27:4221-4229.

[51] Hopkins RA, Jones AL, Wolfinbarger L, Moore MA, Bert AA, Lofland GK. Decellularization reduces calcification while improving both durability and 1-year functional results of pulmonary homograft valves in juvenile sheep. J Thorac Cardiovasc Surg 2009; 137:907-913.

[52] Martin ND, Schaner PJ, Tulenko TN, Shapiro IM, Dimatteo CA, Williams TK, Hager ES, DiMuzio PJ. In vivo behavior of decellularized vein allograft. J Surg Res. 2005; 129:17-23.

[53] Shimada T, Nishibe T, Miura H, Hazama K, Kato H, Kudo F et al. Improved healing of small-caliber, long-fibril expanded polytetrafluoroethylene vascular grafts by covalent bonding of fibronectin. Surg Today. 2004; 34:1025-1030.

[54] Zhou M, Liu Z, Wei Z, Liu C, Qiao T, Ran F et al. Development and validation of small-diameter vascular tissue from a decellularized scaffold coated with heparin and vascular endothelial growth factor. Artif Organs. 2009; 33:230-239.

[55] Budd JS, Allen KE, Bell PR, James RF. The effect of varying fibronectin concentration on the attachment of endothelial cells to polytetrafluoroethylene vascular grafts. J Vasc Surg. 1990; 12:126-130.

[56] Baguneid M, Murray D, Salacinski HJ, Fuller B, Hamilton G, Walker M et al. Shear-stress preconditioning and tissue-engineering-based paradigms for generating arterial substitutes. Biotechnol Appl Biochem. 2004; 39:151-157.

[57] Gwanmesia P, Ziegler H, Eurich R, Barth M, Kamiya H, Karck M et al. Opposite effects of transforming growth factor-β1 and vascular endothelial growth factor on the degeneration of aortic valvular interstitial cell are modified by the extracellular matrix protein fibronectin: implications for heart valve engineering. Tissue Eng Part A. 2010; 16:3737-3746.

[58] Jasińska M, Owczarek J, Orszulak-Michalak D. Statins: a new insight into their mechanisms of action and consequent pleiotropic effects. Pharmacol Rep. 2007; 59:483-499.

[59] Parolari A, Tremoli E, Cavallotti L, Trezzi M, Kassem S, Loardi C, Veglia F, Ferrari G, Pacini D, Alamanni F. Do statins improve outcomes and delay the progression of non-rheumatic calcific aortic stenosis? Heart. 2011; 97:523-529.

[60] Gilmanov D, Bevilacqua S, Mazzone A, Glauber M. Do statins slow the process of calcification of aortic tissue valves? Interact Cardiovasc Thorac Surg. 2010; 11:297-301.

[61] Tang FT, Chen SR, Wu XQ, Wang TQ, Chen JW, Li J, Bao LP, Huang HQ, Liu PQ. Hypercholesterolemia accelerates vascular calcification induced by excessive vitamin D via oxidative stress. Calcif Tissue Int. 2006; 79:326-339.

[62] Drolet MC, Couet J, Arsenault M. Development of aortic valve sclerosis or stenosis in rabbits: role of cholesterol and calcium. J Heart Valve Dis. 2008; 17:381-387.

[63] Ngo DT, Stafford I, Kelly DJ, Sverdlov AL, Wuttke RD, Weedon H, Nightingale AK, Rosenkranz AC, Smith MD, Chirkov YY, Kennedy JA, Horowitz JD. Vitamin D(2) supplementation induces the development of aortic stenosis in rabbits: interactions with endothelial function and thioredoxin-interacting protein. Eur J Pharmacol. 2008; 590:290-296.

[64] Oei FB, Welters MJ, Bonthuis F, Vaessen LM, Marquet RL, Zondervan PE, Weimar W, Bogers AJ. A size-matching heterotopic aortic valve implantation model in the rat. J Surg Res. 1999; 87:239-244.

[65] Li Z, Li L, Zielke R, Cheng L, Xiao R, Crow M, Stetler-Stevenson WG, Froehlich J, Lakatta EG. Increased expression of 72-kD type IV collagenase (MMP2) in human aortic atherosclerotic lesions. Am J Pathol. 1996; 148:121-128.

[66] Loftus IM, Naylor AR, Goodall S, Crowther M, Jones L, Bell PR, Thompson MM. Increased matrix metalloproteinase-9 activity in unstable carotid plaques. A potential role in acute plaque disruption. Stroke. 2000; 31:40-47.

[67] Perrotta I, Russo E, Camastra C, Filice G, Di Mizio G, Colosimo F, Ricci P, Tripepi S, Amorosi A, Triumbari F, Donato G. New evidence for a critical role of elastin in calcification of native heart valves: immunohistochemical and ultrastructural study with literature review. Histopathology. 2011; 59:504-513.
[68] DeBakey ME, Lawrie GM, Glaeser DH. Patterns of atherosclerosis and their surgical significance. Ann Surg. 1985; 201:115-131.
[69] Ross R. Atherosclerosis--an inflammatory disease. N Engl J Med. 1999; 340:115-126.
[70] Bönner F, Borg N, Burghoff S, Schrader J. Resident cardiac immune cells and expression of the ectonucleotidase enzymes CD39 and CD73 after ischemic injury. PLoS One. 2012; 7:e34730.
[71] Ikonen TS, Briffa N, Gummert JF, Honda Y, Hayase M, Hausen B, Billingham ME, Yock PG, Robbins RC, Morris RE. Multidimensional assessment of graft vascular disease (GVD) in aortic grafts by serial intravascular ultrasound in rhesus monkeys. Transplantation. 2000; 70:420-429.
[72] Brockbank KG, Song YC. Morphological analyses of ice-free and frozen cryopreserved heart valve explants. J Heart Valve Dis. 2004; 13:297-301.
[73] Baraki H, Tudorache I, Braun M, Höffler K, Görler A, Lichtenberg A, Bara C, Calistru A, Brandes G, Hewicker-Trautwein M, Hilfiker A, Haverich A, Cebotari S. Orthotopic replacement of the aortic valve with decellularized allograft in a sheep model. Biomaterials. 2009; 30:6240-6246.
[74] Burch PT, Kaza AK, Lambert LM, Holubkov R, Shaddy RE, Hawkins JA. Clinical performance of decellularized cryopreserved valved allografts compared with standard allografts in the right ventricular outflow tract. Ann Thorac Surg. 2010; 90:1301-1305.
[75] Cebotari S, Tudorache I, Ciubotaru A, Boethig D, Sarikouch S, Goerler A, Lichtenberg A, Cheptanaru E, Barnaciuc S, Cazacu A, Maliga O, Repin O, Maniuc L, Breymann T, Haverich A. Use of fresh decellularized allografts for pulmonary valve replacement may reduce the reoperation rate in children and young adults: early report. Circulation. 2011; 124:S115-S123.
[76] da Costa FD, Costa AC, Prestes R, Domanski AC, Balbi EM, Ferreira AD, Lopes SV. The early and midterm function of decellularized aortic valve allografts. Ann Thorac Surg. 2010; 90:1854-1860.
[77] Tavakkol Z, Gelehrter S, Goldberg CS, Bove EL, Devaney EJ, Ohye RG. Superior durability of SynerGraft pulmonary allografts compared with standard cryopreserved allografts. Ann Thorac Surg. 2005; 80:1610-1614.
[78] Ramalanjaona GR, Kempczinski RF, Ogle JD, Silberstein EB. Fibronectin coating of an experimental PTFE vascular prosthesis. J Surg Res. 1986; 41:479-483.
[79] Cha MC, Purslow PP. The activities of MMP-9 and total gelatinase respond differently to substrate coating and cyclic mechanical stretching in fibroblasts and myoblasts. Cell Biol Int. 2010; 34:587-591.
[80] Monzack EL, Masters KS. A time course investigation of the statin paradox among valvular interstitial cell phenotypes. Am J Physiol Heart Circ Physiol. 2012; 303:H903-H909.
[81] Zhao XQ, Yuan C, Hatsukami TS, Frechette EH, Kang XJ, Maravilla KR, Brown BG. Effects of prolonged intensive lipid-lowering therapy on the characteristics of carotid atherosclerotic plaques in vivo by MRI: a case-control study. Arterioscler Thromb Vasc Biol. 2001; 21:1623-1629.
[82] Vaughan CJ, Gotto AM Jr, Basson CT. The evolving role of statins in the management of atherosclerosis. J Am Coll Cardiol. 2000; 35:1-10.
[83] Sun H, Lu X, Wu S, Sun W. The effects of C-reactive protein, interleukin-6, and tumor necrosis factor-alpha in rat allograft adventitial inflammation and allograft arteriosclerosis. Transplant Proc. 2009; 41:3909-3912.

[84] Swartbol P, Truedsson L, Pärsson H, Norgren L. Tumor necrosis factor-alpha and interleukin-6 release from white blood cells induced by different graft materials in vitro are affected by pentoxifylline and iloprost. J Biomed Mater Res. 1997; 36:400-406.

7 Curriculum vitae

Email: alexander.assmann@med.uni-duesseldorf.de

Personal details:

Date of birth:	May the 3rd, 1981
Place of birth:	Fuerstenfeldbruck, Germany
Parents:	Dr. med. Regina Assmann and Dr. med. Rainer Assmann
Nationality:	German

Study:

04/2001-06/2007	Study of medicine at the University of Duesseldorf, Germany
04/2002-06/2007	Stipendiary of the German National Merit Foundation
04–06/2007	Medical state examination (grade *excellent*)

Dissertation:

03/2008	Doctorate in medicine with the thesis "Intracoronary transplantation of HUVECS in the rat myocardium: Feasibility and cell destiny" from the Institute of Heart and Circulatory Physiology of the University of Duesseldorf (grade *summa cum laude*)

Work:

Since 08/2007	Resident in cardiac surgery in the Department of Cardiovascular Surgery at the University of Duesseldorf, Germany
06/2013-05/2014	Research fellowship of the German Heart Foundation at the Biomaterials Innovation Research Center, Division of Biomedical Engineering, Harvard Medical School, Cambridge, MA, USA
02/2014	Ulrich Karsten Scientific Award of the German Society for Thoracic and Cardiovascular Surgery for the research data summarized in this habilitation thesis

Memberships:

German Society for Thoracic and Cardiovascular Surgery
European Association for Cardio-Thoracic Surgery
German Society for Stem Cell Research
Tissue Engineering and Regenerative Medicine International Society
The CardioThoracic Surgery Network

Peer review:

Circulation
PLoS One
Journal of Biomechanics
Artificial Organs
Annals of Biomedical Engineering
International Journal of Cardiovascular Imaging

Duesseldorf, September 2014

Dr. med. Alexander Assmann